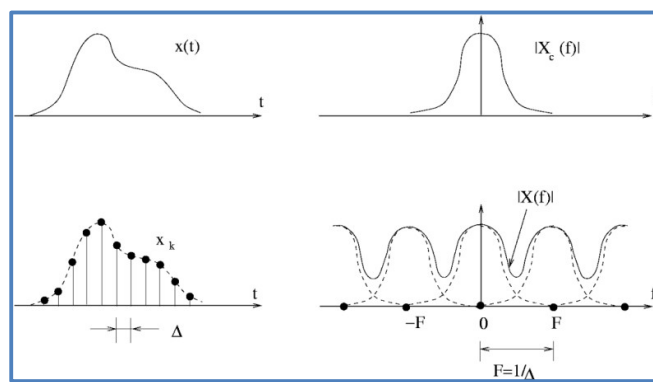


Digital Signal Processing

an introduction



Contents

Preface.....	3
Chapter 1 Signals and systems	4
1.1 Systems.....	4
1.2 Transfer theory of linear invariant systems	6
1.2.1 Impulse response method.....	7
1.2.2 Transmission function method.....	9
1.3 The transmission scheme of a system: convolution and multiplication	12
1.4 Real instead of complex harmonics.....	14
1.5 Filters and their properties.....	15
1.6 Important continuous FT/IFT pairs.....	18
1.7 Exercises	19
Chapter 2 Sampling – Shannon Nyquist Theorem	22
2.1 Introduction.....	22
2.2 Quantization noise	23
2.3 Sampling theorem	25
2.3.1 Sampling and repeating.....	25
2.3.2 The Shannon-Nyquist sampling theorem and signal reconstruction	26
2.4 Alias	30
2.4.1 Alias errors.....	30
2.4.2 Anti-alias filters.....	32
2.4.3 Alias errors at signal edges.....	34
2.5 Continuous and discrete operations	35
2.6 Narrow band signals.....	37
2.7 Exercise.....	38
Chapter 3 Filtering in the time domain - recursive filters.....	39
3.1 Introduction.....	39
3.2 Impulse response	42
3.3 Transmission function	47
3.4 Filters in series.....	60
3.4 Exercises	62
Chapter 4 Filtering in the frequency domain – the Discrete Fourier Transform DFT	65
4.1 Introduction.....	65

4.2	Discrete Fourier Transform	66
4.3	Frequency domain filter	69
4.4	Transmission function of the frequency domain filter.....	72
4.5	Application: noise suppression.....	74
4.7	Exercises	77
Chapter 5 The Discrete Fourier Transform as filter bank – spectral analysis		78
5.1	The ‘sinc’ filter	78
5.2	The tuned ‘sinc’ filter.....	80
5.3	The DFT as filter bank.....	82
5.4	Spectral analysis	83
5.5	Weighting functions to suppress side lobes.....	84
5.6	Exercise.....	87
Chapter 6 Analogy with phased arrays		88
6.1	Introduction.....	88
6.2	Diffraction pattern as Fourier transform of aperture illumination	88
6.3	The analogy	93
6.4	Phased array antennas.....	94
6.5	Applications	99
6.6	Exercise.....	100
Chapter 7 Properties of noise signals – spectral analysis revisited.....		101
7.1	Introduction.....	101
7.2	Mean and variance	101
7.3	Covariance	102
7.4	Spectrum	103
7.5	Wiener-Khintchin relation.....	107
7.6	Spectral analysis	109
7.7	Exercise.....	114
Appendix Analog signal processing		115
Complex impedance and passive filters		115
Exercise.....		124
Circuits with operational amplifiers and active filters		125
Exercises		135
Data acquisition systems.....		137
Exercise.....		142

Preface

This set of lecture notes is an adapted and modernized version of the course given by professor C. van Schooneveld at the University of Leiden in 1980's and can be used as background information on signal processing for the courses AE4431 and AE4463P on aircraft noise. Before doing digital signal processing it is advisable to first learn the very basics of analog signal analysis. The appendix provides the most relevant elements for this.

Professor Dick G. Simons & Professor Mirjam Snellen

Section Aircraft Noise and Climate Effects
Faculty of Aerospace Engineering
Delft University of Technology

April 2023

Chapter 1 Signals and systems

Observations in e.g. physics, astronomy and biology (or nature in general) nearly always provide continuous (analog) signals, i.e. functions of one or more continuous variables. A simple 1D example is the signal $x(t)$, where x is the voltage (in Volt) as a function of time t (in seconds). A 2D example is $s(x, y)$, being light intensity (in W/m^2) in the focal plane of a camera as a function of coordinates x and y (both in m).

For storage and processing of signals in digital systems discrete signals are required. Such discrete signals are rows of numbers that consist of sampled values of the original continuous signal. The sampling distance Δ should be chosen such that the resulting discrete signal remains representative for the continuous signal (see chapter 2).

In this course we will treat only 1D signals. The continuous signal is denoted $x(t)$ and the discrete signal can be indicated by $\dots, x_{k-1}, x_k, x_{k+1}, \dots$ or \dots, x_k, \dots . The shorthand notation for the discrete signal is however often x_k . In practice, discrete signals always are of finite length.

This course is about discrete methods, i.e. numerical operations on sampled signals. This is also denoted ‘digital signal processing’.

1.1 Systems

Basically, a system is a relation between cause and consequence. Both can be considered as signals, i.e. functions of a continuous variable t or a discrete index k , see figure 1.1.

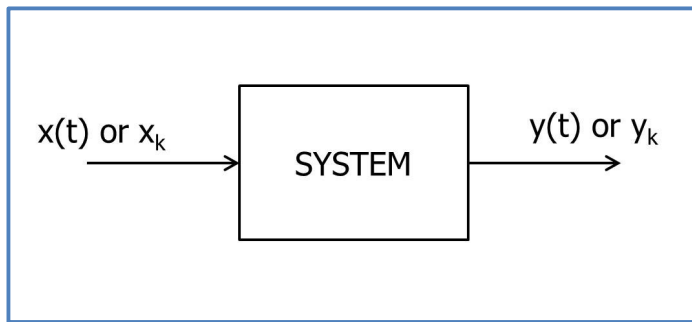


Figure 1.1: System with input $x(t)$ (or x_k) and output $y(t)$ (or y_k).

For continuous signals, $x(t)$ and $y(t)$, the system is continuous, whereas for discrete signals, x_k and y_k , the system is discrete. When x and y depend on a single variable, e.g. time t , then the system is 1D. However, also multi-dimensional systems exist, e.g. 2D when x and y depend on the two coordinates in a plane. Further, x and y (or x_k and y_k) can be both scalar or vector quantities.

In general, the value of $y(t)$ at $t = t_0$ can only be found if $x(t)$ is known for $-\infty < t < \infty$, i.e. all values of $x(t)$ can have their influence on $y(t_0)$. With t representing time, we can distinguish causal and non-causal systems. For physically feasible systems $y(t_0)$ can only depend on the values of $x(t)$ for $t \leq t_0$. Such systems are called causal. However, suppose we first store all values of $x(t)$ in a memory and process them afterwards, then $y(t_0)$ can depend on values of $x(t)$ for $t > t_0$. Such non-causal systems are not physically feasible, but can be made numerically feasible (and are frequently used in digital signal processing).

A system is called invariant when a shift of $x(t)$ along the t -axis only results in the same shift of $y(t)$. Mathematically: if $x(t) \rightarrow y(t)$ then $x(t - t_0) \rightarrow y(t - t_0)$ for all t_0 and all $x(t)$. When t is time in this case, this means that all system properties are fixed (invariable).

A system is linear when the superposition principle holds. This is mathematically formulated as:

if $x_1(t) \rightarrow y_1(t)$ and $x_2(t) \rightarrow y_2(t)$ then $a_1x_1(t) + a_2x_2(t) \rightarrow a_1y_1(t) + a_2y_2(t)$ for all a_1 , a_2 and all x_1 and x_2 . This implies that when $x(t) = 0 \rightarrow y(t) = 0$. In nature non-linear systems occur. In this course however, we only consider linear systems.

As already mentioned, the signals $x(t)$ from nature are nearly always continuous in the variable t and the value x . In order to be able to apply digital signal processing, the signal $x(t)$ is sampled, i.e. discretized in both t and x . The first is performed by taking samples at a fixed spacing Δ , whereas the second is performed by rounding off the values of x on a amplitude grid with fixed spacing q . This is illustrated in figure 1.2.

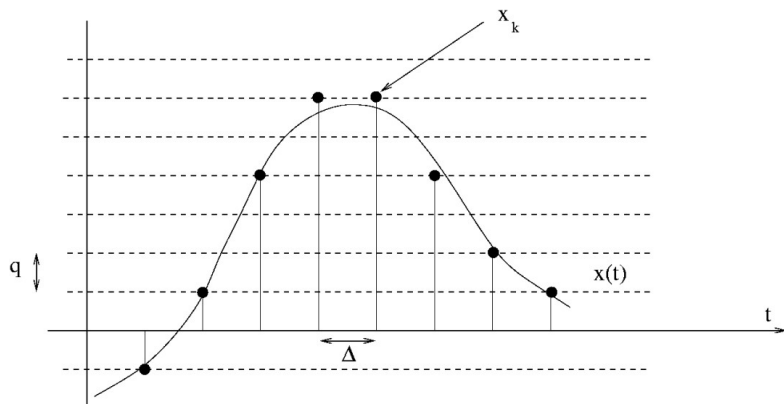


Figure 1.2: Sampling of a continuous signal $x(t)$ resulting in the samples x_k .

This results in the row of numbers x_k , i.e. the samples, given by

$$x_k = x(k\Delta) + r_k \quad (1.1)$$

which is the discrete signal corresponding to the continuous signal $x(t)$. r_k is the residual belonging to x_k with $r_k < \frac{q}{2}$. The theory on sampling is further discussed in chapter 2.

Digital signal processing is useful in the following situations:

- A row of discrete numbers x_k can easily be stored in a digital memory or sent over a digital communication channel. Afterwards the original continuous signal $x(t)$ can be recovered from x_k . Examples of this are digital transmission of speech, music and images.
- Discrete operations can be executed on x_k such that they are equivalent to the desired original operations on the continuous signal $x(t)$. The advantage is that these discrete operations are generally more accurate and more flexible.
- Sometimes a continuous measurement is impossible, e.g. in radar the distance to an aircraft can only be measured by subsequently sending pulses with spacing Δ in time. A row of numbers x_k , containing the distances, is the measurement result.

1.2 Transfer theory of linear invariant systems

We consider linear invariant 1D systems. The independent variable, t or k , is time in seconds. The quantities x and y can be thought of as voltages (in Volt). A generalisation to multi-dimensional systems is trivial. We note that variant systems exist (e.g. adaptive filters), but they are not treated in this course.

The transfer theory for these systems consists of the following two steps:

First, consider the input signal $x(t)$ as a sum of elementary basis functions $e_i(t)$. The system produces for each basis function a response function $T\{e_i(t)\}$ that can easily be calculated. Hence, we can write

$$x(t) = \sum_i p_i e_i(t) \quad (1.2)$$

with all p_i scalar. With basis functions $e(t, \theta)$ with a continuous index θ (instead of discrete i) $x(t)$ can be written as

$$x(t) = \int p(\theta) e(t, \theta) d\theta. \quad (1.2a)$$

Second, we write $y(t)$ as a sum of the responses on the basis functions, i.e.

$$y(t) = \sum_i p_i T\{e_i(t)\} \quad (1.3)$$

or

$$y(t) = \int p(\theta) T\{e(t, \theta)\} d\theta. \quad (1.3a)$$

This is allowed as the system is linear (and invariant).

The transfer theory is now subsequently treated with the so-called ‘impulse response’ and the ‘transmission function’.

1.2.1 Impulse response method

In the discrete situation the elementary input signal is an impulse given as

$$\delta_k = \begin{cases} 1 & k=0 \\ 0 & k \neq 0 \end{cases} \quad (1.4)$$

which is also known as the Kronecker delta.

For the continuous case the elementary input signal is the Dirac function

$$\delta(t) = \begin{cases} \infty & t=0 \\ 0 & t \neq 0 \end{cases} \quad (1.5)$$

with $\int_{-\infty}^{\infty} \delta(t) dt = 1$. The elementary input signals are illustrated in figure 1.3.

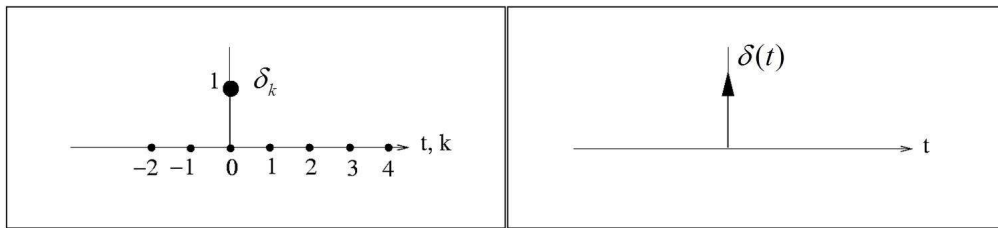


Figure 1.3: Elementary input signal for a discrete system (left) and a continuous system (right).

Conform equation 1.2 we can write the input signal as (discrete case)

$$x_k = \sum_{i=-\infty}^{\infty} x_i \delta_{k-i} \quad (1.6)$$

$$\text{with } \delta_{k-i} = \begin{cases} 1 & k=i \\ 0 & k \neq i \end{cases}.$$

In the continuous case the input signal can be written as

$$a(t) = \int_{-\infty}^{\infty} a(\tau) \delta(t-\tau) d\tau. \quad (1.7)$$

The response of the system to an impulse as input is known as the ‘impulse response’, denoted as h_k and $g(t)$, for the discrete and continuous situation, respectively. The impulse response can be determined from the internal properties of the system (see chapter 3) or experimentally by exciting the system with an impulse. Examples of impulse responses are shown in figure 1.4.

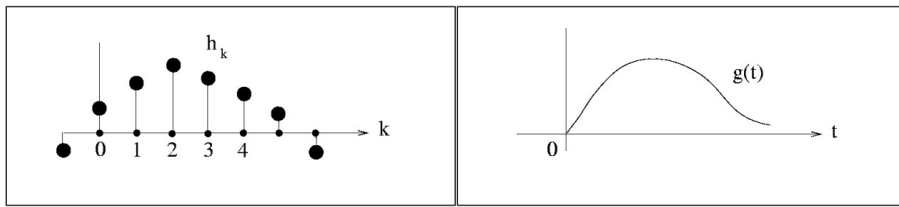


Figure 1.4: An example of an impulse response for a discrete system (left) and for a continuous system (right).

Conform equation 1.3 (and based on linearity and invariance) the output signal in the discrete case can be written as

$$y_k = \sum_{i=-\infty}^{\infty} x_i h_{k-i} = \sum_{i=-\infty}^{\infty} x_{k-i} h_i \quad (1.8)$$

i.e. the ‘convolution’ of x_k and h_k , the shorthand notation of which is $x_k \otimes h_k$. In the continuous situation the output signal is

$$b(t) = \int_{-\infty}^{\infty} a(\tau) g(t-\tau) d\tau = \int_{-\infty}^{\infty} a(t-\tau) g(\tau) d\tau = a(t) \otimes g(t) \quad (1.9)$$

i.e. the convolution of the continuous signals $a(t)$ (the input) and $g(t)$ (the impulse response). This is illustrated schematically in figure 1.5, both for the continuous and discrete system.

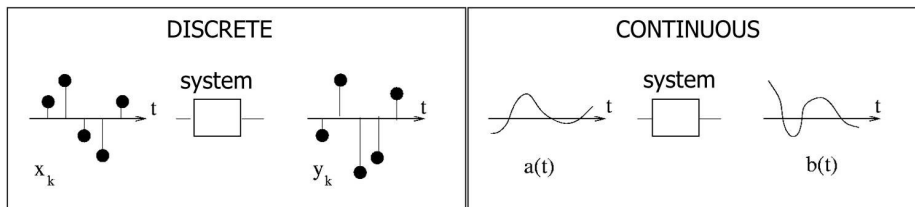


Figure 1.5: Input and output signals for a discrete system (left) and a continuous system (right).

1.2.2 Transmission function method

Now the elementary input signal e_k is a complex harmonic with frequency f (in Hz). At this stage this seems odd, however, later we will see that real signals can be composed of complex parts where the imaginary components cancel. In the discrete case e_k is given as

$$e_k = e^{2\pi j f k \Delta} \quad (1.10)$$

with $j = \sqrt{-1}$. The complex harmonic is visualised in figure 1.6 below.

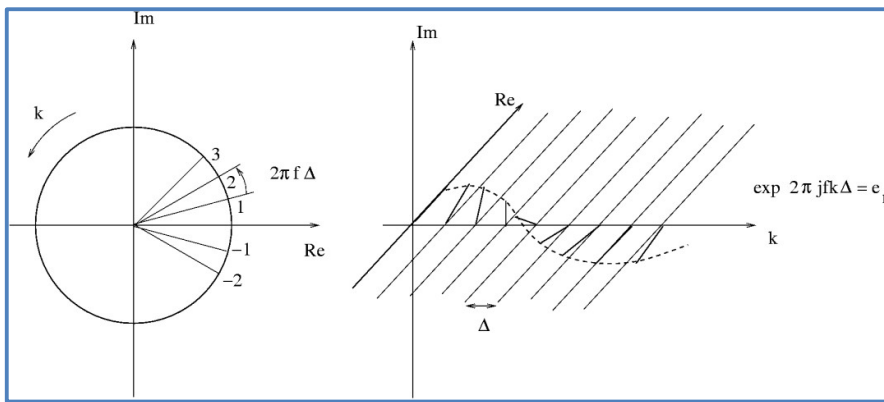


Figure 1.6: The complex harmonic e_k .

In the continuous case the elementary input signal is

$$e(t) = e^{2\pi j f t}. \quad (1.11)$$

Conform equation 1.2a we can write the input signal as (discrete case)

$$x_k = \int_{-\frac{1}{2\Delta}}^{\frac{1}{2\Delta}} X(f) e^{2\pi j f k \Delta} df \quad (1.12)$$

with

$$X(f) = \Delta \sum_{k=-\infty}^{\infty} x_k e^{-2\pi j f k \Delta}. \quad (1.13)$$

The last expression for $X(f)$ can be proven by substituting equation 1.13 into equation 1.12 and

using $\Delta \int_{-\frac{1}{2\Delta}}^{\frac{1}{2\Delta}} e^{2\pi j f (k-k') \Delta} df = \delta_{k-k'}$ for the Kronecker delta. We note that $X(f)$ is the Fourier

transform of x_k and x_k the inverse Fourier transform of $X(f)$. $X(f)$ always converges as in practice the values of x_k are finite and because x_k has finite length. If x_k has infinite length $X(f)$ can still converge provided the row x_k is going to zero sufficiently fast when $k \rightarrow \pm\infty$.

In the continuous case the input signal can be written as

$$a(t) = \int_{-\infty}^{\infty} A(f) e^{2\pi j f t} df \quad (1.14)$$

with

$$A(f) = \int_{-\infty}^{\infty} a(t) e^{-2\pi j f t} dt \quad (1.15)$$

the Fourier transform of $a(t)$. Then, $a(t)$ is the inverse Fourier transform of $A(f)$.

The Fourier transforms, equations 1.13 and 1.15, are Hermitian, i.e.

$$X(-f) = X^*(f) \quad (1.16)$$

and

$$A(-f) = A^*(f) \quad (1.17)$$

provided x_k and $a(t)$ are real valued. $*$ denotes the complex conjugate. Hence, in equation 1.12 and 1.14 the imaginary components for the frequencies $+f$ and $-f$ cancel, such that real signals can indeed be composed of complex parts (see remark at beginning of this section).

The complex harmonics were chosen as elementary functions because they are eigenfunctions of linear invariant systems. This means that the output of a linear invariant system, with a complex harmonic at the input, is the same complex harmonic but multiplied by a complex scalar factor $H(f)$. Hence, $H(f)$ is the eigenvalue corresponding to the eigenfunction $e_k = e^{2\pi j fk\Delta}$ of the system. This can be easily verified by substituting e_k into equation 1.8:

$$y_k = \sum_{k'=-\infty}^{\infty} e_k h_{k'-k} = \sum_{k'=-\infty}^{\infty} e_{k'-k} h_k = \sum_{k'=-\infty}^{\infty} e^{2\pi j f(k'-k)\Delta} h_k = e^{2\pi j fk'\Delta} \sum_{k'=-\infty}^{\infty} e^{-2\pi j fk'\Delta} h_k = e^{2\pi j fk'\Delta} H(f).$$

Hence, the eigenvalue $H(f)$ is given by

$$H(f) = \sum_{k=-\infty}^{\infty} e^{-2\pi j fk\Delta} h_k \quad (1.18)$$

i.e. the Fourier transform of the impulse response h_k (apart from the factor Δ). Therefore, h_k is the inverse Fourier transform (without the factor Δ) of $H(f)$, i.e.

$$h_k = \Delta \int_{-\frac{1}{2\Delta}}^{\frac{1}{2\Delta}} H(f) e^{2\pi j f k \Delta} df. \quad (1.19)$$

In the continuous case the response to the elementary input signal $e(t) = e^{2\pi j ft}$ (equation 1.11) is $G(f) e^{2\pi j ft}$ with

$$G(f) = \int_{-\infty}^{\infty} g(t) e^{-2\pi j ft} dt \quad (1.20)$$

and thus

$$g(t) = \int_{-\infty}^{\infty} G(f) e^{2\pi j ft} df. \quad (1.21)$$

$H(f)$ and $G(f)$ are called the ‘transmission function’ of the discrete and the continuous system (or filter), respectively. $H(f)$ converges when the impulse response h_k is of finite length or is going to zero sufficiently fast. In both cases we have a stable system and we confine ourselves to stable systems in this course. $H(f)$ and h_k form a Fourier transform/inverse Fourier transform (FT/IFT) pair, just like $X(f)$ and x_k . However, note that Δ occurs differently in the equations 1.12/1.13 and the equations 1.18/1.19. This is because both $H(f)$ and h_k are dimensionless, whereas the unit of x_k is Volt and the unit of $X(f)$ is Volt/Hz.

Again, the Hermitian property holds, i.e.

$$H(-f) = H^*(f) \quad (1.22)$$

and

$$G(-f) = G^*(f). \quad (1.23)$$

As the system is assumed linear, the output signal (due to input signal x_k in the discrete case) can be written as an integral of the responses to the basis functions multiplied by $X(f)$, i.e.

$$y_k = \int_{-\frac{1}{2\Delta}}^{\frac{1}{2\Delta}} X(f) H(f) e^{2\pi j fk \Delta} df. \quad (1.24)$$

Hence, the Fourier transform of y_k is

$$Y(f) = X(f) H(f) = Y^*(-f). \quad (1.25)$$

In the continuous case the output signal to an input signal $a(t)$ (with Fourier transform $A(f)$) is

$$b(t) = \int_{-\infty}^{\infty} A(f) G(f) e^{2\pi j f t} df. \quad (1.26)$$

Hence, the Fourier transform of $b(t)$ is

$$B(f) = A(f) G(f) = B^*(-f). \quad (1.27)$$

An important property of discrete systems is that $X(f)$, $H(f)$ and $Y(f)$ are periodic functions in frequency f with period $\frac{1}{\Delta}$ Hz, since from equation 1.13 for $X(f)$ it immediately follows

$$X\left(f + \frac{m}{\Delta}\right) = X(f) \quad (1.28)$$

with m an integer number. The same equation is valid for $H(f)$ and $Y(f)$. The periodicity originates from the fact that the complex harmonic $e^{2\pi j f k \Delta}$ has the same values for f and $f + \frac{m}{\Delta}$.

Hence, a discrete system responds in the same way for all these frequencies. We note that continuous systems do not possess this periodicity property, see figure 1.7.

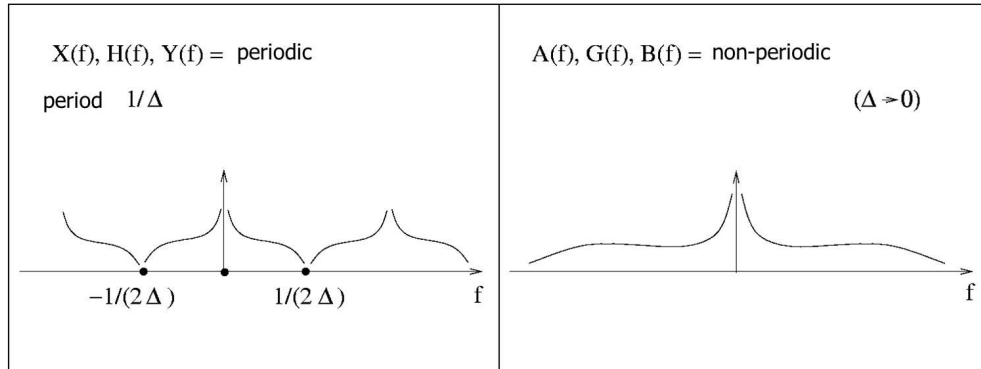


Figure 1.7: Periodicity in discrete systems and non-periodicity in continuous systems.

1.3 The transmission scheme of a system: convolution and multiplication

The main conclusions from the previous section about linear invariant systems are:

- their impulse response h_k and their transmission function $H(f)$ are an FT/IFT pair
- the relation between input and output can be given as

- output signal y_k is a convolution of h_k and the input signal x_k
 - $Y(f)$, the FT of y_k , is the product of $H(f)$ and $X(f)$, the FT of x_k

This is summarized in the schedule of figure 1.8.

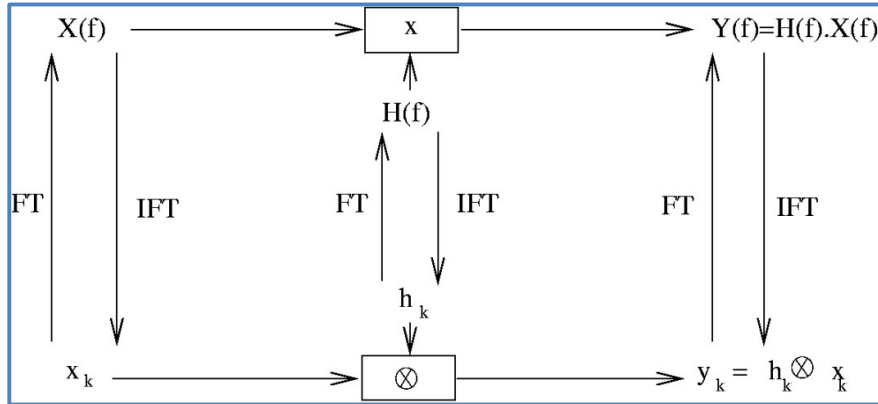


Figure 1.8: Relation between output signal and input signal, both in the time domain and the frequency domain.

We note that the relation between convolution in the time domain and multiplication in the frequency domain is not only valid for transmission of signals through linear systems, but has a more general validity, independent of the physical/electrical context. Suppose we have rows of numbers p_k , q_k and r_k with corresponding Fourier transforms $P(f)$, $Q(f)$ and $R(f)$, i.e.

$$P(f) = \Delta \sum_{k=-\infty}^{\infty} p_k e^{-2\pi j fk\Delta} \quad \text{and} \quad p_k = \int_{-\frac{1}{2\Delta}}^{\frac{1}{2\Delta}} P(f) e^{2\pi j fk\Delta} df. \quad (1.29)$$

(similarly for q_k and r_k)

When

$$r_k = p_k \otimes q_k = \sum_{i=-\infty}^{\infty} p_{k-i} q_i \quad (1.30)$$

then

$$R(f) = \frac{1}{\Delta} P(f) Q(f). \quad (1.31)$$

Note that this deviates slightly from that of figure 1.8 concerning the position of Δ .

Also, the ‘convolution/multiplication’ relation is preserved after swapping time and frequency domain. Suppose that

$$r_k = p_k q_k \quad (1.32)$$

then

$$R(f) = P(f) \otimes_p Q(f) = \int_{-\frac{1}{2\Delta}}^{\frac{1}{2\Delta}} P(f - \eta) Q(\eta) d\eta. \quad (1.33)$$

Here, the symbol \otimes_p refers to convolution of two periodic functions, $P(f)$ and $Q(f)$. This ‘periodic or cyclic convolution’ is illustrated in figure 1.9. More on cyclic convolution can be found in section 4.3.

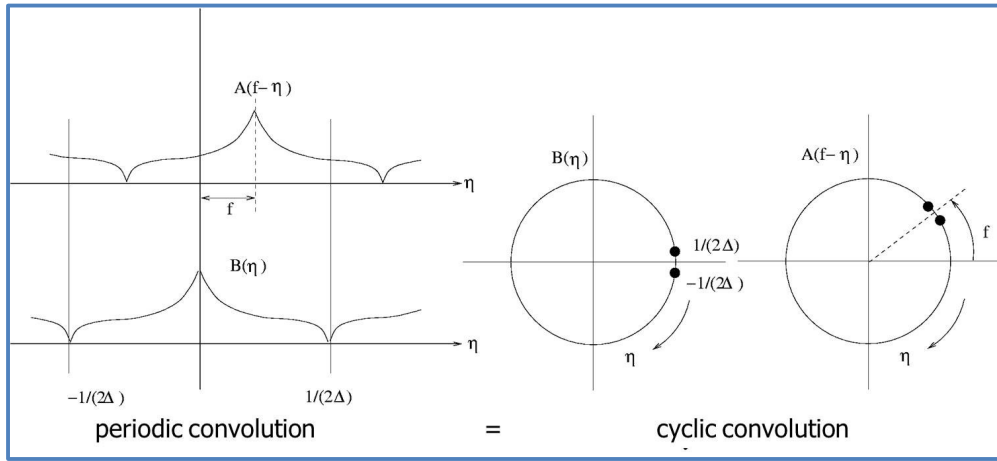


Figure 1.9: Illustration of a periodic or cyclic convolution of two periodic functions A and B .

1.4 Real instead of complex harmonics

When the Fourier transforms $X(f)$, $Y(f)$ and $H(f)$ are decomposed in their amplitude and phase we can rewrite equations 1.12 and 1.24 as

$$x_k = \int_{-\frac{1}{2\Delta}}^{\frac{1}{2\Delta}} |X(f)| e^{j\{2\pi fk\Delta + \arg X(f)\}} df \quad (1.34a)$$

and

$$y_k = \int_{-\frac{1}{2\Delta}}^{\frac{1}{2\Delta}} |H(f)| |X(f)| e^{j\{2\pi fk\Delta + \arg H(f) + \arg X(f)\}} df, \quad (1.34b)$$

respectively. Since $X(f)$, $Y(f)$ and $H(f)$ are Hermitian, we may write

$$x_k = \int_0^{\frac{1}{2\Delta}} 2|X(f)| \cos\{2\pi fk\Delta + \arg X(f)\} df \quad (1.35a)$$

and

$$y_k = \int_0^{\frac{1}{2\Delta}} 2|H(f)||X(f)| \cos\{2\pi fk\Delta + \arg H(f) + \arg X(f)\} df, \quad (1.35b)$$

respectively. Now, these signals are composed of real harmonics with only positive frequencies, i.e. $0 \leq f \leq \frac{1}{2\Delta}$. However, we emphasize that these cosines are not eigenfunctions of the system.

Finally, we note that $|H(f)|$ is the amplification (when > 1) or attenuation (when < 1) of the system at frequency f , whereas $\arg H(f)$ is the phase shift of the system at frequency f . These frequency-dependent amplification/attenuation and phase shift provide the system with filtering properties.

1.5 Filters and their properties

Nowadays, the term ‘filter’ is used for all systems for which $H(f) \neq \text{constant}$, independent of the fact whether the filtering is intentional or unintentional. In the past, the term ‘filter’ was only reserved for electrical circuits with $|H(f)|$ being a desired and thus specific function of f . Figure 1.10 shows $|H(f)|$ for a set of frequently applied filter types.

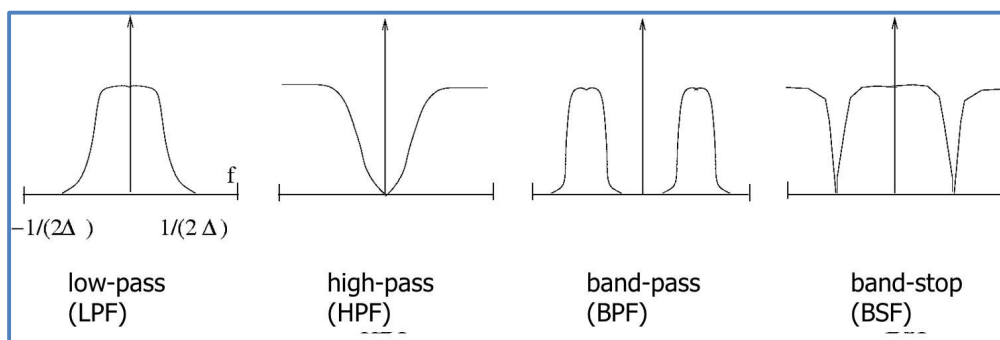


Figure 1.10: Various filters that are frequently applied. LPF = low-pass filter, HPF = high-pass filter, BPF = band-pass filter and BSF = band-stop filter.

Typical examples of naturally occurring filtering effects are:

- The human ear is only sensitive in the frequency band 20 Hz – 20 kHz (BPF);
- The absorption of sound in the atmosphere and in water increases significantly with increasing frequency (LPF);
- A piece of red glass only transmits visible light in a narrow frequency band (BPF).

Examples of unintentional filtering in manmade technical systems are:

- Optical imaging systems produce blurred pictures;
- Frequency-dependent attenuation in electric cables;
- A measured spectrum is always a somewhat blurred version of reality.

Examples of intentional filtering are:

- Separation of the components of a signal that are in different frequency bands;
- Removing the high frequency noise from a low-frequency signal with an LPF filter, see figure 1.11;
- A BSF for suppression of a 50 Hz mains voltage disturbance, see figure 1.12.

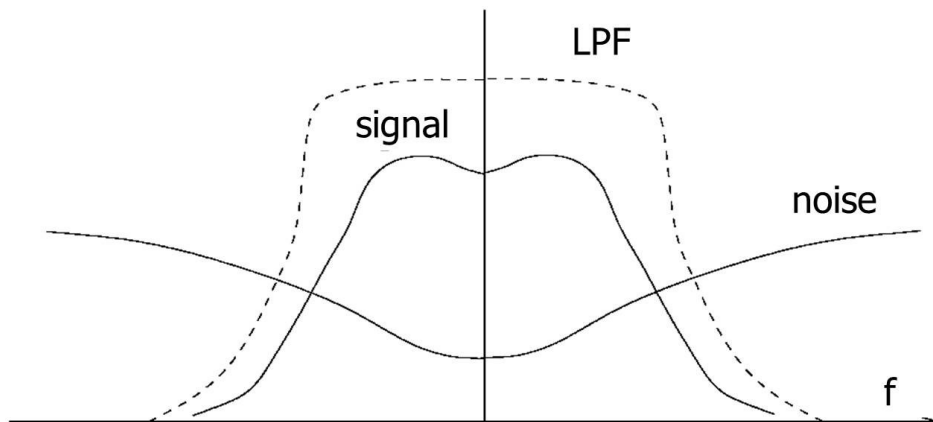


Figure 1.11: Filtering the high frequency noise from a low-frequency signal with an LPF filter.

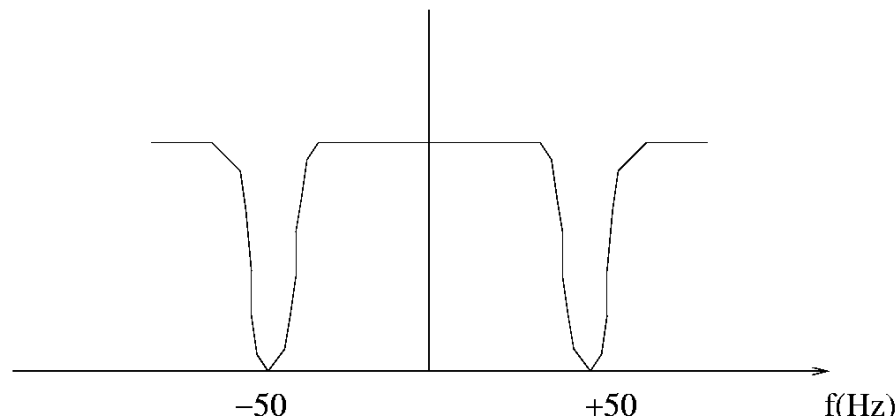


Figure 1.12: Example of a band-stop filter for suppression of a 50 Hz mains voltage disturbance.

Examples of filters designed to change the nature of a signal:

- Filters to smooth a signal by removing the fine structure in the signal thereby obtaining a local average (LPF, see exercise 4);
- HPF for contrast enhancement to strengthen the fine structure in a signal (opposite of previous example);
- Filters for interpolation and decimation of sampled signals.

1.6 Important continuous FT/IFT pairs

In table below the most important continuous FT/IFT pairs are listed.

$a(t)$	$A(f) = \int_{-\infty}^{\infty} a(t) e^{-2\pi j f t} dt$
$a(t - \tau)$	$e^{-2\pi j f \tau} A(f)$
$\frac{da(t)}{dt}$	$2\pi j f A(f)$
1	$\delta(f)$
$\delta(t)$	1
$\delta(t - \tau)$	$e^{-2\pi j f \tau}$
$e^{2\pi j f_1 t}$	$\delta(f - f_1)$
$\cos(2\pi f_1 t)$	$\frac{1}{2} \delta(f + f_1) + \frac{1}{2} \delta(f - f_1)$
$\sin(2\pi f_1 t)$	$\frac{1}{2} j \delta(f + f_1) - \frac{1}{2} j \delta(f - f_1)$
$1 \text{ for } t \leq \tau$ $0 \text{ for } t > \tau$	$\frac{\sin(2\pi f \tau)}{\pi f}$
$\sum_{n=-\infty}^{\infty} \delta(t - n\tau)$	$\frac{1}{\tau} \sum_{n=-\infty}^{\infty} \delta\left(f - \frac{n}{\tau}\right)$
$\sqrt{\frac{\alpha}{\pi}} e^{-\alpha t^2}$	$\frac{\pi^2 f^2}{e^{-\alpha}}$
$\alpha e^{-\alpha t} \text{ for } t \geq 0$ $0 \text{ for } t < 0$	$\frac{1}{1 + 2\pi j \left(\frac{f}{\alpha}\right)}$
$\frac{\alpha}{2} e^{-\alpha t }$	$\frac{1}{1 + 4\pi^2 \left(\frac{f}{\alpha}\right)^2}$
$+1 \text{ for } t > 0$ $-1 \text{ for } t < 0$	$\frac{1}{\pi j f}$
$1 \text{ for } t > 0$ $0 \text{ for } t < 0$	$\frac{1}{2} \delta(f) + \frac{1}{2\pi j f}$

1.7 Exercises

Remark: use Kirchoff's laws to determine the transmission functions of the analog (i.e. continuous) filters in these exercises.

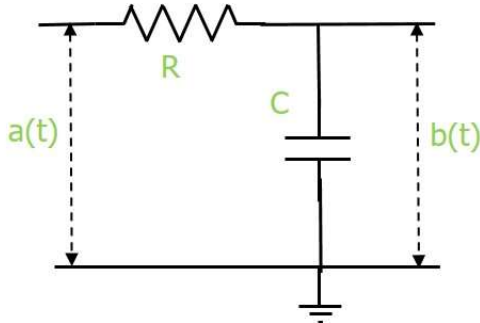
Question 1

Consider the trivial filter for which $h_k = \delta_k = \begin{cases} 1 & k=0 \\ 0 & k \neq 0 \end{cases}$.

Calculate $H(f)$ and explain its behaviour.

Question 2

Consider the following simple continuous filter:



(a) Show that the transmission function of this filter is $G(f) = \frac{1}{1 + 2\pi j fRC}$.

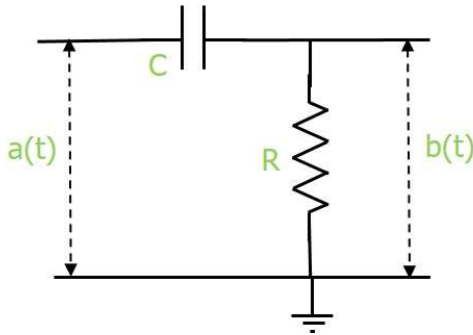
(b) Make a sketch of $|G(f)|$ and $\arg G(f)$ for $-\infty < f < \infty$.

(c) What type of filter is this? LPF, HPF, BPF or BSF?

(d) Show that the impulse response of this filter is $g(t) = \begin{cases} \frac{1}{RC} e^{-\frac{t}{RC}} & \text{for } t \geq 0 \\ 0 & \text{for } t < 0 \end{cases}$

Question 3

Consider the following simple continuous filter:



(a) Show that the transmission function of this filter is $G(f) = \frac{2\pi j fRC}{1 + 2\pi j fRC}$.

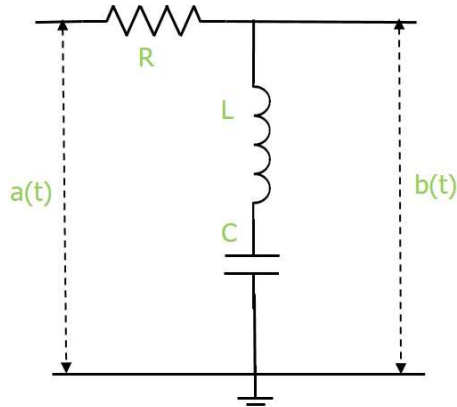
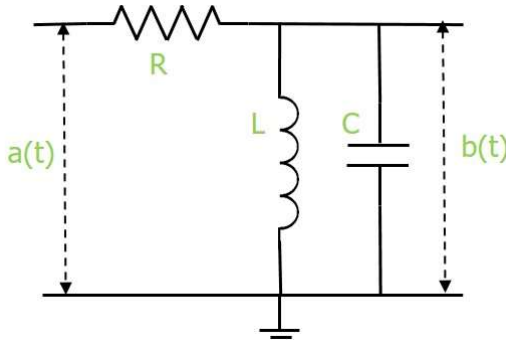
(b) Make a sketch of $|G(f)|$ and $\arg G(f)$ for $-\infty < f < \infty$.

(c) What type of filter is this? LPF, HPF, BPF or BSF?

(d) Show that the impulse response of this filter is $g(t) = \begin{cases} \delta(t) - \frac{1}{RC} e^{-\frac{t}{RC}} & \text{for } t \geq 0 \\ 0 & \text{for } t < 0 \end{cases}$

Question 4

Consider the following continuous filters:



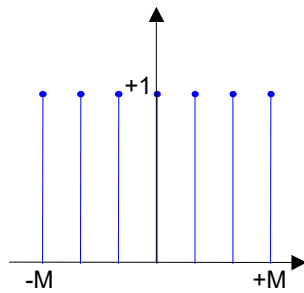
(a) Show that the transmission function of these filters are $G(f) = \frac{1}{1 + jR\left(\omega C - \frac{1}{\omega L}\right)}$ and

$$G(f) = \frac{j\left(\omega L - \frac{1}{\omega C}\right)}{R + j\left(\omega L - \frac{1}{\omega C}\right)}, \text{ respectively.}$$

- (b) Make a sketch of $|G(f)|$ and $\arg G(f)$ for $0 < f < \infty$, for both filters.
(c) What type of filter are these? LPF, HPF, BPF or BSF?

Question 5

Consider the discrete filter with non-causal impulse response:



The output of this filter is a ‘moving average’ of $2M + 1$ consecutive input numbers.

- (a) Show that $H(f) = \frac{\sin(\pi f(2M+1)\Delta)}{\sin(\pi f\Delta)}$.
(b) Make a sketch of $H(f)$. Is $H(f)$ periodic?
(c) What is $H(0)$, the DC amplification?
(d) Why are there frequencies for which $H(f) = 0$?
(e) What type of filter is this? LPF, HPF, BPF or BSF?

Question 6

Given is $x_k = [1 \ 0 \ -1 \ 2 \ 3 \ -1]$ and $h_k = [2 \ 3 \ 1]$.

Show that $y_k = [2 \ 3 \ -1 \ 1 \ 11 \ 9 \ 0 \ -1]$.

Chapter 2 Sampling – Shannon Nyquist Theorem

2.1 Introduction

For the purpose of digitally processing a continuous signal $x(t)$, first the signal needs to be sampled. This means that the signal is quantized on an amplitude grid with spacing q and discretized in time with spacing Δ . This is illustrated in figure 2.1.

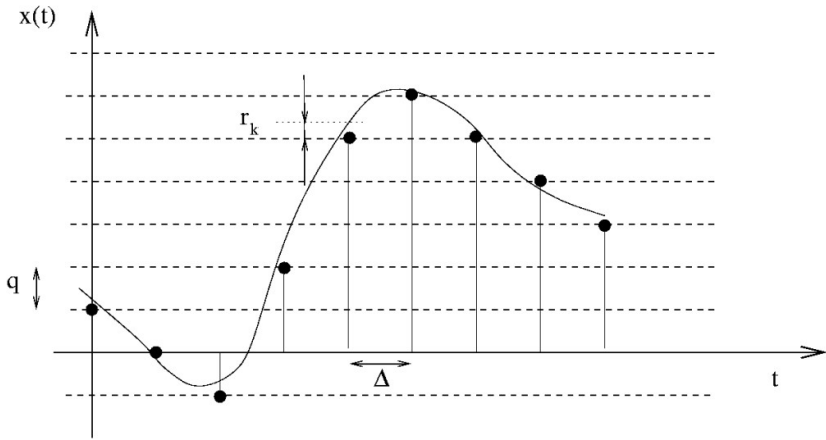


Figure 2.1: Discretization of a continuous signal in time and amplitude.

The samples x_k of $x(t)$ can be written as

$$x_k = x(k\Delta) + r_k \quad (2.1)$$

with r_k the round off errors or residuals (also indicated in figure 2.1). The ‘sample frequency’, i.e. the number of samples per second, is given by

$$F = \frac{1}{\Delta}. \quad (2.2)$$

This sampling gives rise to two important questions:

- How small should we make q so that the added quantization noise r_k is negligible?
- What value of Δ should we choose so that no information is lost due to the discretization in time (assuming r_k to be negligible)?

The current Analog-to-Digital Converters (ADC) with a large number of bits (>12) are cheap and hence the first question is not a serious issue anymore. However, depending on the situation, an ADC with a relatively low number of bits can be selected, while quantization noise is still negligible. Quantization noise is further discussed in section 2.2.

Assuming quantization noise r_k to be negligible, we may write $x_k = x(k\Delta)$ and we continue with the following two accurately formulated questions:

- (1) How big should we choose F so that from the samples x_k the original continuous signal $x(t)$ can be reconstructed without errors?
- (2) How big should we choose F so that a certain desired continuous operation $\int a(t)x(t) dt$ can be replaced by a corresponding discrete operation $\Delta \sum_k a_k x_k$?

Note: Basically, if we can answer the second question with a yes, 'digital signal processing' is allowed.

The answer to both questions is that, when the bandwidth of the continuous signal is B (see figure 2.2), then the requirement on the value of the sample frequency is

$$F \geq F_{\min} = 2B \quad (2.3)$$

with F_{\min} the so-called 'Nyquist rate'. See further section 2.3.

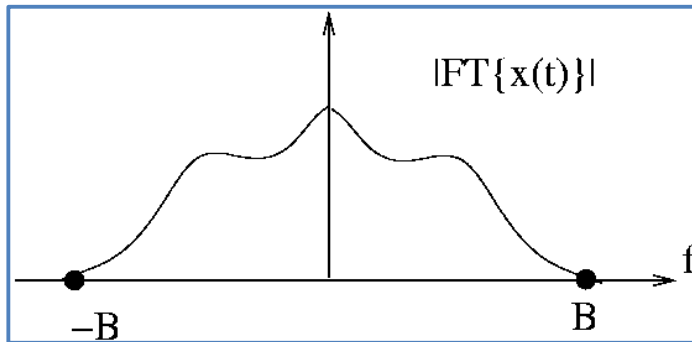


Figure 2.2: A continuous signal with bandwidth B in the frequency domain.

2.2 Quantization noise

For not too large q , all residual values r_k are equally probable within the interval $\left(-\frac{q}{2}, \frac{q}{2}\right)$. Hence,

the random variable r_k has a uniform probability density function (figure 2.3), i.e.

$$p(r_k) = \begin{cases} \frac{1}{q} & \text{for } -\frac{q}{2} < r_k < \frac{q}{2} \\ 0 & \text{elsewhere} \end{cases} \quad (2.4)$$

with expectation value $\bar{r}_k = 0$, variance $\bar{r}_k^2 = \int_{-q/2}^{q/2} r_k^2 p(r_k) dr = \frac{q^2}{12}$ and standard deviation (effective value) $\sqrt{\bar{r}_k^2} = \frac{q}{\sqrt{12}}$.

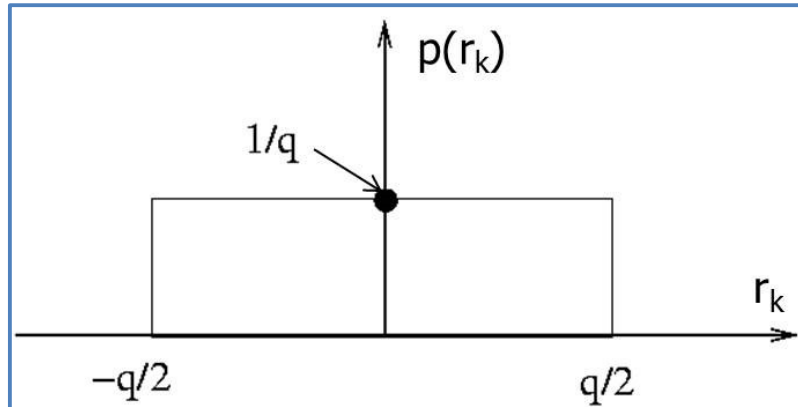


Figure 2.3: The uniform probability density function of the random variable r_k .

Hence, quantization noise decreases linearly with decreasing q , however this does not give an answer to the question when quantization noise can be considered negligible. This depends on the further processing of the sampled signal and should be studied for each situation separately. A general and safe advice is to calculate the final signal-to-noise ratio as a function of q for each specific situation and then decide. For instance, suppose that the continuous signal $x(t)$ exhibits a natural noise component with effective value σ , then q can be chosen such that σ is a few times bigger than the quantization noise (i.e. $\frac{q}{\sqrt{12}}$). Then, the natural noise is still dominating the quantization noise.

Note: As mentioned in the previous section, ADC's with a large number of bits (i.e. small q) are cheap and hence the choice of q is less of a problem nowadays.

For the remainder of this chapter we assume the quantization noise to be negligible, i.e. $x_k = x(k\Delta)$.

2.3 Sampling theorem

2.3.1 Sampling and repeating

We consider a continuous signal $x(t)$ with corresponding samples x_k and Fourier transforms $X_c(f)$ and $X(f)$, respectively. The relation between $x(t)$ and x_k is $x_k = x(k\Delta)$ (no quantisation noise). Hence, for the continuous signal $x(t)$ we have

$$x(t) = \int_{-\infty}^{\infty} X_c(f) e^{2\pi j f t} df \quad \text{and} \quad X_c(f) = \int_{-\infty}^{\infty} x(t) e^{-2\pi j f t} dt \quad (2.5)$$

and for the discrete signal we have

$$x_k = \int_{-\frac{1}{2\Delta}}^{\frac{1}{2\Delta}} X(f) e^{2\pi j fk\Delta} df \quad \text{and} \quad X(f) = \Delta \sum_{k=-\infty}^{\infty} x_k e^{-2\pi j fk\Delta}. \quad (2.6)$$

Below we proof that the relation between $X_c(f)$ and $X(f)$ is

$$X(f) = \sum_{m=-\infty}^{\infty} X_c(f - mF) \quad \text{with} \quad F = \frac{1}{\Delta}. \quad (2.7)$$

Hence, sampling $x(t)$ with frequency F results in a repetition of $X_c(f)$ with ‘repetition distance’ F . Indeed, $X(f)$ becomes a periodic function (as already expected from equation 1.28). This is illustrated in figure 2.4.

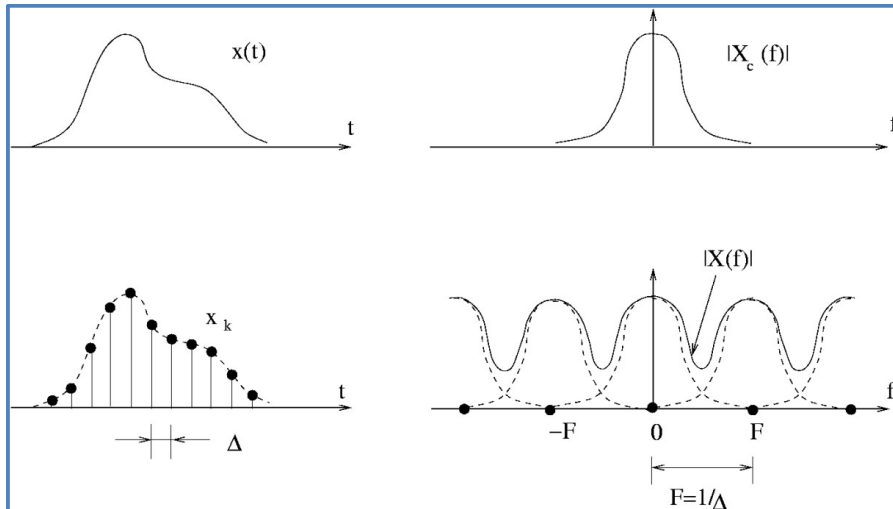


Figure 2.4: Sampling of a signal in the time domain results in repetition in the frequency domain.

The proof of equation 2.7 goes as follows. We can write for the samples

$$x_k = x(k\Delta) = \int_{-\infty}^{\infty} X_c(f) e^{2\pi j f k \Delta} df = \sum_{m=-\infty}^{\infty} \int_{\frac{1}{2\Delta} - \frac{m}{\Delta}}^{\frac{1}{2\Delta} + \frac{m}{\Delta}} X_c(f) e^{2\pi j f k \Delta} df.$$

By applying the transformation $f' = f - \frac{m}{\Delta}$ and swapping the summation and the integral this can be rewritten as

$$x_k = \int_{-\frac{1}{2\Delta}}^{\frac{1}{2\Delta}} \sum_{m=-\infty}^{\infty} X_c\left(f' - \frac{m}{\Delta}\right) e^{2\pi j \left(f' - \frac{m}{\Delta}\right) k \Delta} df' = \int_{-\frac{1}{2\Delta}}^{\frac{1}{2\Delta}} \sum_{m=-\infty}^{\infty} X_c\left(f - \frac{m}{\Delta}\right) e^{2\pi j f k \Delta} df.$$

where we have used $e^{2\pi j m k} = 1$ (as m and k are integers).

Comparing this with $x_k = \int_{-\frac{1}{2\Delta}}^{\frac{1}{2\Delta}} X(f) e^{2\pi j f k \Delta} df$ (equation 2.6) yields $\sum_{m=-\infty}^{\infty} X_c\left(f - \frac{m}{\Delta}\right) = X(f)$.

2.3.2 The Shannon-Nyquist sampling theorem and signal reconstruction

Let the continuous signal $x(t)$ have a bandwidth B , i.e.

$$X_c(f) = 0 \quad \text{for } |f| > B. \quad (2.8)$$

We choose $F \geq 2B$. Then the repeating parts in $X(f)$ do not overlap, see figure 2.5. Hence,

$$X_c(f) = X(f) \quad \text{for } |f| < F - B. \quad (2.9)$$

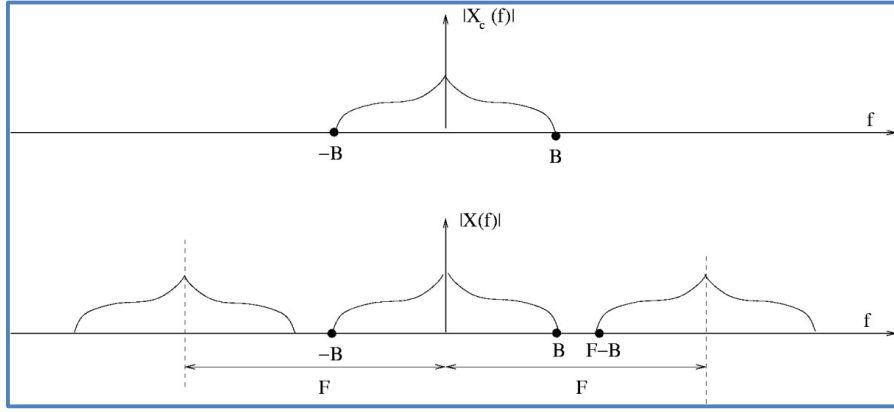


Figure 2.5: The situation $F > 2B$, i.e. the repeating parts in the Fourier transform $X(f)$ of the sampled signal do not overlap.

In this situation $X_c(f)$ can be recovered from $X(f)$ by selecting the central part around $f = 0$. Consequently, the continuous signal $x(t)$ can also be recovered from the samples x_k . Hence, we conclude that the original continuous signal $x(t)$ can be recovered from the samples x_k if $F \geq 2B$. The reconstruction goes as follows:

We select the central part of $X(f) = \Delta \sum_{k=-\infty}^{\infty} x_k e^{-2\pi j fk\Delta}$ (equation 2.6) by multiplying it with the function $G_c(f)$ given by

$$G_c(f) = \begin{cases} 1 & \text{for } |f| < B \\ 0 & \text{for } |f| > F - B \end{cases} \quad (2.10)$$

$G_c(f)$ can be regarded as the transmission function of a continuous filter called ‘reconstruction filter’. The corresponding impulse response is denoted $g(t)$. Hence, we may write

$$X_c(f) = G_c(f)X(f) = \Delta \sum_{k=-\infty}^{\infty} x_k G_c(f) e^{-2\pi j fk\Delta}$$

Applying the IFT of this yields (see table FT/IFT pairs of chapter 1)

$$x(t) = \Delta \sum_{k=-\infty}^{\infty} x_k g(t - k\Delta). \quad (2.11)$$

This processing steps for reconstruction are illustrated in figure 2.6.

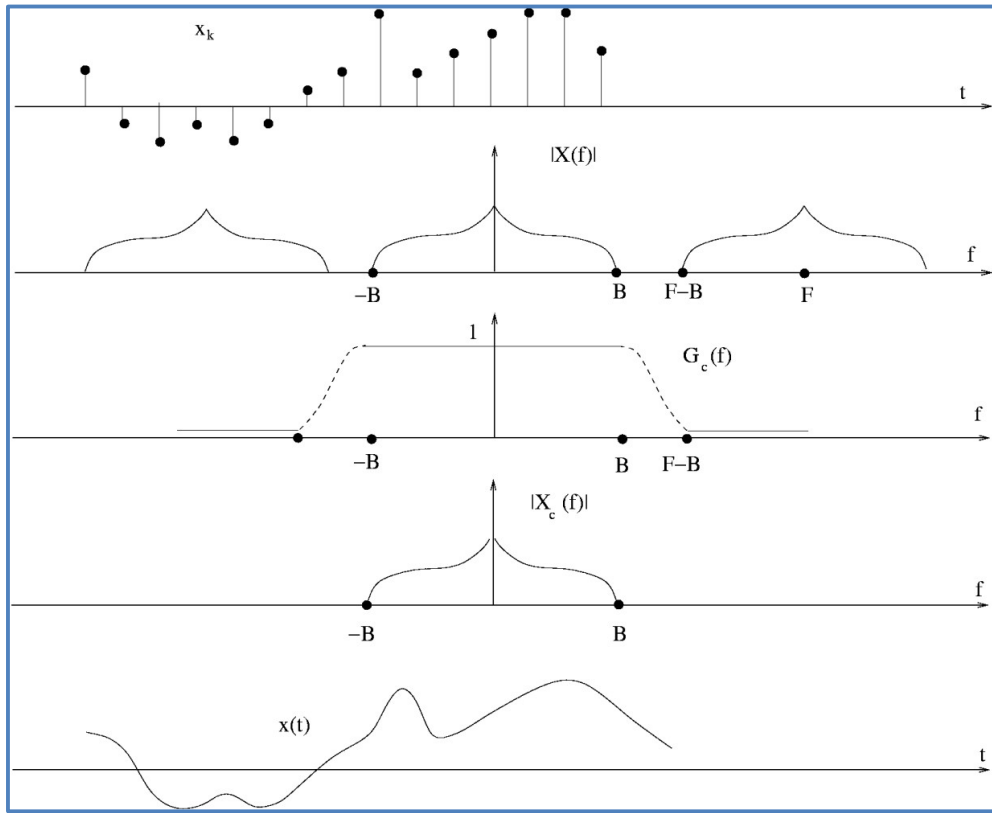


Figure 2.6: Reconstructing the continuous signal from the samples.

The reconstructed signal is thus a summation of shifted impulse responses of the reconstruction filter, each with strength Δx_k . The responses $g(t-k\Delta)$ are long compared to the shifts Δ , such that they strongly overlap and hence a continuous signal is generated. A practical implementation of the reconstruction is shown in figure 2.7.

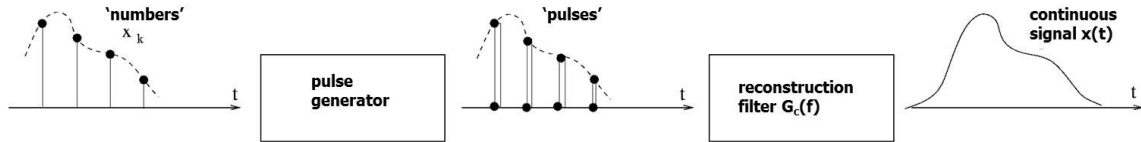


Figure 2.7: A practical implementation of the reconstruction of the continuous signal from the samples.

In practice a certain amount of oversampling is needed, i.e. $F > 2B$, so that between the repetitions in $X(f)$ empty spaces exist with a width in frequency of $F - 2B$, see figure 2.6. In these spaces the transition band of the low pass filter $G_c(f)$ can be placed (as filters with an infinitely fast roll-off cannot be made in practice). In fact, less stringent requirements need to be imposed on the filter

$G_c(f)$ when an increasing amount of oversampling is applied, as then the empty spaces in $X(f)$ become wider.

In theoretical considerations there are no objections to a filter with infinitely fast roll-off (see figure 2.8) and the minimum condition $F = 2B$.

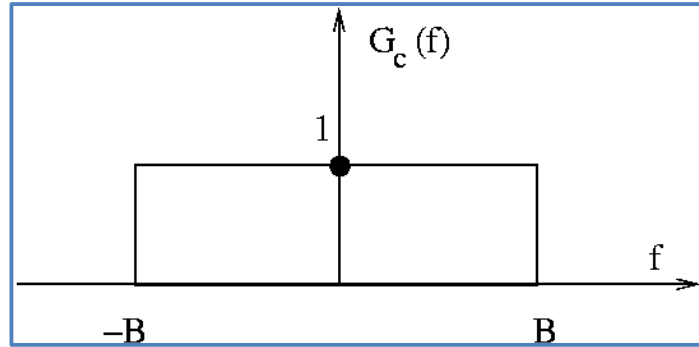


Figure 2.8: The ideal reconstruction filter.

The impulse response of this ideal reconstruction filter is $g(t) = \frac{\sin(2\pi Bt)}{\pi t}$ (see list of FT/IFT pairs in chapter 1). Hence, equation 2.11 becomes

$$x(t) = \sum_k x_k \frac{\sin\{2\pi B(t - k\Delta)\}}{2\pi B(t - k\Delta)} \quad (2.12)$$

where use has been made of $\Delta = \frac{1}{F} = \frac{1}{2B}$. Theoretically, the reconstruction can thus be considered as an interpolation of the samples with a function of the type $\frac{\sin t}{t}$.

Note: The requirement 2.10 means that in the passband of the reconstruction filter we must have

$$|G_c(f)| = 1 \quad \text{and} \quad \arg G_c(f) = 0. \quad (2.13)$$

However, filters without phase shifts cannot be made in practice. Still, to a very good approximation filters with a linear phase shift can be made, i.e.

$$\arg G_c(f) = -2\pi f \tau_0 \quad (2.14)$$

so that the reconstructed signal only shows a time delay of τ_0 (see again list of FT/IFT pairs in chapter 1).

Further note that the requirement 2.10 does not specify the behaviour of the filter in the transition band.

2.4 Alias

2.4.1 Alias errors

A too small sample frequency, i.e. $F < 2B$, generates spectral overlap in $X(f)$, see figure 2.9. In that case reconstruction leads to a signal that differs from the original signal $x(t)$, even if we use the ideal reconstruction filter $G_c(f)$ as shown in figure 2.8. Instead of the desired $X_c(f)$ and $x(t)$ we obtain

$$Y_c(f) = X_c(f) + A_c(f) \quad \text{and hence} \quad y(t) = x(t) + a(t) \quad (2.15)$$

i.e. an extra component $A_c(f)$ (or $a(t)$ in the time domain) appears. This is called the ‘alias component’, which cannot be removed anymore. Hence, the alias effect needs to be avoided (see section 2.4.2).

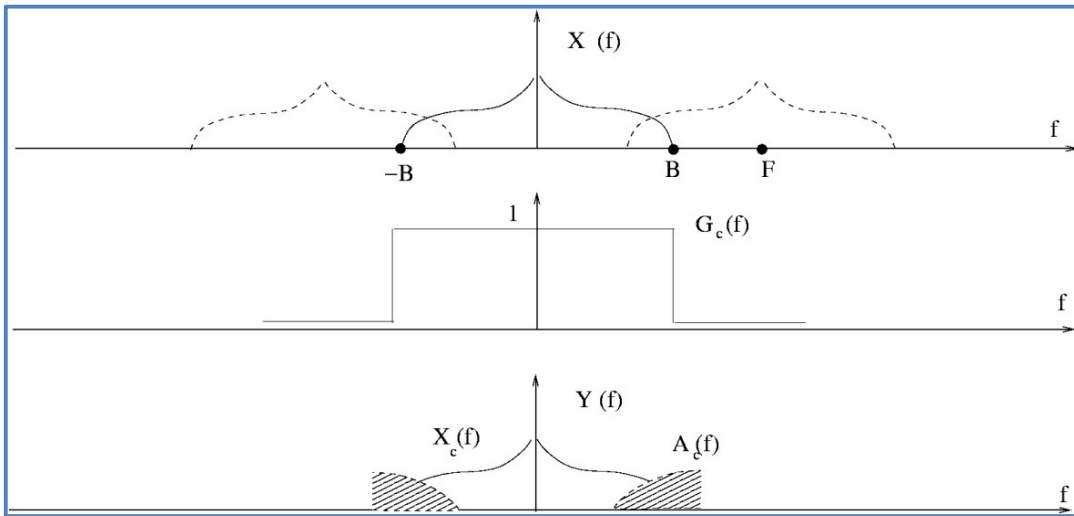


Figure 2.9: Illustration of the alias effect in the frequency domain.

The effect of alias is shown in the examples below. A white noise signal is low-pass filtered, resulting in a continuous bandlimited signal $x_c(t)$ with bandwidth $B \approx 350$ Hz, see figure 2.10.

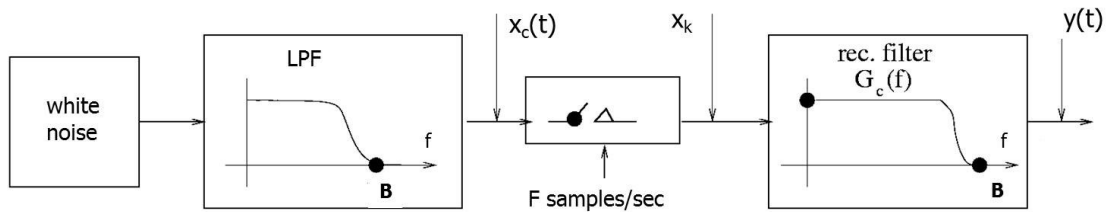


Figure 2.10: Processing chain for simulating alias for various values of the sample frequency F (given a fixed bandwidth B of the signal).

Subsequently, to show the effect of alias, $x_c(t)$ is sampled with F equal to 700 Hz, 600 Hz, 400 Hz and 50 Hz. Finally, reconstruction is applied by filtering the samples x_k with the ideal reconstruction filter shown in figure 2.8 (with $B = 350$ Hz), i.e. using equation 2.12. The original signal $x_c(t)$, the samples x_k and the reconstructed signal $y(t)$ are shown in figure 2.11 for the four sample frequencies. Note that the reconstructed signal is also plotted on top of the original signal for direct comparison. The minimum sample frequency to avoid alias is $F = 2B = 700$ Hz, see figure 2.11a where there is indeed no difference between $x_c(t)$ and $y(t)$. It is clearly observed that for lower F (600 Hz, 400 Hz, see figure 2.11b and c) the reconstructed signal deviates from the original signal, hence undesired alias is clearly visible. At very low F (50 Hz, see figure 2.11d) the non-overlapping individual impulse responses of the reconstruction filter become visible at the sample positions.

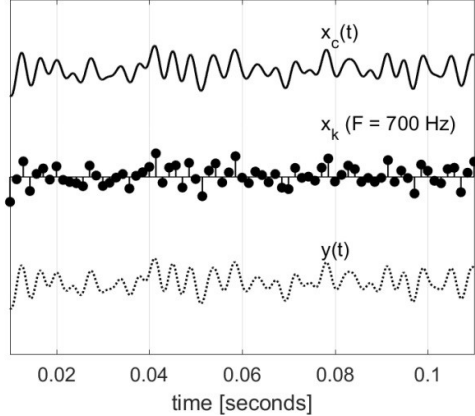


Figure 2.11a: Original signal $x_c(t)$, sampled signal x_k at $F = 700$ Hz and reconstructed signal $y(t)$.

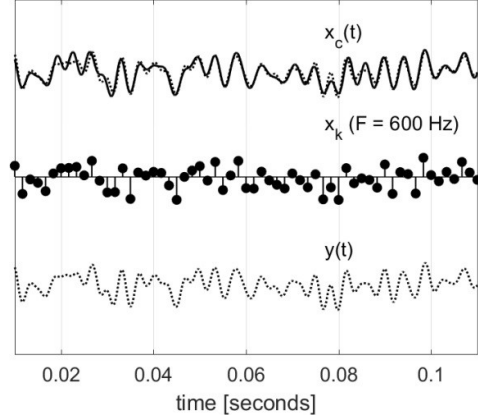


Figure 2.11b: Idem, but now $F = 600$ Hz.

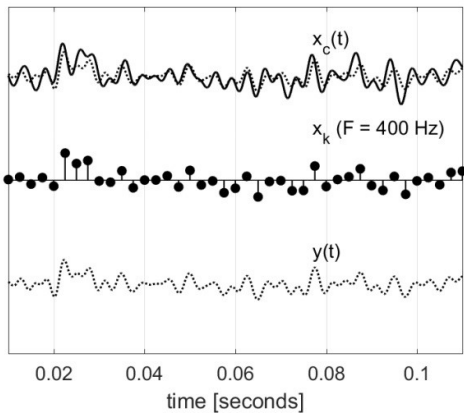


Figure 2.11c Idem, but now $F = 400$ Hz.

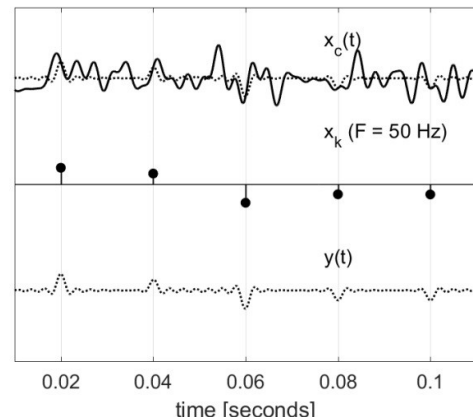


Figure 2.11d: Idem, but now $F = 50$ Hz.

2.4.2 Anti-alias filters

The sampling theorem requires $F \geq 2B$. However, perfectly bandlimited signals, with sharply defined B , hardly exist, as in practice $X_c(f)$ gradually approaches zero. Consequently, there is always alias, even for F large compared to $2B$. This alias is avoided in practice as follows.

Suppose a signal is sampled at F Hz. Then an analog (i.e. continuous) ‘anti-alias filter’ (AAF) with cut-off frequency $\frac{F}{2}$ is applied prior to sampling, see figure 2.12. Hence, this filter eliminates all frequencies $f > \frac{F}{2}$, but these frequencies would have been destroyed anyhow by alias without an AAF. Now, at least we avoid alias for $f < \frac{F}{2}$.

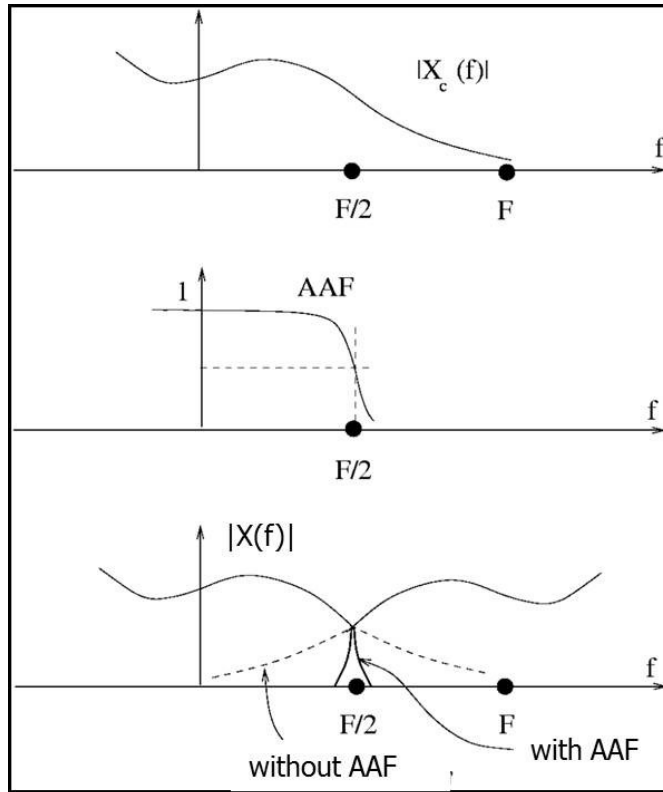


Figure 2.12: The effect of applying an anti-alias filter (AAF), illustrated in the frequency domain.

The AAF should have a steep roll off at $f = \frac{F}{2}$. However, this would lead to a complicated analog

AAF filter. This problem can be solved by using both an analog and digital filter (see chapter 3) for the AAF, see figure 2.13. The analog AAF is simple, hence has a relatively slow roll off. However, the signal is then sampled at such a high sample frequency, e.g. $4F$, that the transition band (i.e. the roll off part) of the analog AAF can easily be positioned in the empty spaces between the repetitions in $X(f)$. Subsequently, a digital AAF is employed with a steep roll off at $f = \frac{F}{2}$ (digital filters with

very steep roll off can easily be made, see chapter 3). Finally, the sample frequency is reduced to F by decimation of the data, i.e. discarding 3 out of each 4 consecutive samples in this example.

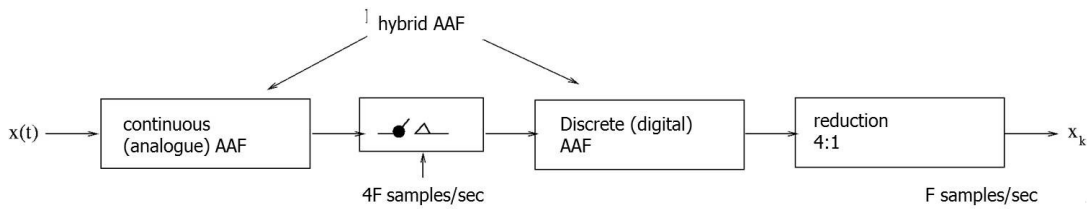


Figure 2.13: Sampling a signal with the 'hybrid' method, i.e. by using both an analog and digital AAF.

2.4.3 Alias errors at signal edges

Generally, in signal processing always time-limited signals are considered, i.e. the continuous signal $x(t)$ with bandwidth B is truncated between the times t_1 and t_2 , such that a new signal $x'(t)$ is generated, see figure 2.14.

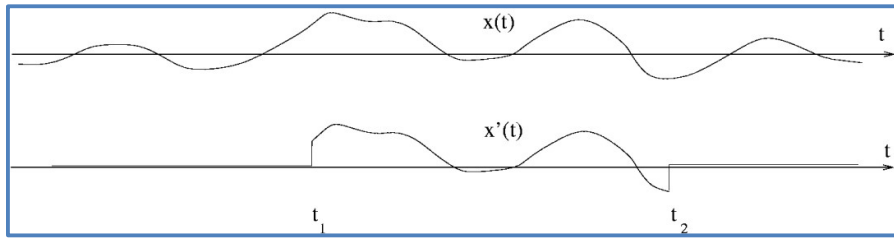


Figure 2.14: Truncation of a continuous signal $x(t)$ at times t_1 and t_2 .

The sampling theorem is not exactly applicable to the truncated signal $x'(t)$, since the FT of $x'(t)$ is non-zero at frequencies higher than B . In fact, the FT of $x'(t)$ contains non-zero power at infinitely high frequencies due to the discontinuities at t_1 and t_2 . Consequently, alias occurs always for finite-length signals and reconstruction errors arise at the signal edges at t_1 and t_2 . The reconstruction is perfect again after a distance of about 5Δ away from t_1 and t_2 , i.e. the alias component is thus manifesting at the signal edges. This is illustrated in figure 2.15.

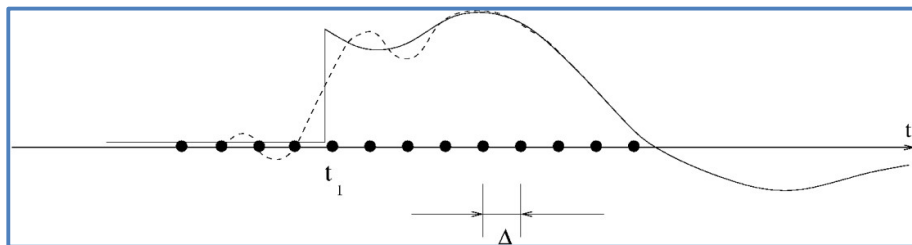


Figure 2.15: Reconstruction errors at the signal edge at time t_1 .

2.5 Continuous and discrete operations

We return to question (2) of section 2.1 about the conditions that allow a continuous operation to be replaced by the corresponding discrete operation, i.e.

$$\int_{-\infty}^{\infty} a(t)x(t)dt \rightarrow \Delta \sum_{k=-\infty}^{\infty} a_k x_k . \quad (2.16)$$

We will shortly see that 2.16 is valid if

$$F = \frac{1}{\Delta} \geq B_1 + B_2 \quad (2.17)$$

with B_1 and B_2 the bandwidth of $a(t)$ and $x(t)$, respectively.

Note: $\int_{-\infty}^{\infty} a(t)x(t)dt$ represents a general linear operation on $x(t)$ (superposition principle) and with $a(t) = h(\theta - t)$ we have the transfer relation of an invariant linear filter, i.e. $z(\theta) = \int h(\theta - t)x(t)dt$. If equation 2.16 is true we may replace this by $z_k = \Delta \sum_i h_{k-i} x_i$.

The proof of 2.16 and 2.17 goes as follows. According to equation 2.5 we can write

$$\int_{-\infty}^{\infty} a(t)x(t)dt = \int_{-\infty}^{\infty} A_c(-f)X_c(f)df \quad (2.18a)$$

whereas from equation 2.6 it follows

$$\Delta \sum_{k=-\infty}^{\infty} a_k x_k = \int_{-\frac{1}{2\Delta}}^{\frac{1}{2\Delta}} A(-f)X(f)df . \quad (2.18b)$$

(Actually, equation 2.18a and 2.18b are generalized forms of Parseval's equation for the continuous and discrete situation, respectively, see also chapter 7).

From figure 2.16 it can be seen that the right-hand sides of equations 2.18a and 2.18b are equal if $F \geq B_1 + B_2$

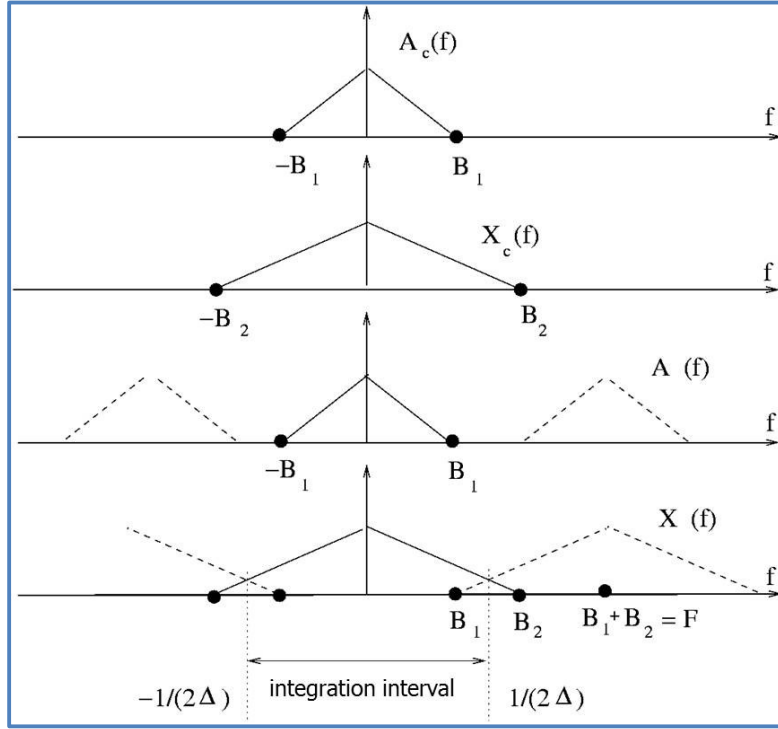


Figure 2.16: Illustration of the fact that a continuous operation on signal $x(t)$ can be replaced by the corresponding discrete operation, see equation 2.16, if the sample frequency $F \geq B_1 + B_2$ (with B_1 and B_2 the bandwidth of $a(t)$ and $x(t)$, respectively).

Note: In practice the integration in 2.16 is over the time interval (t_1, t_2) instead of $(-\infty, \infty)$ and then the discrete operation is an approximation of the continuous one, i.e.

$$\int_{t_1}^{t_2} a(t)x(t) dt \rightarrow \approx \Delta \sum_{k=\frac{t_1}{\Delta}}^{\frac{t_2}{\Delta}} a_k x_k . \quad (2.19)$$

This originates from alias errors at the signal edges t_1 and t_2 , see previous paragraph. For sufficiently long signals the approximation is accurate enough.

2.6 Narrow band signals

In this section we consider narrowband signals defined as a continuous signal with a relatively narrow bandwidth B centred at a frequency f_0 (with $f_0 \gg B$), see figure 2.17.

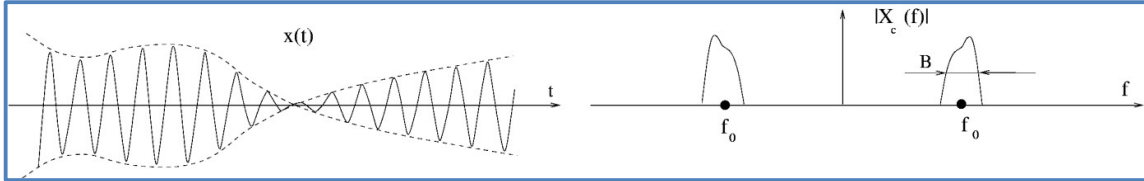


Figure 2.17: A narrow band signal in the time domain (left) and frequency domain (right).

Examples of such narrowband signals are telecommunication signals and radar and sonar signals.

According to 2.3, $F \geq 2B$, the minimum required sample frequency is $F = 2\left(f_0 + \frac{B}{2}\right)$. However,

intuitively we might expect that $F = 2B$ suffices. This much lower sample frequency is indeed allowed (i.e. F somewhat higher than $2B$), if F is chosen such that repetitions in $|X(f)|$ at negative frequencies do not overlap with those at positive frequencies, see figure 2.19. Then reconstruction with a BPF is possible.

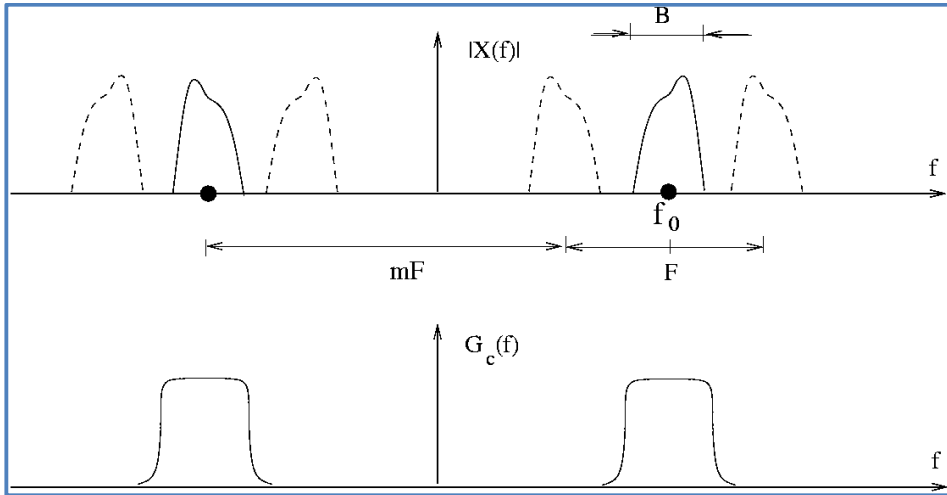


Figure 2.18: A narrow band signal (with bandwidth B centred at a frequency f_0) in the frequency domain (upper figure). The repeating parts in the Fourier transform $X(f)$ of the sampled signal do not overlap, hence reconstruction with the filter shown in the lower part of the figure is possible.

2.7 Exercise

A speech signal with $B = 10$ kHz is sampled at F Hz. For reconstruction a LPF with a fixed transition band of 1 kHz is available. The cut-off frequency f_c of this filter is however flexible, see figure 2.19 below.

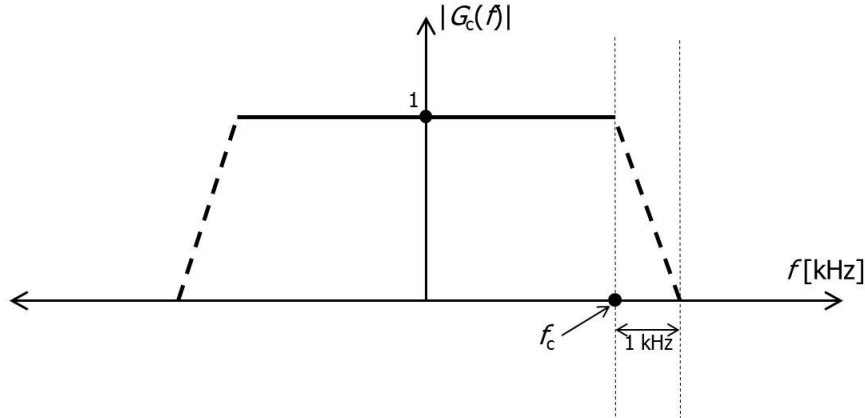


Figure 2.19: Characteristics of the reconstruction filter.

- (a) What value of F and f_c would you choose?
- (b) Suppose F is fixed at 15 kHz (due to a hardware constraint). An analog AAF filter of the type of figure 2.19 is available. What value for the cut-off frequency f_c of the AAF would you choose?

Chapter 3 Filtering in the time domain - recursive filters

3.1 Introduction

In this chapter we discuss digital filters that operate in the time domain. In general, the sample y_k at the output of the filter is a linear combination of the N input samples x_k, \dots, x_{k-N} and the P previous output samples y_{k-1}, \dots, y_{k-P} . Hence, such a ‘recursive filter’ is determined by the linear recursion equation

$$y_k = \sum_{i=0}^N b_i x_{k-i} + \sum_{i=1}^P a_i y_{k-i} \quad (3.1a)$$

or

$$\begin{aligned} y_k = & b_0 x_k + b_1 x_{k-1} + \dots + b_N x_{k-N} + \\ & + a_1 y_{k-1} + a_2 y_{k-2} + \dots + a_P y_{k-P} \end{aligned} \quad (3.1b)$$

Note: The Matlab implementation of the recursion equation is somewhat different:

$$\begin{aligned} y_k = & b_1 x_k + b_2 x_{k-1} + \dots + b_{N+1} x_{k-N} \\ & - a_2 y_{k-1} - a_3 y_{k-2} - \dots - a_{P+1} y_{k-P} \end{aligned} \quad (3.1c)$$

with $a_1 = 1$.

The recursion equation is schematically depicted in figure 3.1. The two rows of memory boxes form two shift registers. For each new input sample all x -values shift one step to the right in the upper shift register, whereas all y -values shift one step to the left in the lower shift register. Subsequently, the new output y_k is calculated. Of course, equation 3.1 is implemented as a few lines of a computer program.

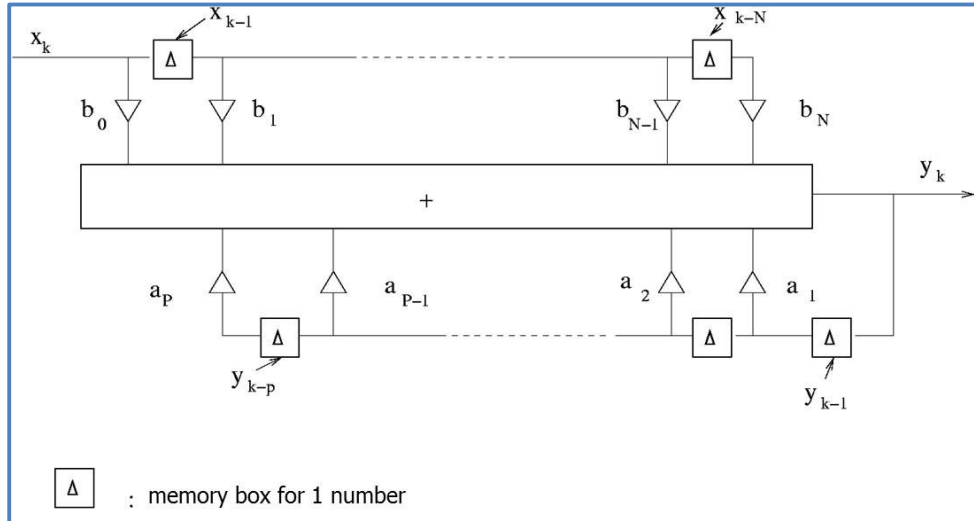


Figure 3.1: Schematic diagram of the recursive filter.

The a -coefficients a_1, \dots, a_p are the feedback coefficients of the filter, hence the name recursive filter. This means that for determining y_k a number of previous output values y_{k-1}, \dots, y_{k-p} are used.

It is easily verified that equation 3.1 is linear and invariant.

All properties of the recursive filter are fully captured by equation 3.1. However, the filter transfer is also fully determined by its impulse response h_k and the convolution relation

$$y_k = \sum_{i=0}^{\infty} h_i x_{k-i}. \quad (3.2)$$

Note that, contrary to equation 1.8, now the index i runs from 0 to ∞ . One can find the impulse response by using an impulse (i.e. Kronecker delta) as input and calculating the output with equation 3.1 (see exercise 1), i.e.

$$h_0 = b_0$$

$$h_1 = b_1 + a_1 h_0 = b_1 + a_1 b_0$$

$$h_2 = b_2 + a_1 h_1 + a_2 h_0 = b_2 + a_1(b_1 + a_1 b_0) + a_2(b_0)$$

$$h_3 = b_3 + a_1 h_2 + a_2 h_1 + a_3 h_0 = b_3 + a_1\{b_2 + a_1(b_1 + a_1 b_0) + a_2(b_0)\} + a_2\{b_1 + a_1 b_0\} + a_3(b_0)$$

etc.

An example is given in figure 3.2.

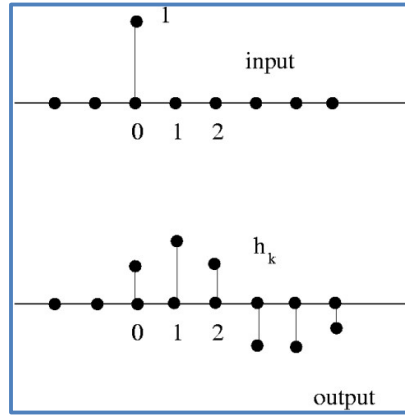


Figure 3.2: The output signal, i.e. the impulse response h_k , due to an impulse (Kronecker delta) as input.

Note that the feedback coefficients a_1, \dots, a_p result in non-zero values for h_{N+1}, h_{N+2}, \dots , which generally gives an infinitely long impulse response.

The transfer or transmission function in the frequency domain can be found by using the complex harmonic $x_k = e^{2\pi j f k \Delta}$ as input signal and using the fact that the output is then the same complex harmonic multiplied by the transmission function $H(f)$, i.e. $y_k = H(f) e^{2\pi j f k \Delta}$.

Hence,

$$y_k = H(f) e^{2\pi j f k \Delta} = \sum_{i=0}^N b_i e^{2\pi j f (k-i) \Delta} + \sum_{i=1}^P a_i H(f) e^{2\pi j f (k-i) \Delta}$$

or

$$H(f) e^{2\pi j f k \Delta} = e^{2\pi j f k \Delta} \sum_{i=0}^N b_i e^{-2\pi j f i \Delta} + H(f) e^{2\pi j f k \Delta} \sum_{i=1}^P a_i e^{-2\pi j f i \Delta}$$

from which we solve $H(f)$ as

$$H(f) = \frac{\sum_{i=0}^N b_i e^{-2\pi j f i \Delta}}{1 - \sum_{i=1}^P a_i e^{-2\pi j f i \Delta}}. \quad (3.3)$$

According to equations 1.18 and 1.19 the relation between h_k and $H(f)$ is

$$H(f) = \sum_{k=0}^{\infty} h_k e^{-2\pi j f k \Delta} \quad (3.4a)$$

and

$$h_k = \Delta \int_{-\frac{1}{2\Delta}}^{\frac{1}{2\Delta}} H(f) e^{2\pi j f k \Delta} df \quad (3.4b)$$

Note again that, contrary to equation 1.18, now the index k runs from 0 to ∞ .

3.2 Impulse response

The simplest recursive filter is given by

$$y_k = x_k + ay_{k-1} \quad (3.5a)$$

i.e. there is only one feedback coefficient ($b_0 = 1, a_1 = a$).

It is easily verified that the impulse response of this filter is given by

$$h_k = \begin{cases} a^k & k \geq 0 \\ 0 & k < 0 \end{cases} \quad (3.5b)$$

i.e. a geometric series. Figure 3.3 shows the impulse response for various values of a . Note that the impulse response of this filter is infinitely long due to the non-zero feedback coefficient.

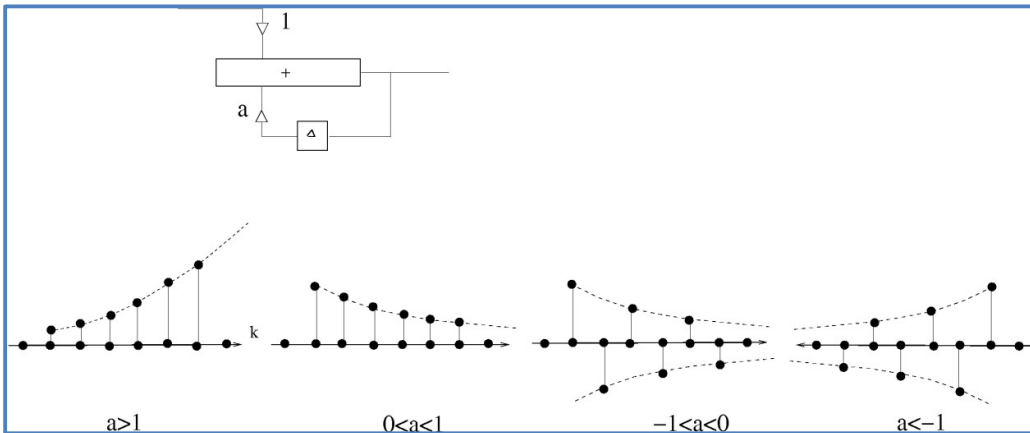


Figure 3.3: Impulse response of the simple filter of equation 3.5a for various values of a .

Starting with the general equation for a recursive filter, a distinction can be made between the following two main filter types:

Transversal or moving average (MA) filters

This filter has no feedback coefficients. Hence, the recursive equation reduces to $y_k = \sum_{i=0}^N b_i x_{k-i}$ and

the impulse response is equal to the b -coefficients b_0, \dots, b_N . Transversal filters thus have a finite length impulse response (length $N+1$) and are therefore also called ‘finite impulse response filters’ (FIR). The transversal filter is schematically depicted in figure 3.4.

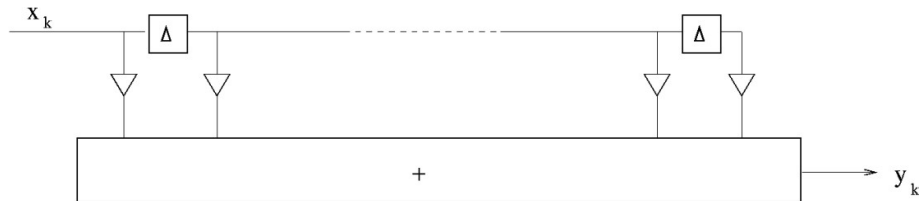


Figure 3.4: Schematic diagram of the transversal or FIR filter.

Autoregressive filter (AR) or infinite impulse response filters (IIR)

This filter has only feedback coefficients in addition to one b -coefficient b_0 , see figure 3.5. The recursive equation is $y_k = b_0 + \sum_{i=1}^P a_i y_{k-i}$. In general the impulse response is infinitely long.

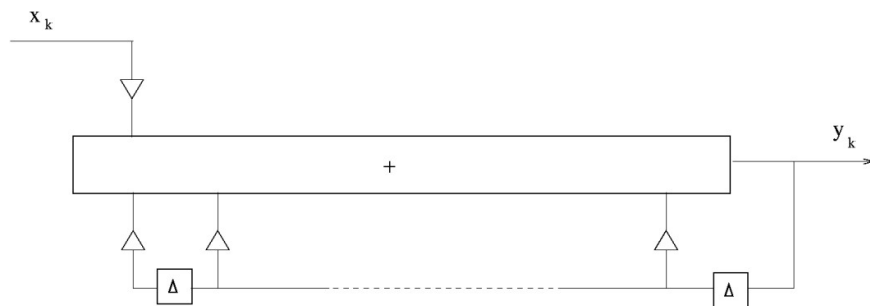


Figure 3.5: Schematic diagram of a IIR filter.

The general recursive filter, equation 3.1, is a combination of both filter types and is hence also called ARMA filter (again having an infinitely long impulse response). The ARMA filter is causal, i.e. $h_k = 0$ for $k < 0$. The filter can be made ‘non-causal’ by an artificial shift of the k -index of the output signal, as illustrated in figure 3.6 for a transversal filter.

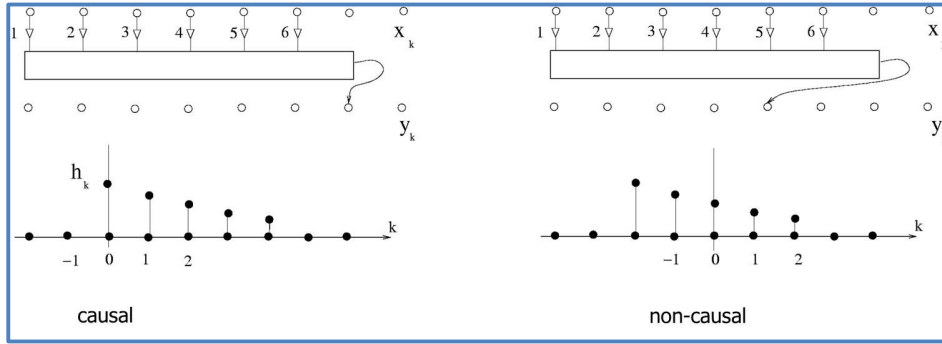


Figure 3.6: Making a causal transversal filter (left diagram) non-causal (right diagram).

For a given recursive filter with known (infinitely long) impulse response h_k we may replace this filter by an equivalent (infinitely long) transversal filter with b – coefficients equal to h_k , see figure 3.7.

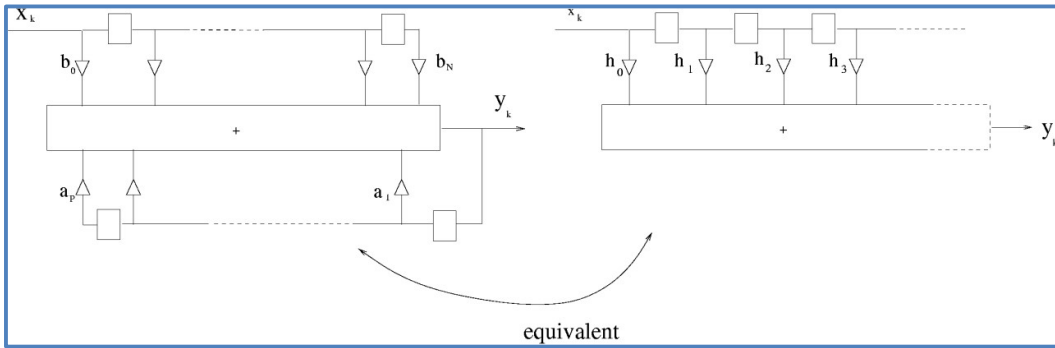


Figure 3.7: The (infinitely long) equivalent transversal filter (right diagram) of the general recursive filter (left diagram).

The convolution relation, equation 3.2, can be written in two ways, i.e.

$$y_k = \sum_{i=0}^{\infty} h_i x_{k-i} = \sum_{i=-\infty}^k h_{k-i} x_i . \quad (3.6a)$$

The shorthand notation for this convolution is $y_k = h_k \otimes x_k$.

For the non-causal filter this becomes

$$y_k = \sum_{i=-\infty}^{\infty} h_i x_{k-i} = \sum_{i=-\infty}^{\infty} h_{k-i} x_i . \quad (3.6b)$$

These equations can be interpreted in two ways. First, equation 3.6 indicates how all input samples $\dots, x_{k-1}, x_k, x_{k+1}, \dots$ contribute to one output sample y_k , see figure 3.8a. The impulse response then indicates the sensitivity of one output sample to the various input samples. Second, equation 3.6

indicates how one input sample x_k contributes to all output samples $\dots, y_{k-1}, y_k, y_{k+1}, \dots$, see figure 3.8b. The impulse response now represents the spreading of one input sample over the various output samples.

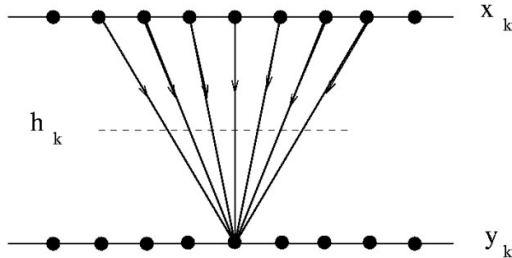


Figure 3.8a: How all input samples contribute to one output sample in a convolution.

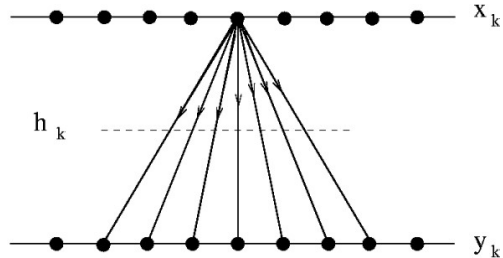


Figure 3.8b: How one input sample contributes to all output samples in a convolution.

These convolution properties also hold for continuous functions, i.e.

$$y(t) = \int h(\tau)x(t-\tau)d\tau = \int h(t-\tau)x(\tau)d\tau = h(t) \otimes x(t).$$

As an example we consider the somewhat blurred image $b(x)$ as obtained in a camera due to the convolution of the object function $O(x)$ with the point spread function (impulse response) $u(x)$ of the camera, i.e. $b(x) = u(x) \otimes O(x)$. This is illustrated in figure 3.9.

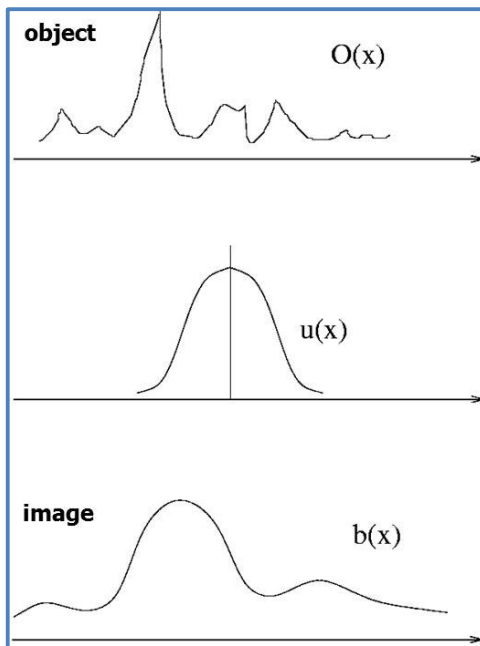


Figure 3.9: In optics the image $b(x)$ is a convolution of the object function $O(x)$ with the point spread function $u(x)$ of the optical system.

It is important to be able to visualize the convolution process, i.e. to be able to have an idea of the shape of the output signal for a given impulse response and a given simple input signal. This can be

done in the following three step. First, swap the impulse response in time. Next, slide it from left to right over the input signal. Finally, calculate the sum of the products in all positions. Try these three steps yourself for the example shown in figure 3.10.

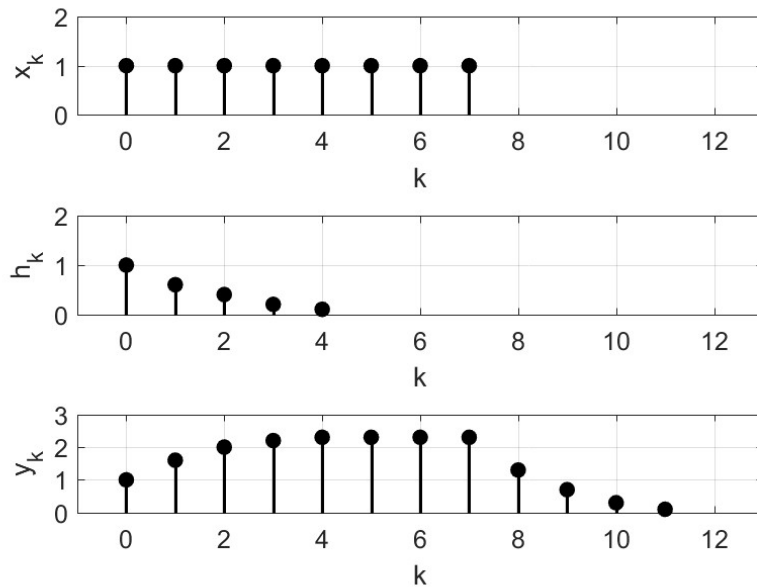


Figure 3.10: The result (y_k) of the convolution of a simple input signal (x_k) with the impulse response (h_k).

Note: the same result is obtained when the input signal is swapped in time and subsequently shifted over the impulse response, see equation 3.6.

The convolution, equation 3.6, can also be computed as a matrix-vector product. Suppose $h = [h_0 \ h_1 \ h_2]$ and $x = [x_0 \ x_1 \ x_2 \ x_3]$ then

$$\begin{bmatrix} y_0 \\ y_1 \\ y_2 \\ y_3 \\ y_4 \\ y_5 \end{bmatrix} = \begin{bmatrix} h_0 & 0 & 0 & 0 \\ h_1 & h_0 & 0 & 0 \\ h_2 & h_1 & h_0 & 0 \\ 0 & h_2 & h_1 & h_0 \\ 0 & 0 & h_2 & h_1 \\ 0 & 0 & 0 & h_2 \end{bmatrix} \begin{bmatrix} x_0 \\ x_1 \\ x_2 \\ x_3 \end{bmatrix}.$$

Note: An important problem in engineering is so-called ‘deconvolution’ (to undo convolution), i.e. find x_k from y_k given h_k . Deconvolution can be difficult in practice due to noise or measurement errors on y_k .

Stability

In general, the recursive filter has an infinitely long impulse response. In this situation we have to avoid that output samples y_k become infinite for finite input sample values x_k . The filter is defined stable if, for every finite input signal ($|x_k| < \infty$), the output signal is finite ($|y_k| < \infty$).

Transversal filters are always stable, since the length of their impulse response is finite. Recursive filters are stable only if their impulse response goes to zero sufficiently fast. It turns out that the condition for stability is

$$\sum_{k=-\infty}^{\infty} |h_k| < \infty. \quad (3.7)$$

A rigorous mathematical proof for this is omitted here.

We return to the example of the beginning of this section, i.e. the simplest recursive filter with only one feedback coefficient equal to a . In this case we have

$$\sum_{k=0}^{\infty} |h_k| = \sum_{k=0}^{\infty} |a|^k = \begin{cases} \frac{1}{1-|a|} & |a| < 1 \\ \infty & |a| \geq 1 \end{cases}$$

i.e. stable for $|a| < 1$ and unstable when $|a| \geq 1$.

3.3 Transmission function

The transmission function $H(f)$ of a recursive filter is given by equations 3.3 and 3.4a and is a periodic function with basis interval $-\frac{1}{2\Delta} < f < \frac{1}{2\Delta}$. Note that the right-hand side of equation 3.3 is only valid for a stable filter.

Let us again take the simple example of the previous section, but now we take $b_0 = 1 - x$, $a_1 = x$. We apply equation 3.4a and obtain

$$H(f) = \sum_{k=0}^{\infty} h_k e^{-2\pi j f k \Delta} = (1-x) \sum_{k=0}^{\infty} x^k e^{-2\pi j f k \Delta} = (1-x) \sum_{k=0}^{\infty} (x e^{-2\pi j f \Delta})^k = \frac{1-x}{1-x e^{-2\pi j f \Delta}}.$$

The geometric series only converges when $|x| < 1$ (i.e. when the filter is stable). This result is directly obtained when we substitute b_0 and a_1 in equation 3.3 (however the result is only valid for a stable filter i.e. $|x| < 1$). The transmission function is depicted in figure 3.11a for $x = a_1 = 0.8$ and $b_0 = 1 - x = 0.2$. (The time step Δ is chosen to be 1 s, i.e. $F = 1$ Hz and the frequency axis goes from

-0.5 Hz to +0.5 Hz). Both $|H(f)|$ on a linear scale and in dB units are shown. The phase shift of the filter, i.e. $\arg H(f)$ in degrees, is also indicated. Apparently, this choice of the filter coefficients results into a LPF. Note that with $b_0 = 1 - x = 0.2$ instead of $b_0 = 1$, $|H(f)|$ is normalized, i.e. its maximum value is 1 (0 dB).

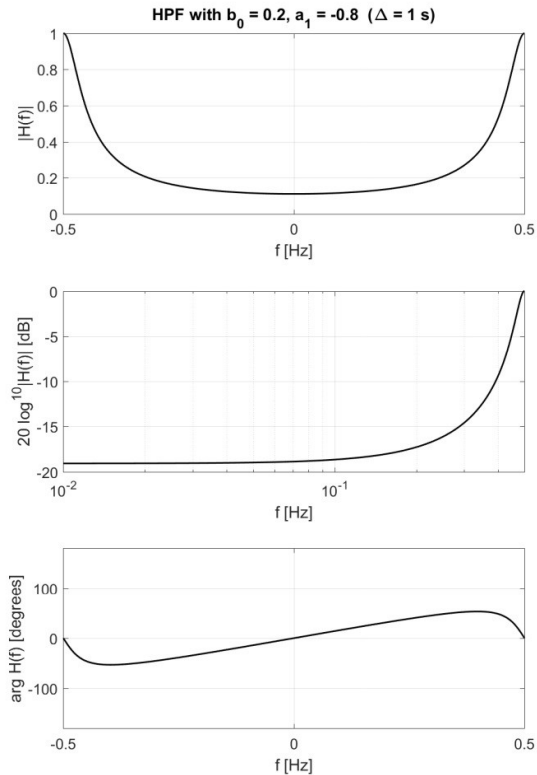
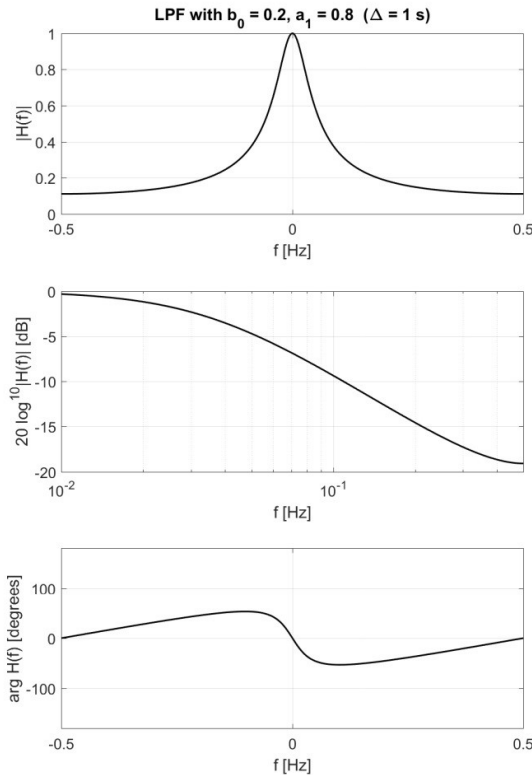


Figure 3.11a: Transmission function of the simplest recursive LPF.

Figure 3.11b: Transmission function of the simplest recursive HPF.

Figure 3.11b shows the transmission function for $b_0 = 0.2$ and $a_1 = -0.8$. Clearly, this results in a HPF.

Note: in Matlab the feedback coefficients a_i are $[1 -0.8]$ and $[1 +0.8]$ for the LPF and the HPF, respectively (the first a coefficient should always be equal to 1 in Matlab, see equation 3.1c).

As can be seen from e.g. equation 1.12, each signal can be thought of as consisting of many harmonic signals. Each of these harmonic signals will appear at the output of a filter as

$$|H(f)| e^{j\{2\pi fk\Delta + \arg H(f)\}} = |H(f)| e^{j\left\{2\pi f\left(k\Delta - \frac{-\arg H(f)}{2\pi f}\right)\right\}}.$$

Hence, the two reasons for the output y_k to differ from the input x_k are (1) a frequency-dependent amplification or attenuation $|H(f)|$ and (2) a frequency-dependent phase shift $\arg H(f)$. The effect of the phase shift can be interpreted as a frequency-dependent delay given by

$$\tau(f) = \frac{-\arg H(f)}{2\pi f}. \quad (3.8)$$

We note that this delay does not necessarily have values equal to multiples of Δ . When τ is indeed varying with f , then the filter exhibits so-called ‘dispersion’, i.e. delays that are not the same for the various frequencies.

In many filter applications a given behaviour of $|H(f)|$ is required, whereas the requirements on $\arg H(f)$ are minimal. Still, often a dispersion-free filter is necessary. This is e.g. the case in the situation of a useful signal corrupted with noise where signal and noise are concentrated in separate frequency bands (see the example at the end of this section). A filter with a passband centred around the signal frequencies is then used and to avoid unnecessary signal distortion, the filter needs to be dispersion-free in the passband.

A transversal filter with symmetrical impulse response, i.e. $h_k = h_{-k}$, $k = 0, \dots, N$, is perfectly dispersion-free. The filter is then non-causal. According to equation 3.4a, $H(f)$ is then real-valued and $\tau(f) = 0$. Such filters can be made causal by shifting the impulse response to the right. Then $\tau(f)$ becomes nonzero, but it is the same for all frequencies. Hence, there is no dispersion.

Poles and zeros

A disadvantage of formula 3.3 for $H(f)$ is that, for given coefficients a_i and b_i , the nature of $H(f)$ is not clear. To obtain a qualitative impression of $H(f)$, we therefore introduce the concept of ‘poles and zeros’. In chapter 1 we already saw that the signal $x_k = e^{2\pi jfk\Delta}$ is an eigenfunction of a linear invariant system. This can be written as the geometric series $x_k = (e^{2\pi jf\Delta})^k$. In fact, any geometric series $x_k = z^k$, with z an arbitrary complex number, is an eigenfunction of a linear invariant system. Substituting $x_k = z^k$ and $y_k = H(z)z^k$ in the recursion equation 3.1 gives

$$H(z) = \frac{\sum_{i=0}^N b_i z^{-i}}{1 - \sum_{i=1}^P a_i z^{-i}} \quad (3.9)$$

and from equation 3.4a we obtain

$$H(z) = \sum_{i=0}^{\infty} h_i z^{-i}. \quad (3.10)$$

$H(z)$ is the so-called z -transform of h_i . It is a function above the complex plane. If we choose z on the unit circle in the complex plane, i.e. $z = e^{2\pi j f \Delta}$, then we again obtain the formulas 3.3 and 3.4a for the transmission function, i.e. $H(f) = H(z = e^{2\pi j f \Delta})$. The basis frequency interval $\left(-\frac{1}{2\Delta}, \frac{1}{2\Delta}\right)$ of the periodic function $H(f)$ corresponds to going once along the unit circle in the complex plane, see figure 3.12.

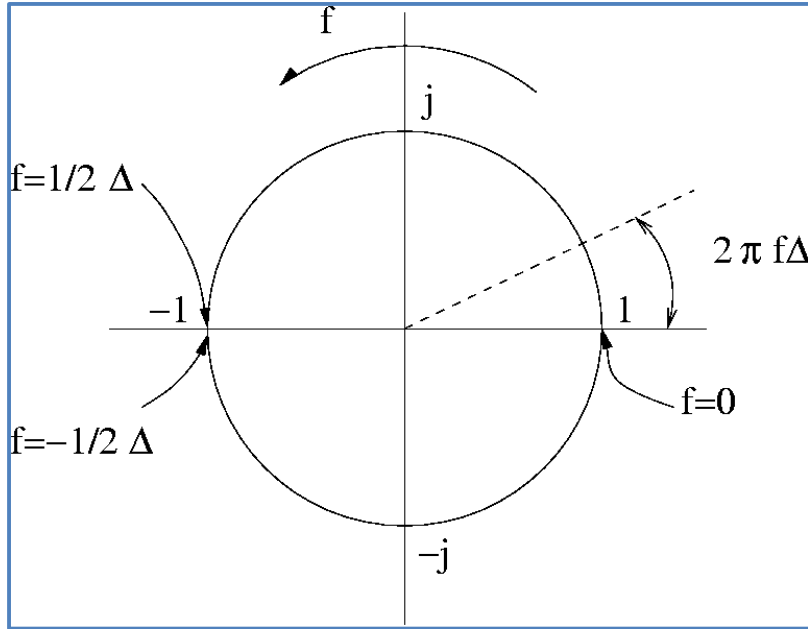


Figure 3.12: The unit circle in the complex plane and the basis frequency interval of the periodic function $H(f)$.

We write $H(z)$ as a function of z instead of z^{-1} , i.e.

$$H(z) = z^{P-N} \frac{\sum_{i=0}^N b_i z^{N-i}}{z^P - \sum_{i=1}^P a_i z^{P-i}}. \quad (3.11)$$

which can be written as

$$H(z) = b_0 z^{P-N} \frac{(z - n_1)(z - n_2) \dots (z - n_N)}{(z - p_1)(z - p_2) \dots (z - p_P)}. \quad (3.12)$$

The nominator of this equation is, apart from the factor z^{P-N} , a polynomial of degree N , which has N roots n_1, \dots, n_N that are either real-valued or complex conjugate pairs. These are called the 'active zeros' of $H(z)$. The denominator of equation 3.12 is a polynomial of degree P , which has

P roots p_1, \dots, p_P , again either real-valued or complex conjugate pairs. These are called the ‘active poles’ of $H(z)$. The factor z^{P-N} results in so-called ‘passive poles or zeros’, depending on the sign of $P - N$. They have no influence on $|H(f)|$.

Note: Transversal filters only have zeros and autoregressive filters only have poles. The general recursive filter has both poles and zeros.

Let $|p_i|, i=1, \dots, P$ be the absolute values of the poles and let R be the largest of these. Then, for a causal recursive filter, the series in equation 3.10 converges for $|z| > R$. Further, $H(z)$ should converge on the unit circle in the complex plane, otherwise $H(f)$ would be undefined. Hence, the unit circle must lie in the area $|z| > R$. Consequently, for the filter to be stable all poles must lie inside the unit circle, i.e. $|p_i| < 1, i=1, \dots, P$. The zeros are allowed to lie anywhere in the complex plane.

The position of the poles and zeros in the complex plane can provide insight in the nature of the transmission function. According to equation 3.12 the absolute value of the transmission function can be written as

$$|H(f)| = |b_0| \frac{\prod_{i=1}^N |e^{2\pi j f \Delta} - n_i|}{\prod_{i=1}^P |e^{2\pi j f \Delta} - p_i|} \quad (3.13)$$

i.e. for a given frequency f , $|H(f)|$ depends on the distances of point f on the unit circle to the poles and zeros. This is illustrated in figure 3.13 for a filter with three poles p_1 , p_2 and p_3 and two zeros n_1 and n_2 . The distance of point f on the unit circle (indicated by the black dot in figure 3.13) to the three poles are denoted A_1 , A_2 and A_3 , respectively, whereas the distance of point f to the zeros are denoted B_1 and B_2 . In this case $|H(f)|$ is thus given by

$$|H(f)| = |b_0| \frac{B_1 B_2}{A_1 A_2 A_3}$$

Now, attenuation or amplification of the filter at a certain frequency can be accomplished as follows.

A pole close to the unit circle, see figure 3.14a, gives a strong resonance peak in $|H(f)|$, i.e. strong amplification at that point f on the unit circle close to the pole. Similarly, a strong attenuation is obtained for a zero close or on the unit circle, see figure 3.14b. Both can be strengthened and made sharper by placing a pole and zero closely together (and close to the unit circle), see figure 3.14c and 3.14 d. For points f on the unit circle close to this pole or zero, either the pole or the zero dominates. For points f further away, the effects of the pole and zero compensate each other.

Note: Each pole or zero is always accompanied by its complex conjugate, see examples of figure 3.14.

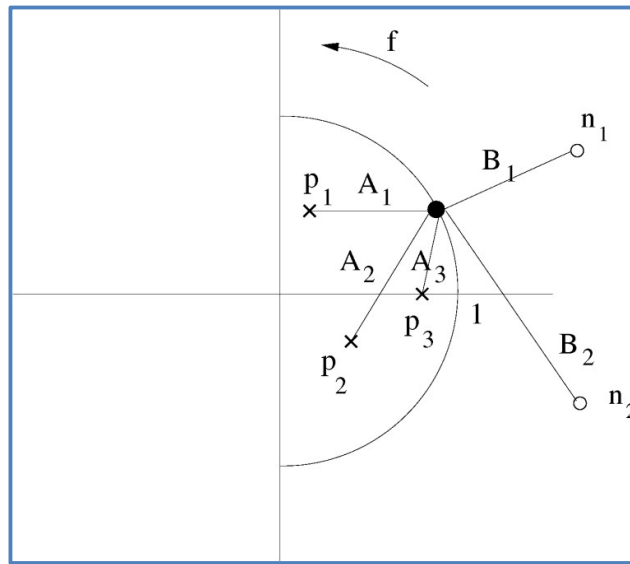


Figure 3.13: Distances of point f on the unit circle (black dot) to the poles and zeros of a recursive filter. Note: this is not a pole-zero diagram of a recursive filter as the poles are not complex conjugates. The diagram is merely intended to illustrate the working of equation 3.13.

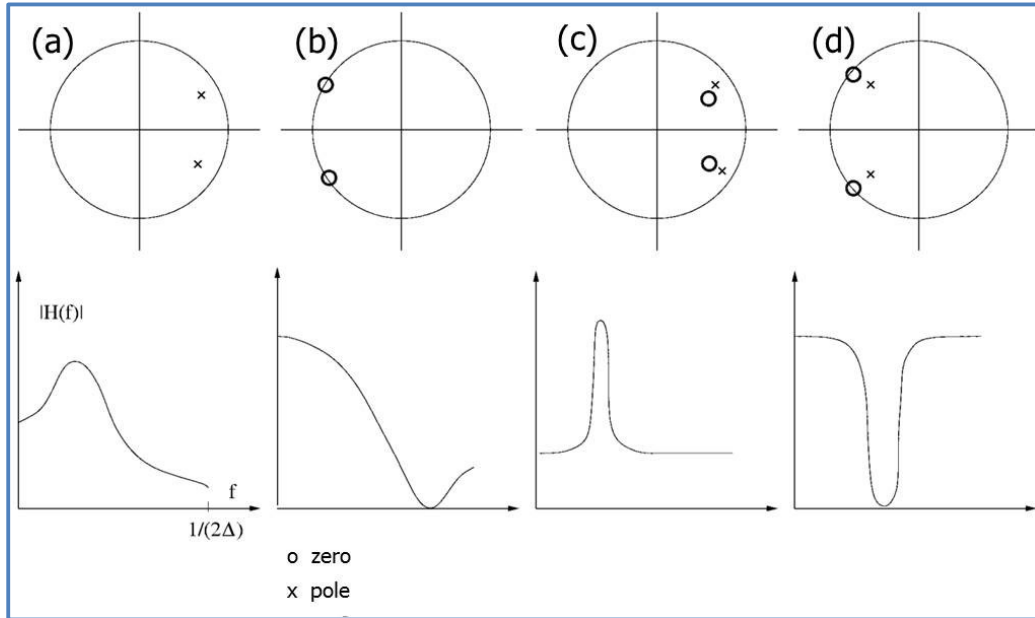


Figure 3.14: $|H(f)|$ of a few simple filters and their corresponding poles and zeros.

In principle, any desired transmission function can be obtained, simply by moving poles and zeros across the complex plane. For given pole- and zero positions, the coefficients a_i and b_i can be obtained from equation 3.12.

In general, the filter design problem is as follows. Given a desired transmission function $H(f)$, find the corresponding coefficients a_i and b_i . Today, software tools like Matlab provide ready-to-use routines that are able to do this job fast and in a user-friendly manner. An example is routine ‘fir1’ that determines the filter coefficients $b_i, i = 0, \dots, N$ of a transversal LPF for given N and cut-off frequency f_c (relative to the Nyquist frequency $f_N = \frac{F}{2}$, F being the sample frequency).

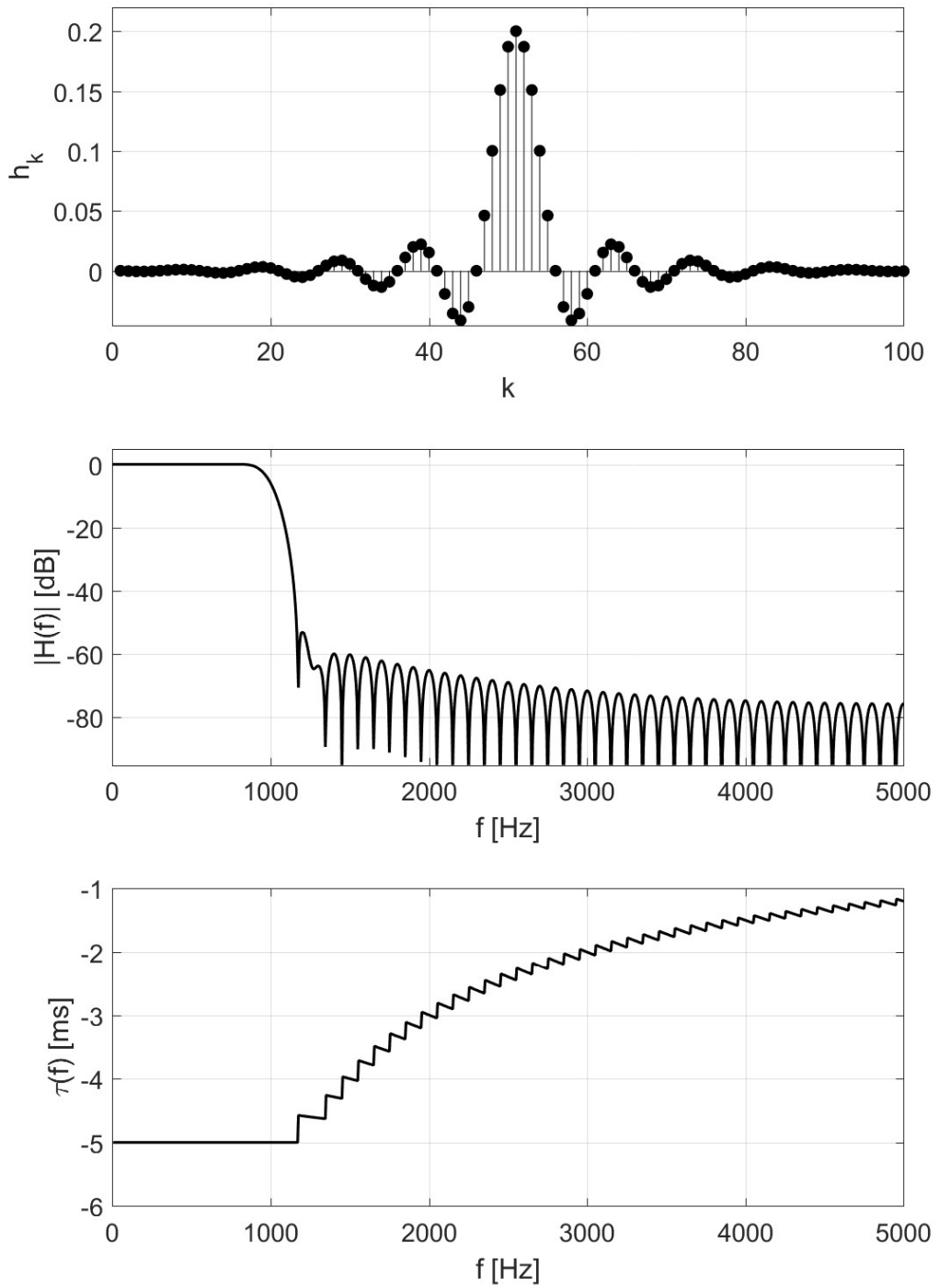
Figure 3.15 shows the impulse response h_k and transmission function $H(f)$ for a LPF with $f_c = 1000$ Hz ($F = 10000$ Hz, $f_N = 5000$ Hz) and $N = 100$. Both $|H(f)|$ in dB and $\tau(f) = \frac{-\arg H(f)}{2\pi f}$ in ms (see equation 3.8) are shown.

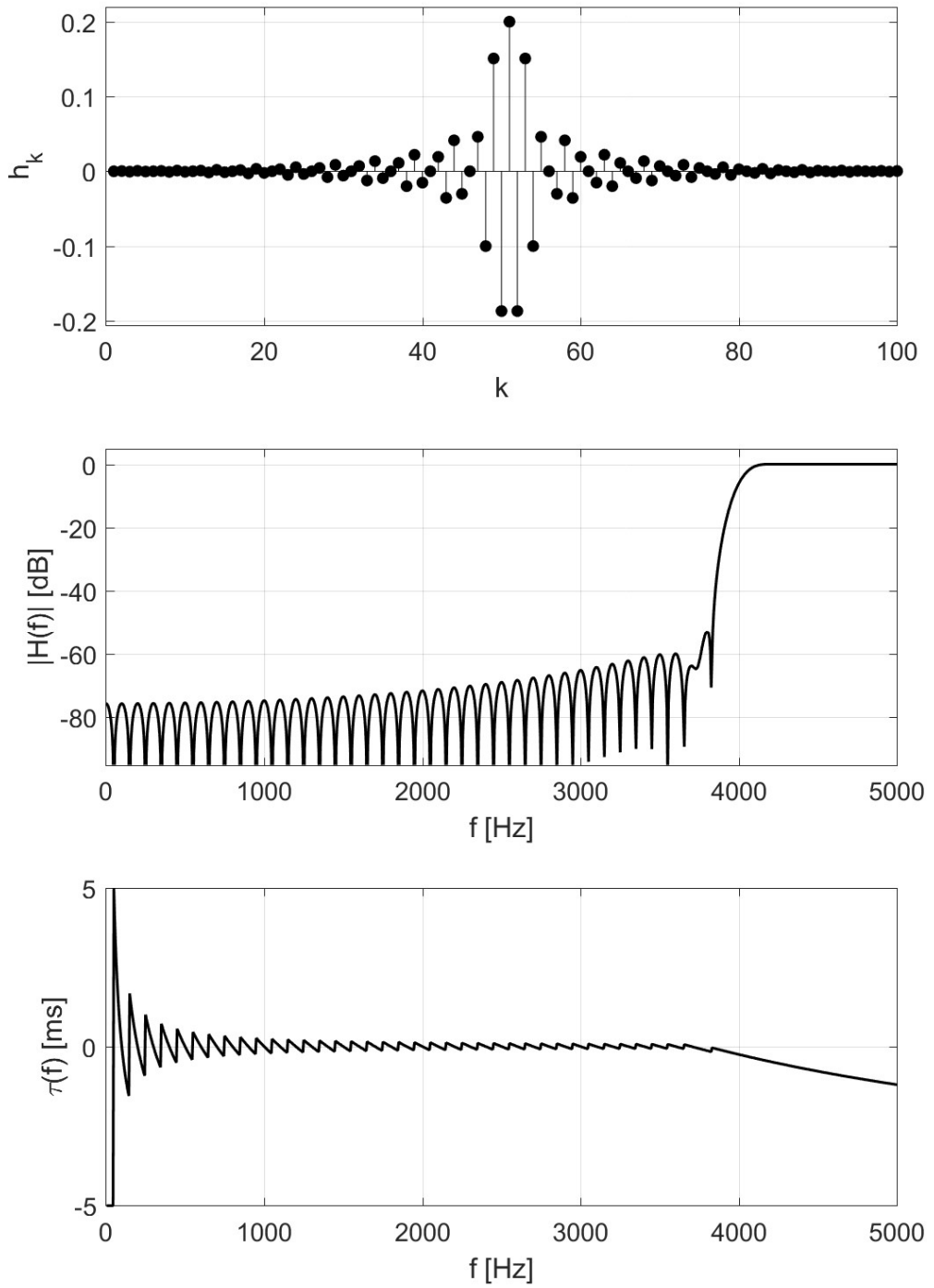
Notes:

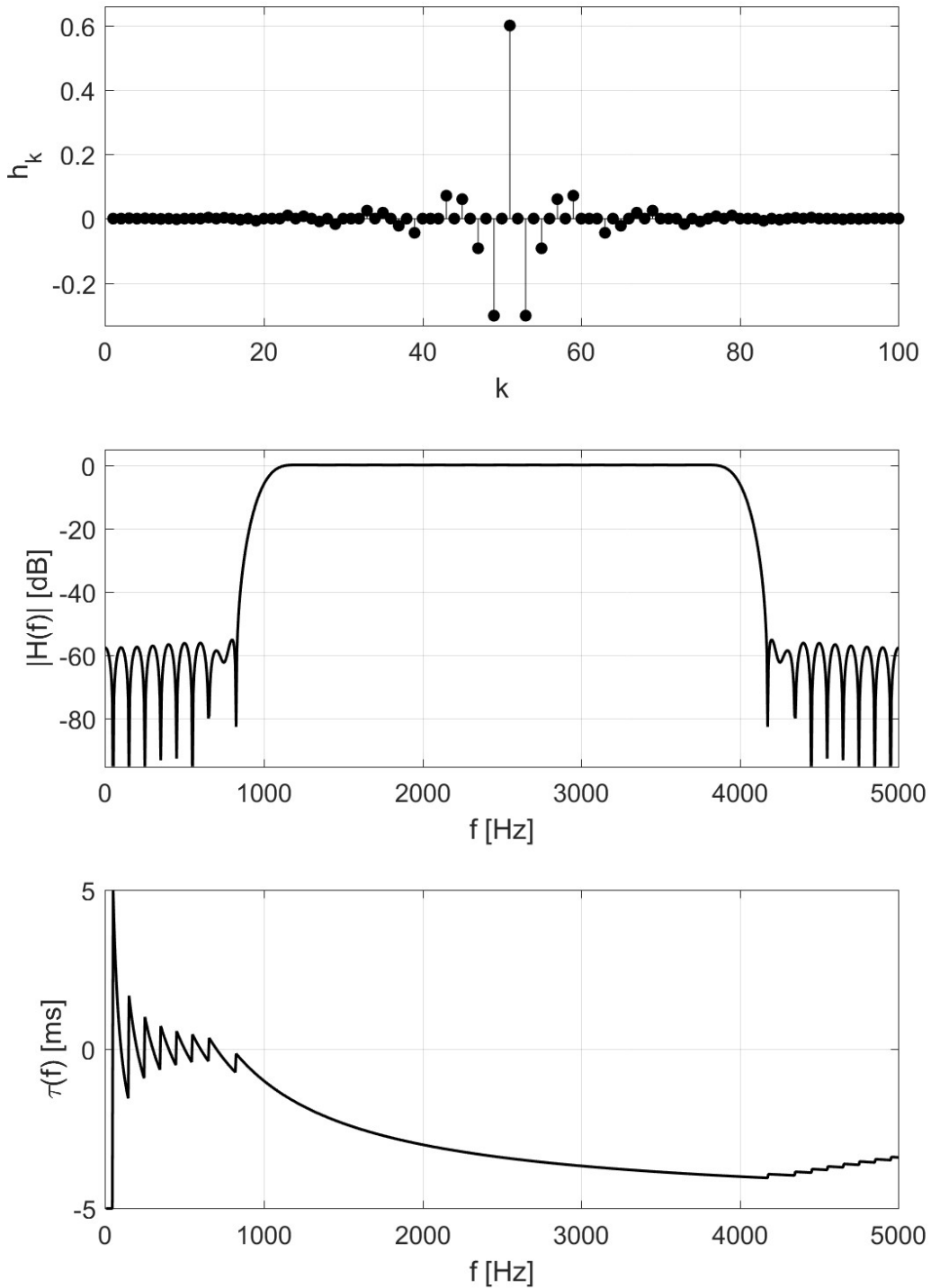
- For this transversal (i.e. FIR) filter, the impulse response is the equal to the filter coefficients $b_i, i = 0, \dots, N$;
- The filter has only zeros, positioned in such a way on the unit circle that the desired attenuation occurs (actually, the frequencies for which the deep negative peaks in $20\log(|H(f)|)$ occur correspond to these zeros on the unit circle);
- It is observed that in the passband ($0 < f < f_c$) the filter has the desired property that $\tau(f)$ is a constant, i.e. independent of f (no dispersion).
- For a LPF, routine ‘fir1’ is called in Matlab as $b = \text{fir1}\left(N, \frac{f_c}{f_N}\right)$, i.e. the two parameters of the routine are filter length N and cut-off frequency (relative to the Nyquist frequency). Parameter N can be increased up to value for which a sufficient attenuation in the stopband and a sufficiently fast roll-off in the transition band is obtained.

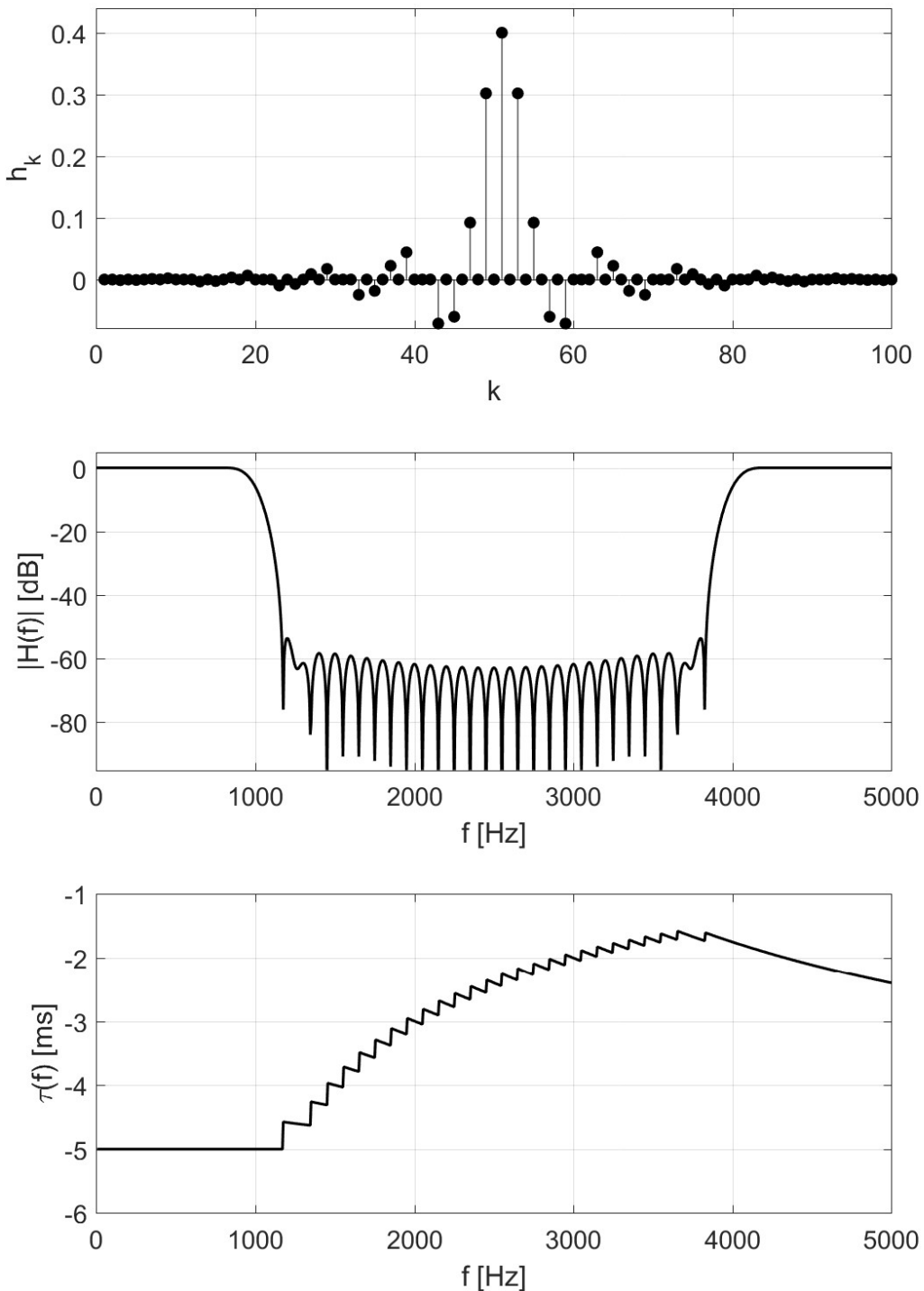
Routine ‘fir1’ can also provide a transversal HPF, BPF and BSF. For HPF routine ‘fir1’ is called in Matlab as $b = \text{fir1}\left(N, \frac{f_c}{f_N}, \text{'high'}$). Figure 3.16 shows the result for $f_c = 4000$ Hz (same N and F as for the LPF of figure 3.15).

A BPF can be implemented with ‘fir1’ by specifying two cut-off frequencies, the result of which is show in figure 3.17 for the band (1000 Hz, 4000 Hz). Calling the routine as $b = \text{fir1}(N, [1000 \ 4000], \text{'stop'})$ results in a BSF with the same cut-off frequencies, see figure 3.18.

Figure 3.15: Example of a finite impulse response Low Pass Filter (LPF) with $N = 100$.

Figure 3.16: Example of a finite impulse response High Pass Filter (HPF) with $N = 100$.

Figure 3.17: Example of a finite impulse response Band Pass Filter (BPF) for $N = 100$.

Figure 3.18: Example of a finite impulse response Band Stop Filter (BSF) for $N = 100$.

As a final filter design example we show the transmission function of a recursive LPF obtained with Matlab routine 'ellip' (which generates a so-called 'elliptical filter'). The routine is called in Matlab as $[b,a] = \text{ellip}(N, R_p, R_s, \frac{f_c}{f_N})$ with R_p the so-called bandpass ripple and R_s the stopband attenuation (both in dB). Figure 3.19 shows the result for an allowed R_p of 0.2 dB and a required R_s of -60 dB ($|H(f)| \leq 10^{-3}$). This can be accomplished with $N = 8$.

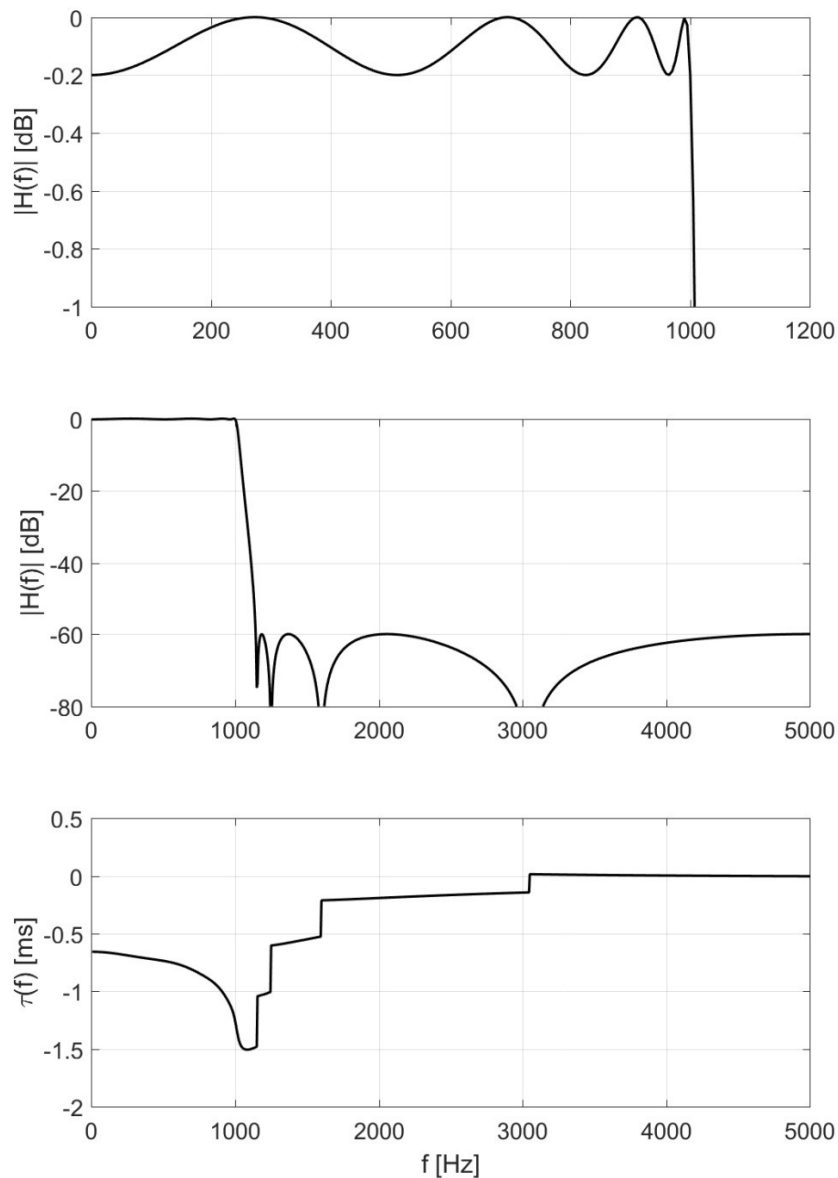


Figure 3.19: Transmission function of the recursive elliptical filter.

Notes:

- The main difference between the transversal filters of figures 3.15 to 3.18 and the recursive filter of figure 3.19 is the filter length, i.e. much less filter coefficients are needed for a recursive filter with approximately the same performance as a transversal filter (e.g. with stopband attenuation -60 dB in these cases). This is because transversal filters only have zeros to do the job;
- The positions of the poles and zeros of this recursive filter (as shown in figure 3.20) directly correspond to the ripples in the passband and the strong negative peaks in the stopband;
- As can be observed from the bottom plot of figure 3.19, the recursive filter is not dispersion-free in its passband;
- With N equal to eight as input parameter to routine 'ellip', we obtain nine b -coefficients ($b_i, i = 0, \dots, N$) and eight a -coefficients, resulting in eight poles and eight zeros (see also figure 3.20).

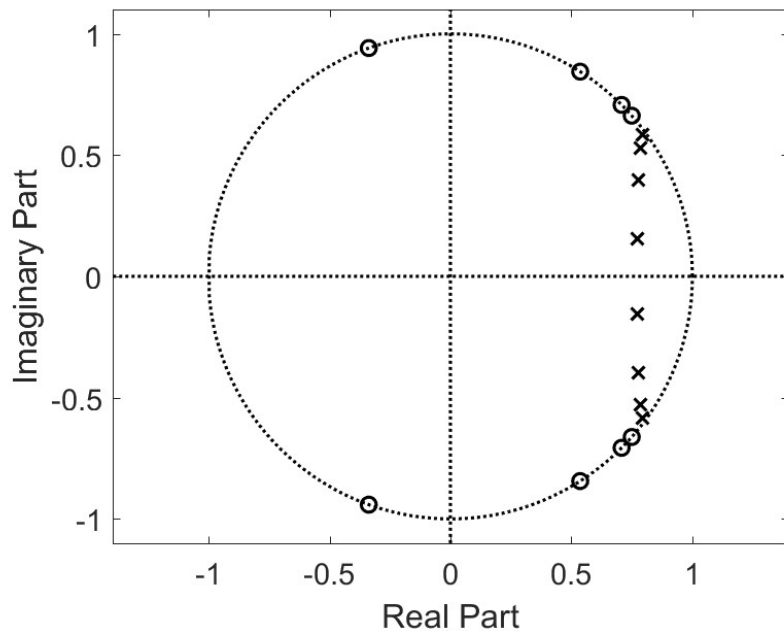


Figure 3.20: Poles and zeros of the recursive elliptical filter.

Depending on the required stopband attenuation, transition band roll-off, allowed passband ripple and dispersion behaviour, other types of recursive filters can be utilized, such as 'butterworth' and 'chebyshev' filters.

As an example of the application of a transversal BPF, we consider a useful narrowband signal (with bandwidth $B \approx 500$ Hz centred at a frequency $f_0 = 15000$ Hz) corrupted with low-frequency noise.

The clean signal is shown in the upper plot of figure 3.21. The middle plot of the figure shows the signal totally buried in the noise. The filtered signal, obtained by applying a transversal BPF with $N = 100$ and cut-off frequencies of 14750 Hz and 15250 Hz, is shown in the bottom plot of figure 3.21 and

illustrates the strength of digital filtering in recovering the signal of interest. Note that the filtered signal exhibits a delay. Also, the signal is somewhat distorted caused by dispersion of the filter.

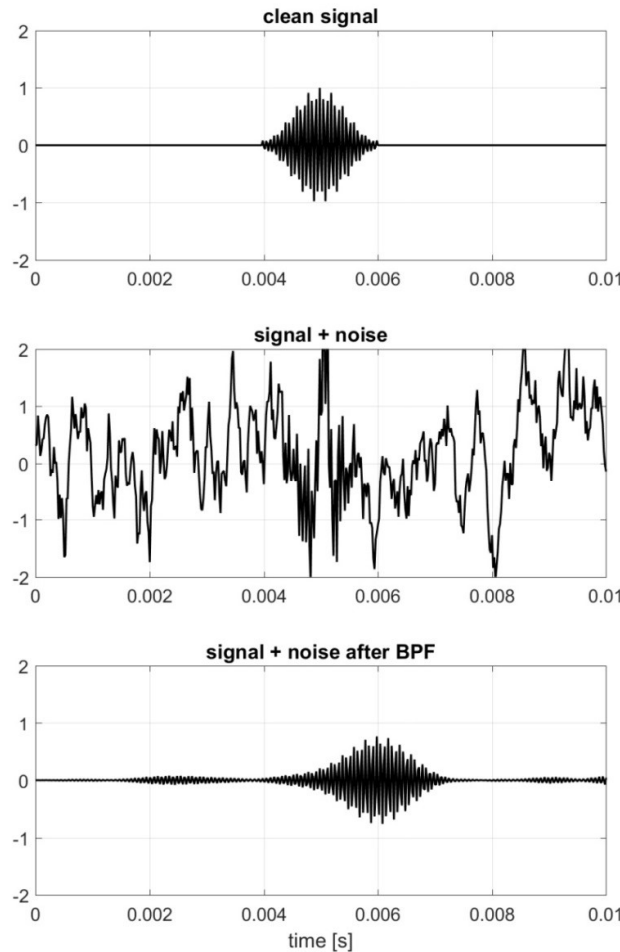


Figure 3.21: Narrow band signal at 15 kHz buried in low-frequency noise before (middle plot) and after bandpass filtering (lower plot). The original clean signal without the noise is shown in the upper plot.

3.4 Filters in series

In this section we consider two (or more) filters in series, see figure 3.22.

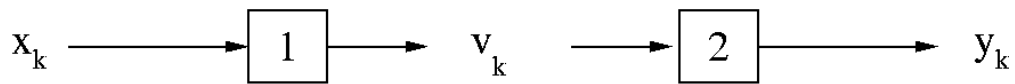


Figure 3.22: Filters 1 and 2 in series.

Using equation 3.6 it is easily verified that the output signal y_k of the combined filter is given by

$$y_k = h_k^{(2)} \otimes (h_k^{(1)} \otimes x_k) = (h_k^{(2)} \otimes h_k^{(1)}) \otimes x_k = (h_k^{(1)} \otimes h_k^{(2)}) \otimes x_k$$

with x_k the signal at the input of filter 1 and $h_k^{(1)}$ and $h_k^{(2)}$ the impulse response of filter 1 and 2, respectively. Hence, the combined impulse response is

$$h_k = h_k^{(1)} \otimes h_k^{(2)} \quad (3.14)$$

Equations 3.4a and 3.4b give the relations between h_k and $H(f)$, i.e. they are each other's Fourier transform, and thus

$$H(f) = H^{(1)}(f)H^{(2)}(f) \quad (3.15)$$

with $H^{(1)}(f)$ and $H^{(2)}(f)$ the transmission function of filter 1 and 2, respectively. This confirms that 'convolution in the time domain' corresponds to 'multiplication in the frequency domain'.

Note: The order of the two filters can be swapped without changing the result.

3.4 Exercises

Question 1

Consider the recursive filter $y_k = x_k + x_{k-1} - x_{k-2} + \frac{1}{10}y_{k-1} + \frac{1}{5}y_{k-2}$. Calculate the first five terms h_0, \dots, h_4 of the impulse response.

Question 2

Consider the recursive filter $y_k = x_k + \frac{1}{2}y_{k-1}$. Give the expression for the output signal y_k for the input signal $x_k = \begin{cases} 0 & k < 0 \\ k^2 & k \geq 0 \end{cases}$.

Question 3

Calculate the impulse response and transmission function of the recursive filters $y_k = x_k + \frac{3}{4}y_{k-1}$ and $y_k = 3x_k - 3x_{k-1} + \frac{3}{4}y_{k-1}$. What type of filter are these? LPF, HPF, BPF or BSF?

Question 4

A transversal filter has impulse response $\left[\frac{1}{9} \quad \frac{2}{9} \quad \frac{3}{9} \quad \frac{2}{9} \quad \frac{1}{9} \right]$.

(a) Is this a LPF or HPF? Check your answer by calculating the response to a constant signal $x_k = 1$ for all k .

(b) Calculate the response to the signal

$$x_k = [\dots \quad 0 \quad 0 \quad 0 \quad 9 \quad -9 \quad 18 \quad 0 \quad -9 \quad -9 \quad 9 \quad 0 \quad -18 \quad 9 \quad -9 \quad 0 \quad 9 \quad 0 \quad 0 \quad 0 \quad \dots]$$

(c) Calculate $H(f)$ and make a sketch of it.

- (d) Calculate and sketch $H(f)$ for the filter with impulse response $\left[\frac{1}{5} \quad \frac{1}{5} \quad \frac{1}{5} \quad \frac{1}{5} \quad \frac{1}{5} \right]$.

Question 5

A transversal filter has impulse response $\left[-\frac{1}{8} \quad -\frac{3}{8} \quad \frac{8}{8} \quad -\frac{3}{8} \quad -\frac{1}{8} \right]$.

- (a) Show that this is a HPF by calculating the response to quickly fluctuating signal

$$x_k = [\dots \quad +1 \quad -1 \quad +1 \quad -1 \quad +1 \quad -1 \quad \dots].$$

- (b) Calculate the response to a constant signal $x_k = 1$ for all k .

- (c) Calculate the response to the signal

$$x_k = [\dots \quad 0 \quad 16 \quad 8 \quad 0 \quad \dots]$$

Question 6

Consider the recursive filters $y_k = x_k + ay_{k-1}$ and $y_k = x_k + by_{k-1}$ in series.

- (a) Calculate the impulse response h_k .
 (b) Calculate the transmission function $H(f)$.
 (c) Again calculate $H(f)$ by Fourier transforming h_k .

Question 7

The transmission function of a digital filter is $H(f) = 1 - \frac{1}{2}\cos(2\pi f\Delta) - \frac{1}{4}\cos(4\pi f\Delta)$.

- (a) Make a sketch of $H(f)$ (take $\Delta = 1$ s).
 (b) Calculate and sketch the impulse response h_k .
 (c) Is this filter causal or non-causal?
 (d) Find the recursive equation?
 (e) Is the filter dispersion-free?

Question 8

Consider the transversal filter with $b_0 = b_1 = \dots = b_{N-1} = \frac{1}{N}$.

- (a) Show that $H(f) = e^{-\pi j f(N-1)\Delta} \frac{\sin(\pi f N \Delta)}{N \sin(\pi f \Delta)}$.
- (b) Make a sketch of $|H(f)|$ for $N = 10$ and $\Delta = 1$ s.
- (c) What type of filter is this? LPF, HPF, BPF or BSF?
- (d) Suppose $\Delta = 1$ ms and the first zero of $H(f)$ should be at 40 Hz, what should be the value of N ?

Chapter 4 Filtering in the frequency domain – the Discrete Fourier Transform DFT

4.1 Introduction

The recursive filters of the previous chapter are time domain filters, i.e. the filtering occurs by taking weighted combinations of delayed input- and output numbers (see equation 3.1). These filters are suitable for real-time processing of a continuously incoming input signal. The filter transfer is characterized by the convolution relation

$$y_k = h_k \otimes x_k = \sum_i h_{k-i} x_i \quad (4.1)$$

and the product relation

$$Y(f) = H(f)X(f) \quad (4.2)$$

with h_k , x_k and y_k the impulse response of the filter and the input- and output signal in the time domain, respectively. $H(f)$, $X(f)$ and $Y(f)$ are the corresponding Fourier transforms. $H(f)$ is called the transmission function of the filter.

Filtering can also be performed in the frequency domain by executing the following three steps, see also figure 4.1:

- Transform the input signal x_k to $X(f)$:

$$X(f) = \Delta \sum_k x_k e^{-2\pi jfk\Delta} \quad (4.3)$$

- Multiply $X(f)$ with the desired $H(f)$:

$$Y(f) = H(f)X(f) \quad (4.4)$$

- Transform $Y(f)$ to y_k :

$$y_k = \int_{-\frac{1}{2\Delta}}^{\frac{1}{2\Delta}} Y(f) e^{2\pi jfk\Delta} df \quad (4.5)$$

Note that $H(f)$, $X(f)$ and $Y(f)$ are continuous functions of f , i.e. they need to be defined on an infinite number of points on the interval $-\frac{1}{2\Delta} < f < \frac{1}{2\Delta}$. This is not convenient for digital signal processing. In the next section it will however become clear that it suffices to use a finite number of samples for $H(f)$, $X(f)$ and $Y(f)$. The integral of equation 4.5 then becomes a summation.

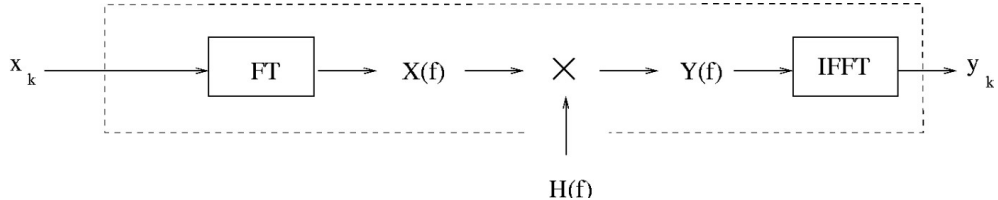


Figure 4.1: The three steps for frequency domain filtering.

Notes:

- Indeed the filtering is performed in the frequency domain, see equation 4.4.
- For this method to work a finite length input signal x_0, \dots, x_{N-1} must be available (N can be large).
- The advantage, with respect to recursive time domain filters, is that the desired $H(f)$ can be immediately substituted in equation 4.4. There is no need to find corresponding $a-$ and $b-$ coefficients. However, not all arbitrary $H(f)$ can be used, i.e. we are limited by transmission functions corresponding to finite length impulse responses h_0, \dots, h_{N-1} . This is caused by the fact that $H(f)$ needs to be represented by a finite number of samples, see section 4.2. As a consequence only transversal filters can be made (i.e. no poles, only zeros).
- We can also start with a desired impulse response h_k , calculate $H(f)$ with
$$H(f) = \sum_{k=0}^{N-1} h_k e^{-2\pi jfk\Delta}$$
 (equation 1.18) and then apply 4.4.
- The Fourier transforms, equation 4.3 and 4.5, are usually implemented as ‘Fast Fourier Transforms’ (FFT). In software tools like Matlab, efficient ready-to-use FFT routines are available.

4.2 Discrete Fourier Transform

For frequency domain filtering in digital signal processing, the continuous functions $H(f)$, $X(f)$ and $Y(f)$ need to be replaced by finite length rows of numbers. Intuitively, one might expect that this should be allowed: when $X(f)$ is the Fourier transform of a finite length signal x_0, \dots, x_{N-1} ,

then it must be possible that also $X(f)$ is described in terms of N numbers. We will show that the ‘Discrete Fourier Transform’ (DFT) is the solution. The DFT X_r of time signal x_k is defined as

$$X_r = \Delta \sum_{k=0}^{N-1} x_k e^{-2\pi j \frac{kr}{N}}, \quad r = 0, \dots, N-1 \quad (4.6a)$$

The Inverse Discrete Fourier Transform (IDFT) of X_r , resulting in the original time signal x_k , is then given as

$$x_k = \frac{1}{N\Delta} \sum_{r=0}^{N-1} X_r e^{2\pi j \frac{kr}{N}}, \quad k = 0, \dots, N-1 \quad (4.6b)$$

Proof:

We substitute equation 4.6a in equation 4.6b yielding

$$x_k = \frac{1}{N\Delta} \sum_{r=0}^{N-1} X_r e^{2\pi j \frac{kr}{N}} = \frac{1}{N\Delta} \sum_{r=0}^{N-1} \left(\Delta \sum_{k'=0}^{N-1} x_{k'} e^{-2\pi j \frac{k'r}{N}} \right) e^{2\pi j \frac{kr}{N}} = \sum_{k'=0}^{N-1} x_{k'} \left(\frac{1}{N} \sum_{r=0}^{N-1} e^{2\pi j \frac{(k-k')r}{N}} \right)$$

with $\frac{1}{N} \sum_{r=0}^{N-1} e^{2\pi j \frac{(k-k')r}{N}} = \delta_{k-k'+mN}$ where m is any positive or negative integer number (including 0),

i.e. $\frac{1}{N} \sum_{r=0}^{N-1} e^{2\pi j \frac{(k-k')r}{N}}$ is a periodic Kronecker delta with period N .

As the summation over k' goes from 0 to $N-1$, we have

$$\sum_{k'=0}^{N-1} x_{k'} \left(\frac{1}{N} \sum_{r=0}^{N-1} e^{2\pi j \frac{(k-k')r}{N}} \right) = \sum_{k'=0}^{N-1} x_{k'} \delta_{k-k'} = x_k$$

Note:

For the same discrete signal x_0, \dots, x_{N-1} we thus have two Fourier transforms, i.e.

$$X(f) = \Delta \sum_{k=0}^{N-1} x_k e^{-2\pi j kf\Delta} \quad (4.7)$$

and

$$X_r = \Delta \sum_{k=0}^{N-1} x_k e^{-2\pi j \frac{kr}{N}}. \quad (4.8)$$

Equation 4.7 is a continuous function of f on $-\frac{1}{2\Delta} < f < \frac{1}{2\Delta}$ and is called the Fourier Transform (FT) of x_k . Equation 4.8 is a row of discrete numbers ($r = 0, \dots, N-1$) and is called the Discrete Fourier Transform (DFT) of x_k . Inversion of the DFT now goes through the summation of equation 4.6b (and not the integral of equation 1.12). Comparing equations 4.7 and 4.8 shows that X_r are samples of $X(f)$ at frequency 'distance' $\frac{1}{N\Delta}$ Hz, i.e.

$$X_r = X\left(f = \frac{r}{N\Delta}\right), \quad r = 0, \dots, N-1 \quad (4.9)$$

This is illustrated in figure 4.2.

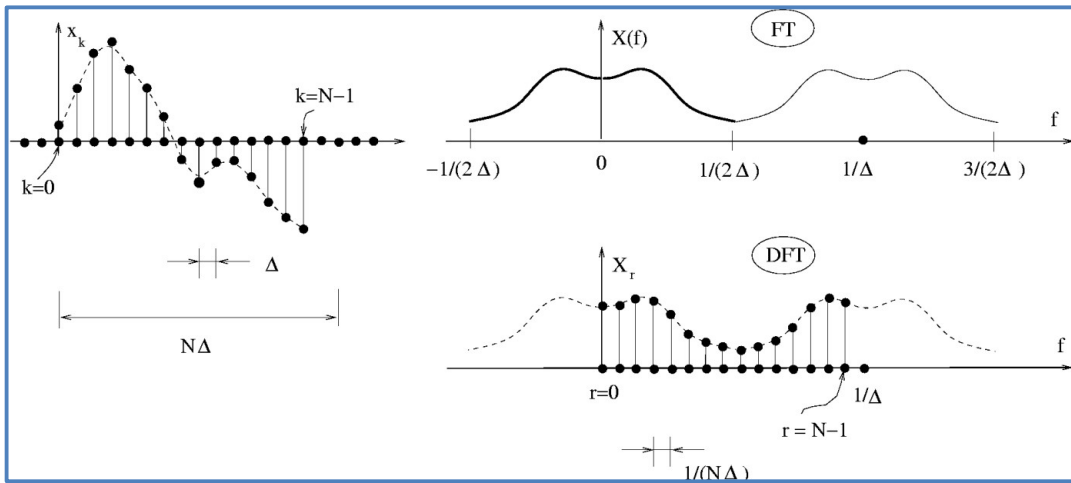


Figure 4.2: The FT and DFT of discrete signal x_k .

Note:

The basis interval of the FT is $\left(-\frac{1}{2\Delta}, \frac{1}{2\Delta}\right)$ and that of the DFT is $\left(0, \frac{1}{\Delta}\right)$, see figure 4.2. This convention is adopted to obtain maximum symmetry in equation 4.6. The negative frequencies $-\frac{1}{2\Delta} < f < 0$ in the FT are now located in the interval $\frac{1}{2\Delta} < f < \frac{1}{\Delta}$ for the DFT. For a real-valued signal, the Hermitian symmetry $X(-f) = X^*(f)$ now becomes

$$X_{N-r} = X_r^* \quad (4.10)$$

For a real-valued signal x_0, \dots, x_{N-1} , only the DFT for $r = 0, \dots, \frac{N}{2}-1$ (N assumed even) needs to be calculated. The rest follows immediately from equation 4.10.

Note:

The DTF is implemented as a FFT, see last note of section 4.1

4.3 Frequency domain filter

The schedule of figure 4.1 (with the continuous FT) can be implemented with the DFT according to the schedule given in figure 4.3 below. Note that all variables are now rows of discrete numbers of length N .

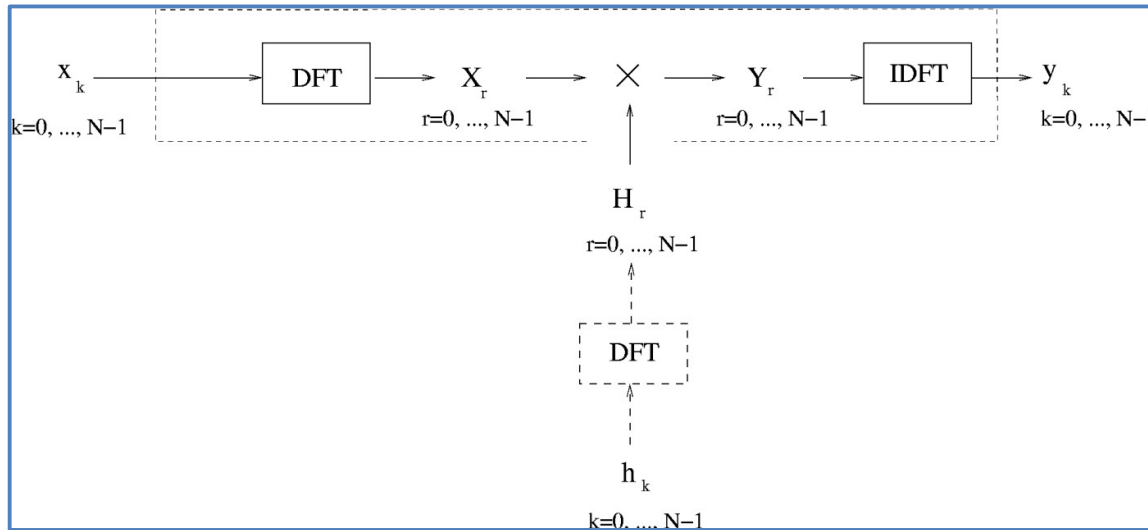


Figure 4.3: Frequency domain filtering with the DFT.

Filtering in the time domain means the ‘linear convolution’ of equation 4.1, which has the following property. When the input signal x_i is of length N_x and the impulse response h_i is of length N_h , then the output signal y_k has length $N_y = N_x + N_h - 1$. Also, with figure 4.3 we have $Y_r = H_r X_r$ instead of $Y(f) = H(f)X(f)$ (equation 4.2). Therefore, filtering in the frequency domain with the DFT will result in a different convolution than the linear convolution of equation 4.1.

Assume $H_r = \sum_{l=0}^{N-1} h_l e^{-2\pi j \frac{rl}{N}}$, i.e. the DFT of h_l according to equation 4.6a (without the Δ factor). We

also have $X_r = \Delta \sum_{i=0}^{N-1} x_i e^{-2\pi j \frac{ir}{N}}$, i.e. the DFT of x_i . The output signal y_k is the IDFT of Y_r (see equation 4.6b):

$$y_k = \frac{1}{N\Delta} \sum_{r=0}^{N-1} H_r X_r e^{2\pi j \frac{kr}{N}} = \frac{1}{N\Delta} \sum_{r=0}^{N-1} \left(\left(\sum_{l=0}^{N-1} h_l e^{-2\pi j \frac{rl}{N}} \right) \left(\Delta \sum_{i=0}^{N-1} x_i e^{-2\pi j \frac{ir}{N}} \right) e^{2\pi j \frac{kr}{N}} \right)$$

which can be written as

$$y_k = \sum_{i=0}^{N-1} \sum_{l=0}^{N-1} x_i h_l \left(\frac{1}{N} \sum_{r=0}^{N-1} e^{2\pi j \frac{r(k-i-l)}{N}} \right) = \sum_{i=0}^{N-1} \sum_{l=0}^{N-1} x_i h_l \delta_{k-i-l+mN}$$

with m any positive or negative integer number (see proof in section 4.2). Hence,

$$y_k = \sum_{i=0}^k x_i h_{k-i} + \sum_{i=k+1}^{N-1} x_i h_{k-i+N} \quad (4.11)$$

We introduce the periodic continuations of x_k , h_k and y_k and denote these as x_k^P , h_k^P and y_k^P , respectively. Then equation 4.11 can be interpreted as the 'periodic convolution' of x_k and h_k :

$$y_k^P = h_k^P \otimes x_k^P = \sum_{i=0}^{N-1} h_{k-i}^P x_i^P \quad (4.12)$$

Note: This periodic convolution can be visualised as follows. Put the N numbers of x_k and h_k along a circle, subsequently rotate the circles for one revolution and sum the products of x_k and h_k , see figure 4.4.

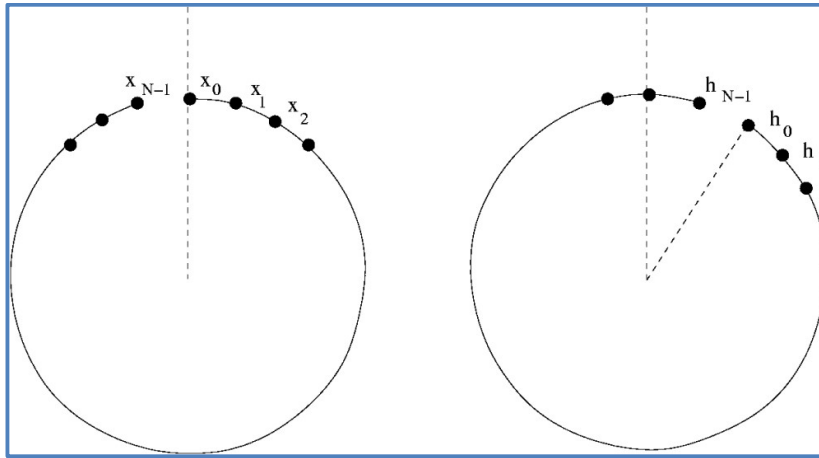


Figure 4.4: Visualization of the periodic convolution.

Apparently, the operation $Y_r = H_r X_r$, $r = 0, \dots, N-1$ results in the periodic convolution $y_k^P = h_k^P \otimes x_k^P$, $k = 0, \dots, N-1$, which is undesired. Hence, the remaining question is how to make

this periodic convolution equal to the linear convolution of equation 4.1. This can easily be accomplished by adding zeros to x_k and h_k up to length N with the condition

$$N \geq N_y = N_x + N_h - 1 \quad (4.13)$$

This length N is now used in the DFT/IDFT schedule of figure 4.3. In this way sufficient zeros are added to x_k and h_k , see figure 4.5. One period of y_k^P , $k = 0, \dots, N-1$ then equals the desired linear convolution $y_k = h_k \otimes x_k$.

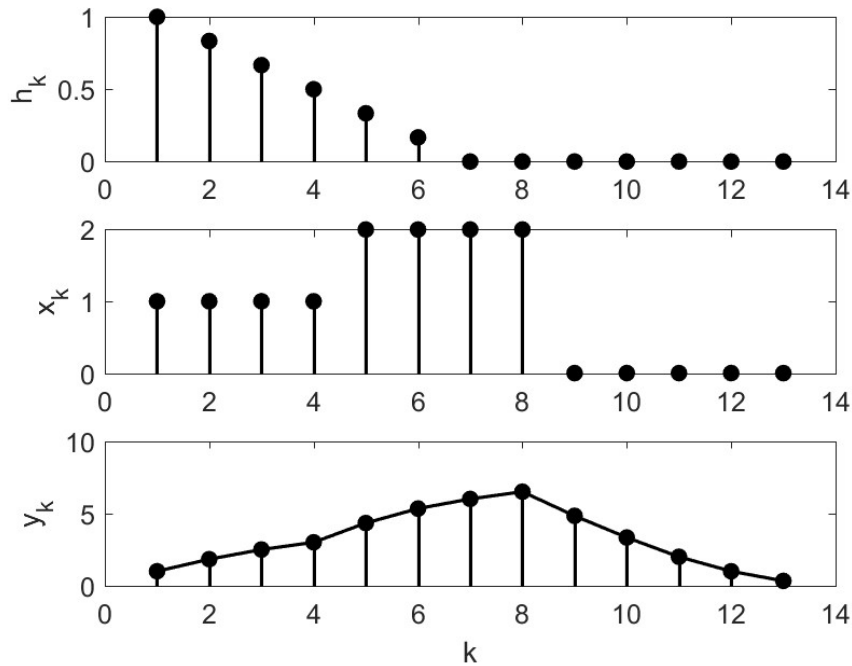


Figure 4.5: Adding sufficient zeros to the signal x_k and the impulse response h_k .

Note: The discussion here about periodic and linear convolution can also be considered as an application of the sampling theorem of chapter 2. In the frequency domain filter (figure 4.3) we use sampled Fourier transforms X_r , H_r and Y_r , implying that the corresponding time signals x_k , h_k and y_k are repeating. By oversampling X_r and H_r , i.e. using a smaller frequency step ($\frac{1}{N\Delta}$) than that required according to the Shannon-Nyquist theorem, empty spaces between the repetitions are created such that the periodic convolution equals the linear convolution.

4.4 Transmission function of the frequency domain filter

For frequency domain filtering an arbitrary transmission function can directly be specified, i.e. we simply specify a row of N numbers $H_r, r = 0, \dots, N-1$. However, the transmission function $H(f)$, i.e. the transmission function with which we actually filter, is different. In principle, $H(f)$ can be calculated according to the schedule of figure 4.6.

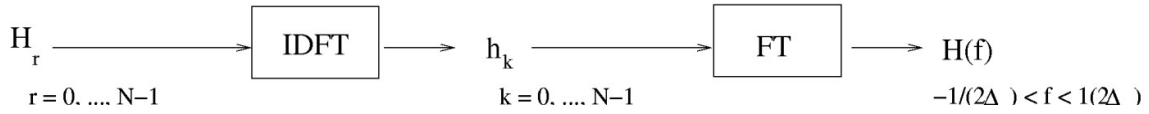


Figure 4.6: The two steps to calculate the actual transmission function $H(f)$ from the specified transmission function H_r .

According to this schedule $H(f)$ is

$$H(f) = \Delta \sum_{k=0}^{N-1} h_k e^{-2\pi jfk\Delta} = \Delta \sum_{k=0}^{N-1} \left(\frac{1}{N\Delta} \sum_{r=0}^{N-1} H_r e^{2\pi j \frac{kr}{N}} \right) e^{-2\pi jfk\Delta}.$$

This can be rewritten as

$$H(f) = \sum_{r=0}^{N-1} H_r \left(\frac{1}{N} \sum_{k=0}^{N-1} e^{2\pi jk \left(\frac{r}{N} - f\Delta \right)} \right).$$

The part of this formula in parentheses is a geometric series, the sum of which is

$$\begin{aligned} \frac{1}{N} \sum_{k=0}^{N-1} e^{2\pi jk \left(\frac{r}{N} - f\Delta \right)} &= \frac{1}{N} \frac{1 - e^{2\pi j \left(\frac{r}{N} - f\Delta \right) N}}{1 - e^{2\pi j \left(\frac{r}{N} - f\Delta \right)}} = e^{-\pi j \left(f - \frac{r}{N\Delta} \right) (N-1)\Delta} \frac{1}{N} \frac{e^{\pi j \left(f - \frac{r}{N\Delta} \right) N\Delta} - e^{-\pi j \left(f - \frac{r}{N\Delta} \right) N\Delta}}{e^{\pi j \left(f - \frac{r}{N\Delta} \right) \Delta} - e^{-\pi j \left(f - \frac{r}{N\Delta} \right) \Delta}} \\ &\approx \frac{\sin \left(\pi \left(f - \frac{r}{N\Delta} \right) N\Delta \right)}{N \sin \left(\pi \left(f - \frac{r}{N\Delta} \right) \Delta \right)} \end{aligned}$$

Hence,

$$H(f) = \sum_{r=0}^{N-1} H_r I \left(f - \frac{r}{N\Delta} \right) \quad \text{with} \tag{4.14}$$

$$I(f) = \frac{\sin(\pi f N\Delta)}{N \sin(\pi f \Delta)}$$

i.e. an interpolation of H_r with the function $I(f)$. This implies that $H(f)$ can exhibit unexpected behaviour between the specified points H_r . This is illustrated in figure 4.7 where we specified a bandpass filter by setting $H_r = 1$ in the passband and $H_r = 0$ outside this passband (i.e. in the stopbands).

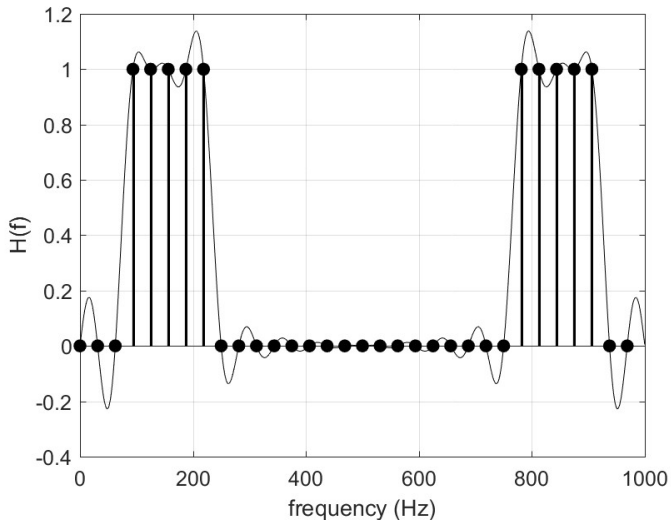


Figure 4.7: Specified transmission function (black dots) and actual transmission function $H(f)$ illustrating the Gibbs effect.

It is observed that in the stopband a significant transmission exists, i.e. they are not perfect stopbands. Furthermore, the passband shows a significant ripple. This is the so-called ‘Gibbs phenomenon’. A second problem is that for the specified H_r it is not guaranteed that equation 4.13 is satisfied. If not, a periodic convolution occurs due to overlap of repetitions of x_k and h_k . In practice, both problems can be made negligible by avoiding abrupt jumps in the specified H_r . This is illustrated in figure 4.8 where a smooth transition from passband to stopband is realized by two intermediate samples in H_r with values 0.11 and 0.59, respectively. Indeed, this eliminates the Gibbs effect and, at the same time, reduces the length of the impulse response (not shown here) and hence reduces the effect of periodic convolution.

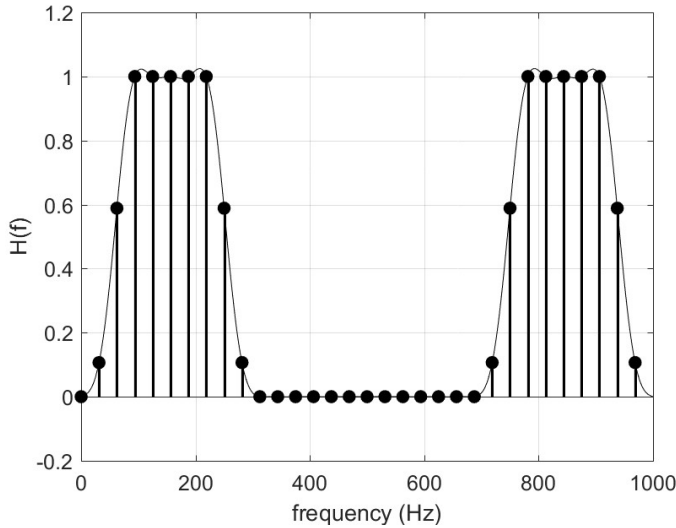


Figure 4.8: Specified transmission function (black dots), now with a smooth transition between passband and stopband. The interpolated transmission function $H(f)$, i.e. the actual transmission function with which the signal is filtered, is now virtually free of the Gibbs effect.

4.5 Application: noise suppression

In this section we illustrate frequency domain filtering for a narrow band signal s_k buried in white noise r_k . The useful signal s_k has a bandwidth of about 75-120 Hz. Hence, the noisy signal is $x_k = s_k + r_k$, see figure 4.9. s_k and x_k are shown in the upper and middle plot of figure 4.10a, respectively. The signal-to-noise-ratio was chosen such that the useful signal is hardly visible in the mixture x_k .

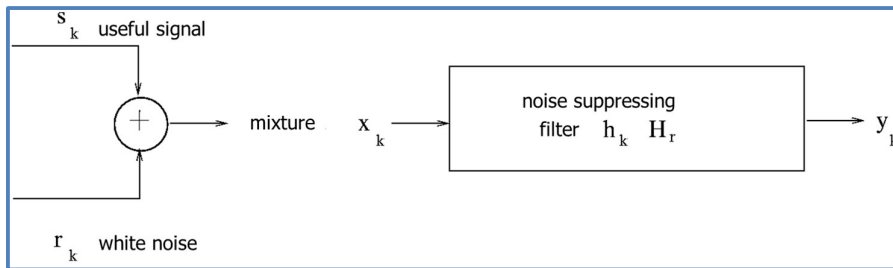


Figure 4.9: Filtering in the frequency domain of a noise-corrupted useful signal.

The signals s_k and r_k have a duration of 0.3 s and are sampled at a frequency of 1000 Hz. Hence, both s_k and r_k consist of 300 samples. The Fourier transforms of s_k and x_k have been determined and are denoted S_r and X_r , the absolute value of which are shown in figure 4.10b. The N in the

DFT of equation 4.6a is equal to 512, i.e. 212 zeros are added to x_k . The frequency distance $\frac{1}{N\Delta}$ of the DFT is thus equal to 2.0 Hz.

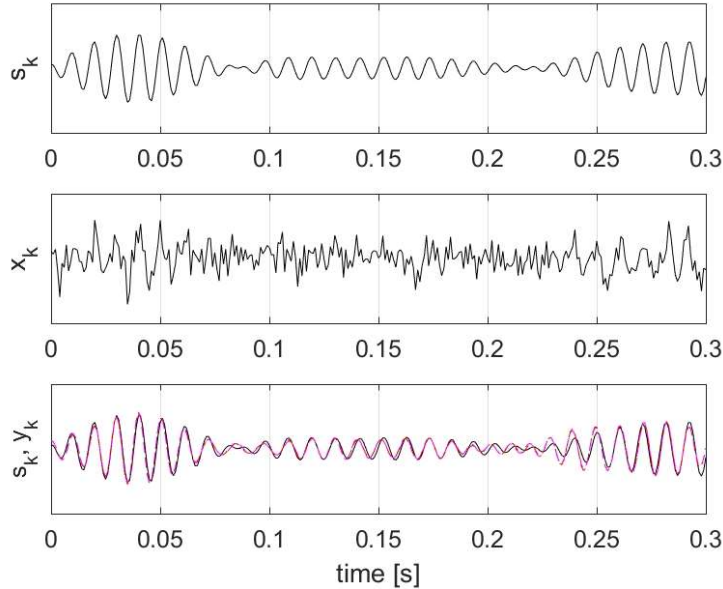


Figure 4.10a: Useful signal s_k (top plot), noise-corrupted signal x_k (middle plot) and filtered signal y_k (bottom plot, red and pink curve). The clean useful signal (black curve) is also plotted in the bottom plot for comparison.

We will apply frequency domain filtering to x_k by multiplying X_r with a transmission function H_r with $H_r = 1$ in the passband (75-120 Hz and 880-925 Hz) and $H_r = 0$ outside this passband. The frequency bins for which $H_r = 1$ are indicated by red crosses in figure 4.10b. Hence, the DFT of the output signal y_k of the noise suppression filter is $Y_r = X_r H_r$. The output signal y_k in the time domain is obtained by taking the IDFT of Y_r and is shown in the bottom plot of figure 4.10a (red curve). For comparison, the original signal s_k is also shown in this plot (black curve). y_k and s_k almost coincide, i.e. the filter operation has been successful. Note that the output signal y_k shows no delay, i.e. the filter H_r (real numbers) is free of dispersion. Also shown in the bottom plot of figure 4.10a (pink curve) is the output signal in case a smooth transition from passband to stopband is applied (see previous section). For this problem no noticeable improvement is observed.

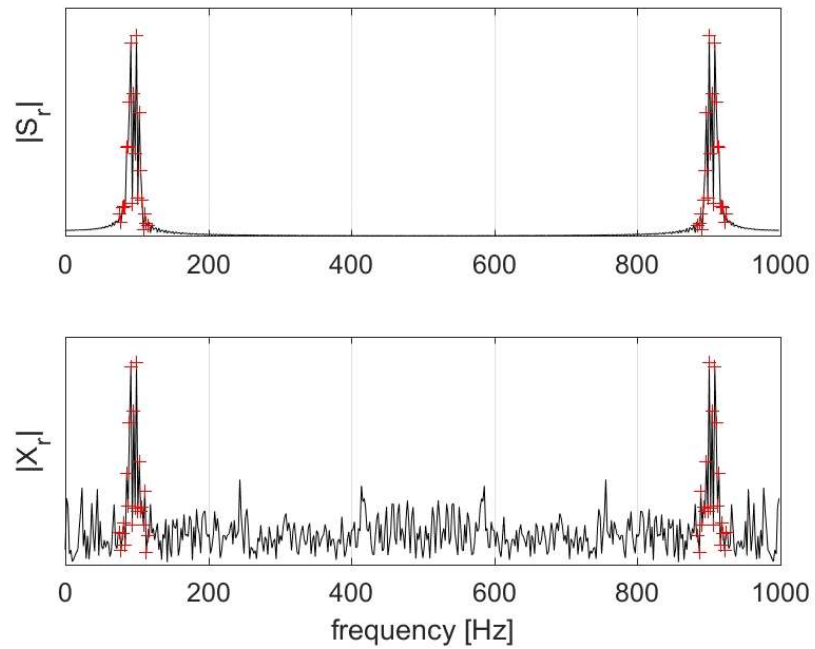


Figure 4.10b: Absolute value of the DFT of useful signal s_k (top plot) and noise-corrupted signal x_k (bottom plot). The frequency bins for which $H_r = 1$ are indicated by red crosses.

4.7 Exercises

Question 1

- (a) A continuous signal $x(t)$ with bandwidth 450 Hz is sampled with $F = 1000$ Hz. We want to make a plot of $|X(f)|$, using 0.25 seconds of the signal, with a frequency step of 1 Hz. Find the required length N of your DFT.
- (b) Next, we want to have twice as many frequencies, i.e. a DFT with a frequency step of 0.5 Hz. Find the required length N of your DFT.
- (c) Finally, we want to convolve 1 second of $x(t)$ with an impulse response of duration 0.5 seconds. This operation is performed in the frequency domain. Find the required length N of your DFT's.

Question 2

Given is the discrete signal $x_k = e^{2\pi j f_0 k \Delta}$, $k = 0, \dots, N-1$.

- (a) Calculate $X(f)$.
- (b) Make a sketch of $|X_r|$ when f_0 is a multiple of $\frac{1}{N\Delta}$, i.e. f_0 is coinciding with a frequency point of the DFT.
- (c) Same as (b), but now f_0 is located in between two frequency points of the DFT.

Chapter 5 The Discrete Fourier Transform as filter bank – spectral analysis

5.1 The ‘sinc’ filter

In this chapter we discuss an important interpretation of the Discrete Fourier Transform (DFT), i.e. the DFT as a set (or bank) of parallel narrow-band filters. Further, we introduce the technique of ‘spectral analysis’ of a (time) signal using the DFT.

We consider the non-causal transversal filter with uniform impulse response

$$h_k = \begin{cases} 1 & k = -M, \dots, +M \\ 0 & \text{elsewhere} \end{cases} \quad (5.1)$$

This impulse response, graphically depicted in figure 5.1, has an effective length of $L = N\Delta = (2M + 1)\Delta$.

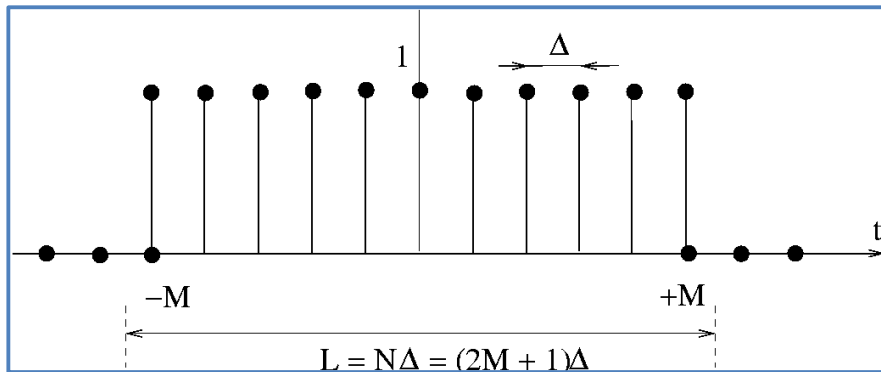


Figure 5.1: The uniform non-causal impulse response of equation 5.1.

The transmission function of this filter is

$$H(f) = \sum_{k=-\infty}^{\infty} e^{-2\pi j f k \Delta} h_k = \frac{\sin(\pi f(2M+1)\Delta)}{\sin(\pi f\Delta)} = \frac{\sin(\pi fL)}{\sin(\pi f\Delta)} \quad (5.2)$$

The derivation of $H(f)$ has already been done in exercise 5 of chapter 1 using equation 1.18 and the equation for the sum of a geometric series: $\sum_{k=0}^N a^k = \frac{1-a^{N+1}}{1-a}$. This $H(f)$, shown in figure 5.2, is called the ‘digital sinc function’, which is closely related to the ‘continuous sinc function’ $\text{sinc}(x) = \frac{\sin(\pi x)}{\pi x}$. In fact, the digital sinc is a repetition of the continuous sinc as caused by the sampling.

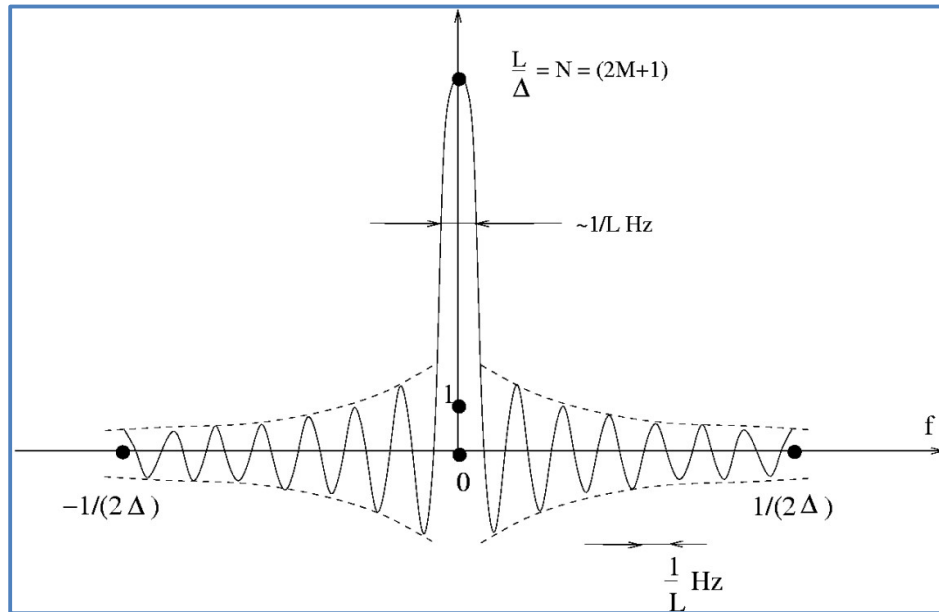


Figure 5.2: Transmission function corresponding to the impulse response of equation 5.1.

Notes:

- This filter is a low-pass filter (LPF). It has a ‘resonance’ peak at $f = 0$. The bandwidth of the peak is $B \approx \frac{1}{L}$ Hz, i.e. inversely proportional to the time duration $L = N\Delta$ of the impulse response.
- There are fairly high ‘side lobes’ in the stopband, which can be suppressed through the application of a weighting function (see section 5.5).
- The filter considered as a transversal filter is a moving average filter that smooths the time signal over $N = (2M + 1)$ points.
- Because of the output bandwidth $B \approx \frac{1}{L}$ Hz, it is allowed to sample the output of the transversal filter with $\geq \frac{2}{L}$ Hz, instead of $\frac{1}{\Delta}$ Hz, i.e. at the filter output the sample frequency may be reduced by a factor $\frac{N}{2}$. This means that the filter output value needs to be calculated only every $\frac{L}{2}$ seconds. This is illustrated in figure 5.3.

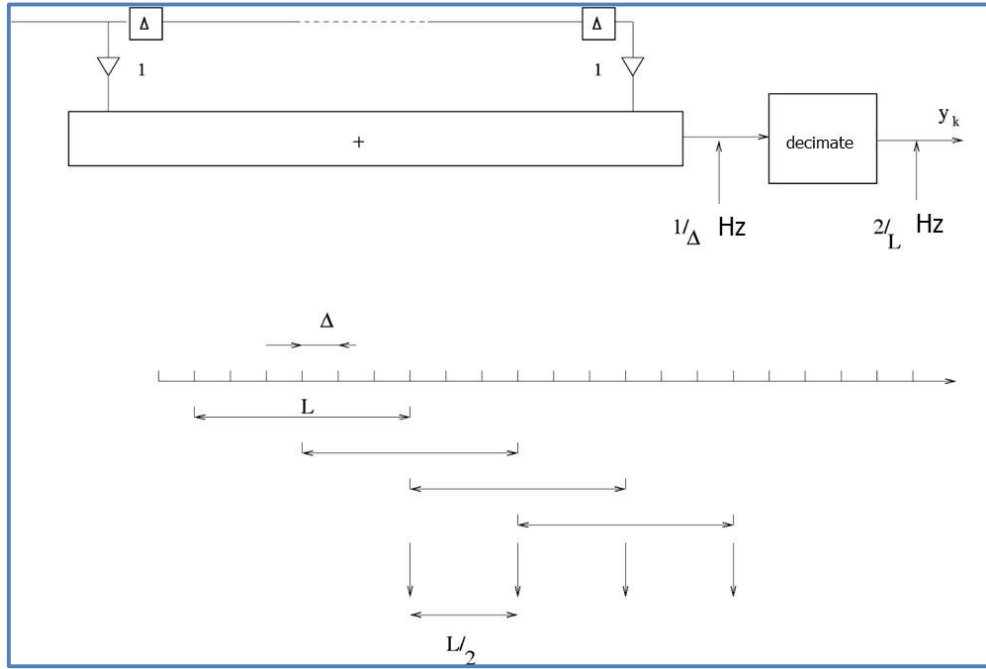


Figure 5.3: A schematic of the processing steps of the moving average filter with the impulse response of equation 5.1.

5.2 The tuned ‘sinc’ filter

We now consider the filter with impulse response

$$h_k = \begin{cases} e^{2\pi j f_0 k \Delta} & k = -M, \dots, +M \\ 0 & \text{elsewhere} \end{cases} \quad (5.3)$$

This is quite a special filter as the impulse response is complex-valued. Hence, the output signal y_k also becomes complex-valued. Such a filter is composed of two real-valued filters, one for $\text{Re}(y_k)$ and one for $\text{Im}(y_k)$, see figure 5.4.

When $A(f)$ is the Fourier transform of a_k , then $A(f - f_0)$ is the Fourier transform of $a_k e^{2\pi j f_0 k \Delta}$ (see section 1.6). Hence, the transmission function of this filter is

$$H(f) = \frac{\sin(\pi(f - f_0)L)}{\sin(\pi(f - f_0)\Delta)}. \quad (5.4)$$

We note that this is a real-valued function.

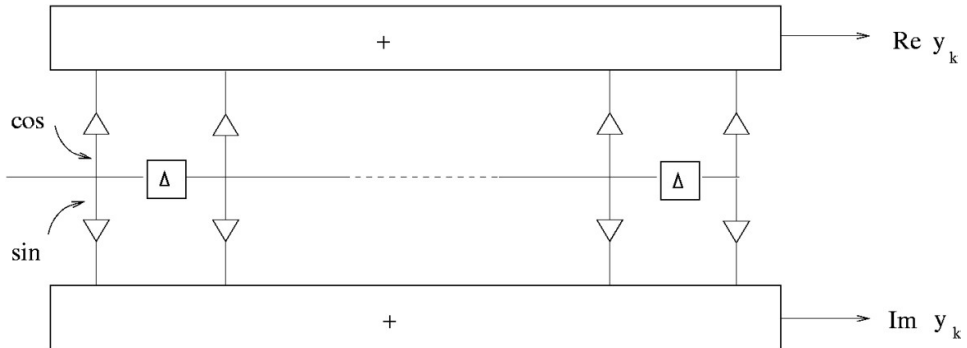


Figure 5.4: Practical implementation of the filter with the impulse response given by equation 5.3.

The transmission function, equation 5.4, is shown in figure 5.5. It is seen that the 'resonance peak' has shifted to $f = f_0$. Note that there is only a transmission peak at $f = +f_0$ and not at $f = -f_0$, i.e. $H(f)$ is asymmetric. The complex-valued impulse response has broken down the Hermitian symmetry, i.e. $H(-f) \neq H^*(f)$. A cosine or sine in the impulse response of equation 5.3 (instead of the exponential) would have resulted in a symmetric $H(f)$, i.e. with a peak at $f = +f_0$ and at $f = -f_0$.

Because of the single transmission peak at $f = +f_0$, we are still allowed to sample the output of the filter at $\geq \frac{2}{L}$ Hz.

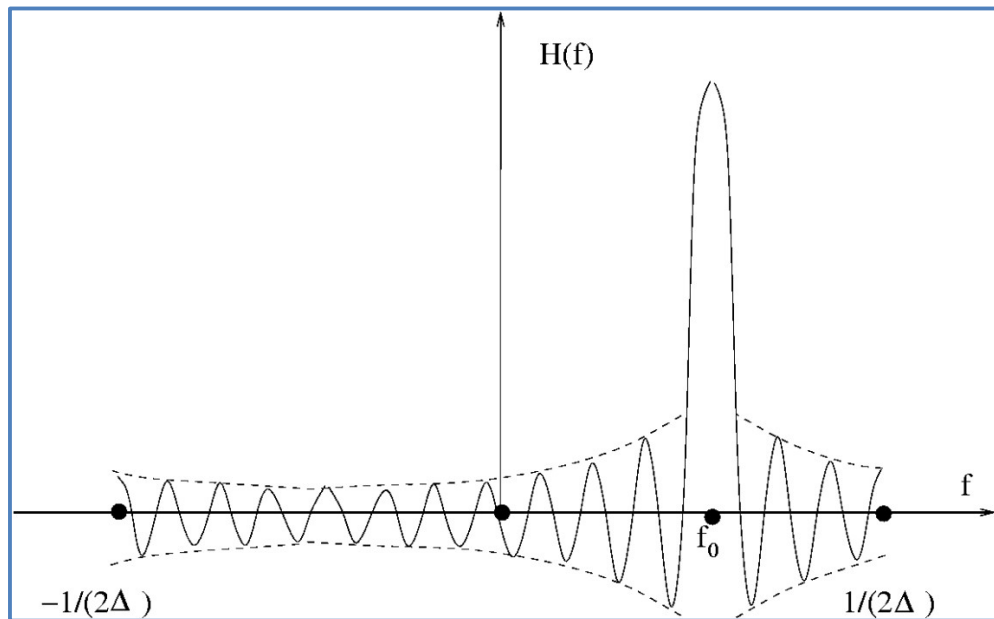


Figure 5.5: Transmission function corresponding to the impulse response of equation 5.3.

5.3 The DFT as filter bank

Recall that, given the input x_k , the output of a filter is $y_i = \sum_{k=-M}^M h_k x_{i-k}$. For $i=0$ this is

$y_0 = \sum_{k=-M}^M h_k x_{-k}$. For the filter of equation 5.3 this becomes

$$y_0 = \sum_{k=-M}^M x_k e^{-2\pi j f_0 k \Delta}. \quad (5.5)$$

Apart from the factor Δ and a shift in the summation index k , equation 5.5 is the expression for the Discrete Fourier Transform (DFT), equation 4.6a:

$$X_r = \Delta \sum_{k=0}^{N-1} x_k e^{-2\pi j \frac{kr}{N}}, \quad r = 0, \dots, N-1 \quad (5.6)$$

Hence, we may conclude that a DFT of size N can be considered as the output, at a single time instant, of a set or bank of N transversal filters tuned at the frequencies $f_r = \frac{r}{N\Delta}$, $r = 0, \dots, N-1$ (see figure 5.6).

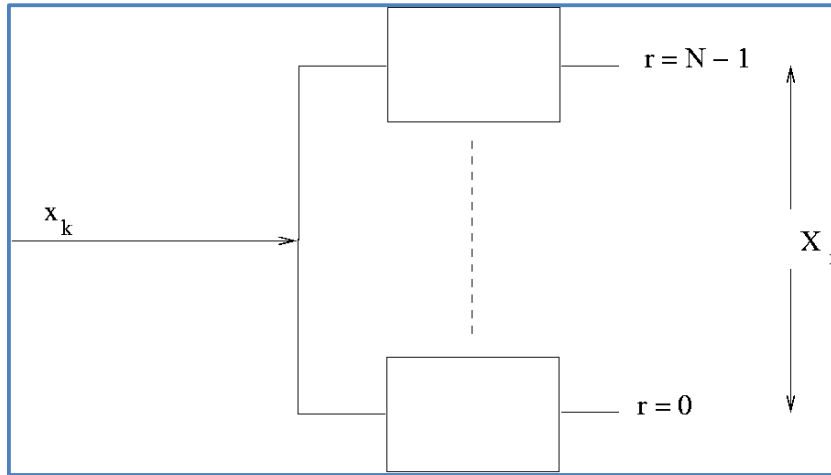
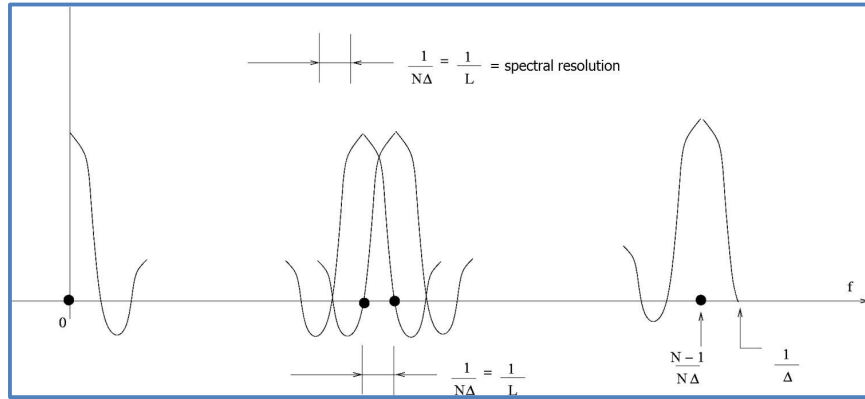


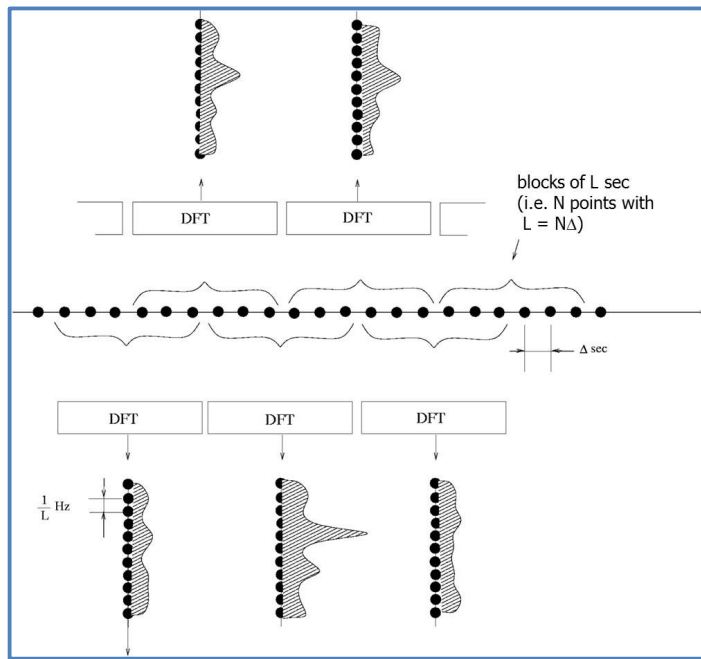
Figure 5.6: The Fourier transform as a bank of N transversal filters.

Each transversal filter has a transmission function according to equation 5.4 with $f_0 = f_r = \frac{r}{N\Delta}$ for $r = 0, \dots, N-1$. The peak bandwidth for each filter is the same and equal to $\frac{1}{L}$, see figure 5.7.

Figure 5.7: Transmission functions (cf. equation 5.4) of the N transversal filters of figure 5.6.

5.4 Spectral analysis

The Discrete Fourier Transform DFT is commonly used for ‘spectral analysis’ of discrete time signals. To this end the DFT is calculated for subsequent blocks of N points (i.e. $L = N\Delta$ seconds) of the time signal. Usually, these data blocks are chosen to be half-overlapping. Then the output rate of this spectral analysis is $\frac{2}{L}$ DFT spectra per second. In this way, each $\frac{L}{2}$ seconds the presence of spectral components in each of the N frequency channels is investigated, see figure 5.8. The topic of spectral analysis is further discussed in chapter 6.

Figure 5.8: Spectral analysis using subsequent (overlapping) blocks of the time signal, each of length L seconds.

5.5 Weighting functions to suppress side lobes

The significantly high side lobes of the sinc transmission function of equation 5.4 give rise to substantial sensitivity at frequencies away from the resonance peak. In addition, a weak signal at a certain frequency can be totally masked by a side lobe from a stronger signal. This phenomenon is commonly referred to as ‘leakage’ and is caused by the abrupt beginning and ending (at $k = \pm M$) of the impulse responses of equations 5.1 and 5.3. Leakage can be counteracted by taking an impulse response that smoothly goes to zero at the edges at $k = \pm M$, which can be accomplished by applying a suitable weighting function to the impulse response. Then the effect on the transmission function is twofold:

- The side lobes become considerably lower;
- The main lobe gets broader.

The desired effect of lower side lobes is obtained at the cost of a broader main lobe. However, typically the side lobe level is reduced by a factor of 1000, whereas the main lobe only gets wider by a factor of typically 1.5 to 2.

An example of a frequently used weighting function is the so-called ‘Hanning’ or ‘raised cosine’ function given by

$$g_k = 1 + \cos\left(2\pi k \frac{\Delta}{L}\right) \quad k = -M, \dots, +M \quad (5.7)$$

which can be written as $g_k = \left(\frac{1}{2}e^{-2\pi j k \frac{\Delta}{L}}\right) + (1) + \left(\frac{1}{2}e^{2\pi j k \frac{\Delta}{L}}\right)$. The transmission function of g_k is

$$G(f) = \frac{1}{2} \frac{\sin\left(\pi\left(f + \frac{1}{L}\right)L\right)}{\sin\left(\pi\left(f + \frac{1}{L}\right)\Delta\right)} + \frac{\sin(\pi f L)}{\sin(\pi f \Delta)} + \frac{1}{2} \frac{\sin\left(\pi\left(f - \frac{1}{L}\right)L\right)}{\sin\left(\pi\left(f - \frac{1}{L}\right)\Delta\right)}. \quad (5.8)$$

Note that the first and the third term in this equation are shifted versions of $H(f)$ (i.e. the middle term of the equation) with a shift equal to one frequency bin, i.e. $\frac{1}{L} = +\frac{1}{N\Delta}$ and $-\frac{1}{L} = -\frac{1}{N\Delta}$, respectively.

Figure 5.9 shows the unweighted and the weighted impulse response (equations 5.1 and 5.7, both for $M = 10$) and their corresponding transmission functions, $H(f)$ and $G(f)$, respectively. It is observed (right bottom plot) that the side lobe reduction is the result of a compensation of the negative first side lobe of $H(f)$ by positive side lobes of the first and the third term of equation 5.8.

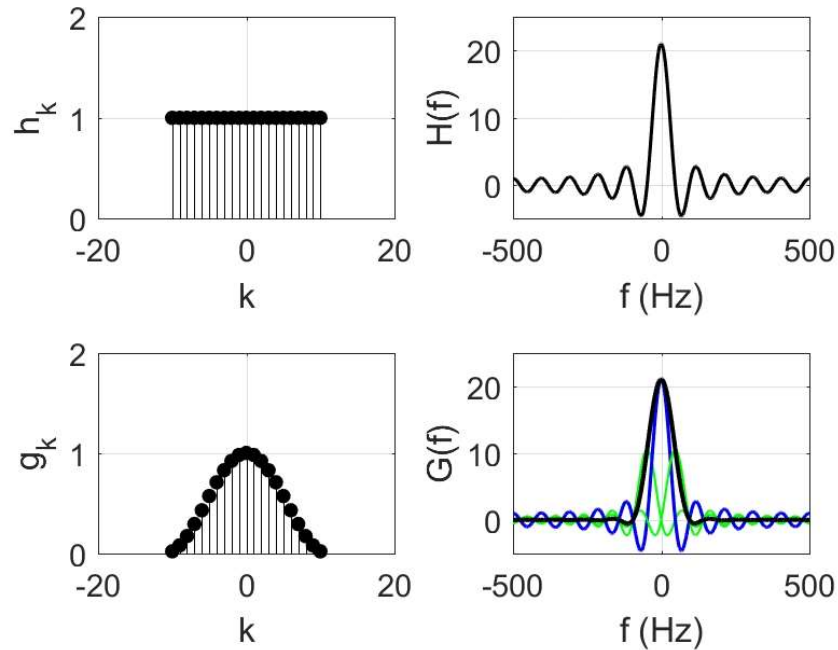


Figure 5.9: Unweighted and weighted impulse responses (left figures) and their corresponding transmission functions (right figures, black lines). The right bottom plot illustrates how the side lobe reduction is obtained. A sample frequency of 1000 Hz ($\Delta = 1$ ms) is chosen.

The transmission functions of the unweighted and the weighted impulse response , $H(f)$ and $G(f)$, are shown in figure 5.10 on a dB scale to emphasize the side lobe reduction.

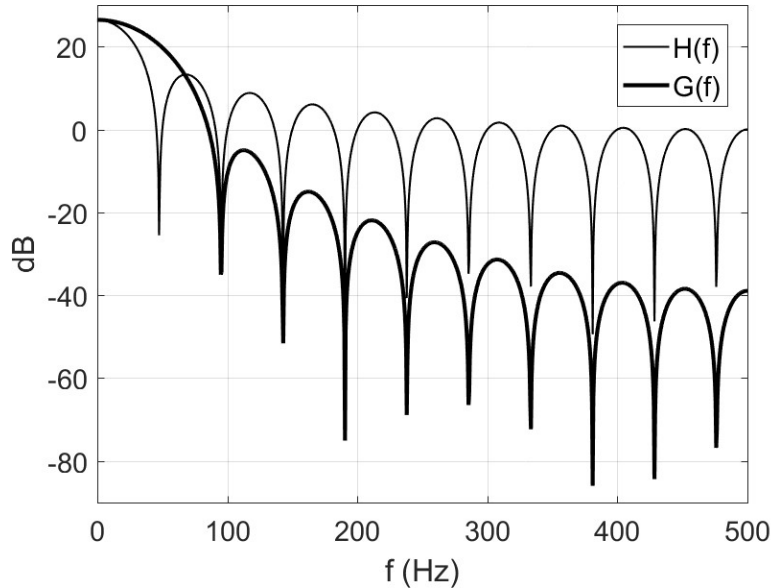


Figure 5.10: Transmission functions $H(f)$ and $G(f)$ on a dB scale (only positive frequencies shown).

Note: Also in spectral analysis with the DFT, weighting functions are applied. The expression for the DFT, equation 5.6, is then replaced by

$$X'_r = \Delta \sum_{k=0}^{N-1} g_k x_k e^{-2\pi j \frac{kr}{N}}, \quad r = 0, \dots, N-1. \quad (5.9)$$

5.6 Exercise

Consider the signal $x_k = \sin(2\pi f_1 k \Delta) + 0.1 \sin(2\pi f_2 k \Delta)$ $k = 0, \dots, N-1$

with $\Delta = 1$ ms, $N = 128$ and $f_1 = 100$ Hz and $f_2 = 125$ Hz.

- (a) Calculate the DFT X_r of x_k and make a plot of $|X_r|$. Estimate the relative amplitude of the second sine in the signal from this plot.
- (b) Add zeros to the signal x_k up to 1024 samples, i.e. 896 zeros are added to the signal (called ‘zero padding’). Calculate again the DFT X_r of x_k and make a plot of $|X_r|$. Estimate the relative amplitude of the second sine in the signal from this plot. Compare with the result of question (a).
- (c) Now first apply Hanning weighting to the original signal x_k (consisting of 128 samples). Subsequently apply zero padding to the signal up to 1024 samples. Finally, calculate again the DFT X_r of x_k and make a plot of $|X_r|$. Estimate the relative amplitude of the second sine in the signal from this plot. Compare with the result of question (b).

Note: for this exercise you need Matlab.

Chapter 6 Analogy with phased arrays

6.1 Introduction

There exists an analogy between the transmission function $H(f)$ (equations 5.2 and 5.4) of the transversal filters of the previous chapter 5 and the beam patterns of so-called ‘phased array antennas’. Through this analogy chapter 5 almost completely provides the foundations of electronically steered phased arrays. However, there is also an analogy with optical diffraction with which we will start.

6.2 Diffraction pattern as Fourier transform of aperture illumination

We consider a 1D opening or aperture along the x -axis from $x = -\frac{L}{2}$ to $x = +\frac{L}{2}$, see figure 6.1.

Point O is the origin and point S an arbitrary point along the x -axis within the aperture.

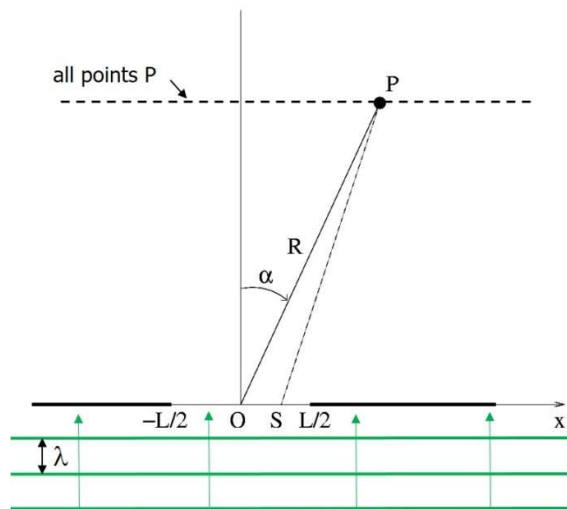


Figure 6.1: Plane wave impinging from below on an aperture of size L .

Assume that a plane and coherent wave front of monochromatic laser light arrives from below at the aperture (with wave fronts parallel to the x -axis). With f being the frequency of the light (i.e.

wavelength $\lambda = \frac{c}{f}$, c being the speed of light), the light oscillation in the aperture is given by

$$a(x) e^{2\pi j f t} \quad (6.1)$$

with $a(x)$ the aperture illumination. When the illumination over the aperture is uniform we have $a(x) = 1$.

We consider the point P at distance R from the centre O of the aperture, PO making an angle α with respect to the vertical, see figure 6.1. To determine the contribution from S to the light oscillation in P , we have to account for the delay due to the path length PS . According to the cosine rule for triangle OSP we have

$$PS^2 = R^2 + x^2 - 2xR \cos\left(\frac{\pi}{2} - \alpha\right).$$

Hence, distance PS is

$$PS = \sqrt{R^2 + x^2 - 2xR \sin \alpha} = R \sqrt{1 + \left(\frac{x}{R}\right)^2 - 2\left(\frac{x}{R}\right) \sin \alpha}.$$

Assuming $x \ll R$, this can be approximated by

$$PS \approx R \sqrt{1 - 2\left(\frac{x}{R}\right) \sin \alpha} \approx R \left(1 - \frac{1}{2} \left(\frac{2x}{R}\right) \sin \alpha\right).$$

Hence, we obtain

$$PS(x) \approx PO - x \sin \alpha = R - x \sin \alpha. \quad (6.2)$$

In this approximation, where PS depends linearly on x , we assume that all rays from S to P are parallel. This so-called Fraunhofer or far field approximation is correct at sufficiently large distances R .

The travel time of the light from S to P is $\frac{PS(x)}{c}$ and hence the light oscillation in P becomes the ‘sum’ of all the delayed contributions, i.e.

$$\int_{-L/2}^{L/2} e^{2\pi j f(t-PS(x)/c)} dx = e^{2\pi j f t} e^{-2\pi j f \frac{R}{c}} \int_{-L/2}^{L/2} e^{2\pi j f \frac{x \sin \alpha}{c}} dx. \quad (6.3)$$

In this formula we have omitted the attenuation due to the spherical spreading of the wave between S and P (and we have assumed that this attenuation is independent of x). This is part of the Fraunhofer approximation where the x -dependence is only accounted for in the delay time $\frac{PS(x)}{c}$.

We now consider all possible points P along a line parallel to x -axis, see figure 6.1. Assuming these to be at the same distance R , the delay factor $e^{-2\pi j f R/c}$ in equation 6.3 becomes a constant that is omitted hereafter. Hence, the light amplitude at P becomes

$$\int_{-L/2}^{L/2} e^{2\pi j \frac{x \sin \alpha}{\lambda}} dx. \quad (6.4)$$

Finally, we replace the direction α by a new direction coordinate k given by

$$k = \frac{\sin \alpha}{\lambda} \quad \text{with} \quad -\frac{1}{\lambda} < k < \frac{1}{\lambda} \quad (6.5)$$

k is also called the ‘spatial frequency’. The light amplitude in P can now be written as

$$A(k) = \int_{-L/2}^{L/2} e^{2\pi j k x} dx = L \frac{\sin(\pi k L)}{\pi k L} \quad (6.6)$$

i.e. the well-known ‘sinc’-shaped diffraction pattern of a 1D slit. Note that $A(k)$ is the Fourier transform of the block function

$$a(x) = \begin{cases} 1 & \text{for } -\frac{L}{2} \leq x \leq \frac{L}{2} \\ 0 & \text{elsewhere} \end{cases}$$

(see section 1.6). The function $A(k)$ is shown in figure 6.2. Note that this is not a periodic function, in contrast to the result of section 6.4 for phased arrays.

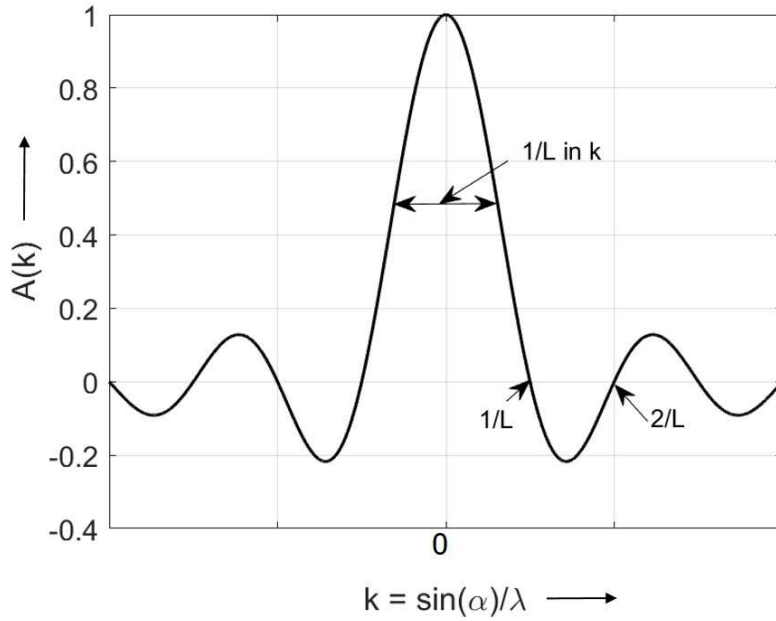


Figure 6.2: The diffraction pattern function $A(k)$ cf. equation 6.6 and its properties.

Note: For $\lambda \ll L$ the width of the main 'lobe' (in angle α) of the function $A(k)$ is equal to $\frac{\lambda}{L}$ (radians).

Now assume we put a glass in the aperture that has an optical transmission and/or optical thickness that depend on x , see figure 6.3. Then the illumination of the aperture at the exit side of the glass becomes

$$a(x) = |a(x)| e^{j\arg a(x)} \quad (6.7)$$

with $|a(x)|$ the optical transmission of the glass and $\arg a(x)$ the phase shift due to varying optical thickness.

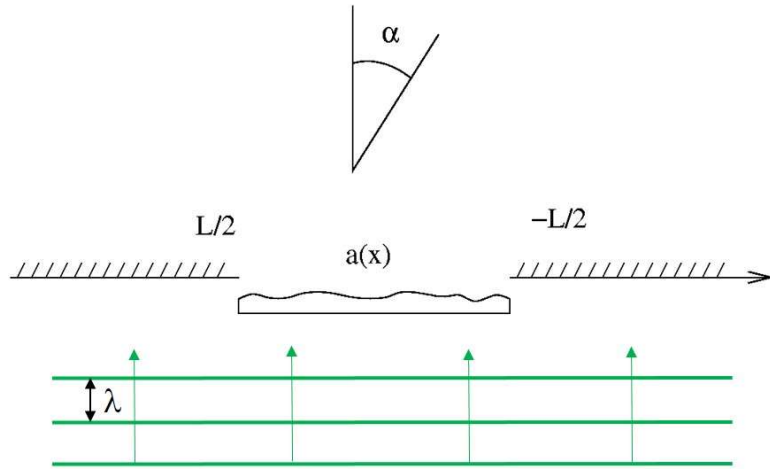


Figure 6.3: Plane wave impinging from below on an aperture with varying thickness $a(x)$.

The Fraunhofer approximation remains valid, but now the contribution from the point S in the aperture equals $a(x)$. Instead of equation 6.6 we obtain

$$A(k) = \int_{-L/2}^{L/2} a(x) e^{2\pi j kx} dx \quad (6.8)$$

i.e. the Fourier transform of the aperture illumination $a(x)$. Again, the mechanism of diffraction results in a Fourier transform.

Note: For the notation to be consistent with the previous chapters a minus sign in the exponent of equation (6.8) is needed. This is however not essential.

Note: In reality optical diffraction should be treated in a 2D way, i.e. the aperture is a hole in a (x, y) -plane with illumination $a(x, y)$ and the far field point P is determined by the two directions $\sin \alpha$ and $\sin \beta$. Using the Fraunhofer approximation we obtain the 2D diffraction pattern

$$A(k_x, k_y) = \iint_{\text{aperture}} a(x, y) e^{2\pi j (xk_x + yk_y)} dx dy \quad (6.9)$$

with $k_x = \frac{\sin \alpha}{\lambda}$ and $k_y = \frac{\sin \beta}{\lambda}$.

i.e. a 2D Fourier transform of $a(x, y)$. As this is not important for the basic principle, we continue with the 1D case.

6.3 The analogy

The table below gives the analogy between the diffraction pattern $A(k)$ and the transmission function $H(f)$ of a continuous filter (see chapter 1).

<u>Filter</u>	<u>Diffraction</u>
impulse response $h(t)$ t = time (sec)	aperture illumination $a(x)$ x = position (m)
transmission function $H(f)$ $H(f) = \int h(t) e^{-2\pi j f t} dt$ f = frequency (s^{-1})	diffraction pattern $A(k)$ $A(k) = \int_{-L/2}^{L/2} a(x) e^{2\pi j k x} dx$ k = spatial frequency (m^{-1})

It is important to understand why $k = \frac{\sin \alpha}{\lambda}$ in equation 6.8 is called spatial frequency. The dimension of k is indeed m^{-1} . Further, the interpretation of equation 6.8 is that $A(k)$ is the amplitude of the Fourier component $e^{-2\pi j k x}$ occurring in $a(x)$, because

$$a(x) = \int_{-1/\lambda}^{1/\lambda} A(k) e^{-2\pi j k x} dk.$$

Now suppose that $a(x)$ only consists of this one Fourier component, i.e.

$$a(x) = e^{-2\pi j k x} = e^{-2\pi j \frac{\sin \alpha}{\lambda} x}.$$

This is a light wave with wavelength λ propagating in the direction α , projected along the x -axis.

This wave has a wavelength $\frac{\lambda}{\sin \alpha}$ along the x -axis and hence a spatial frequency of $\frac{\sin \alpha}{\lambda}$ (m^{-1}).

This is illustrated in figure 6.4. Each Fourier component $e^{-2\pi j k x}$ of $a(x)$ corresponds to its own plane wave direction $\alpha = \sin^{-1}(k\lambda)$. The complete set of plane waves gives the diffraction pattern $A(k)$ in the far field.

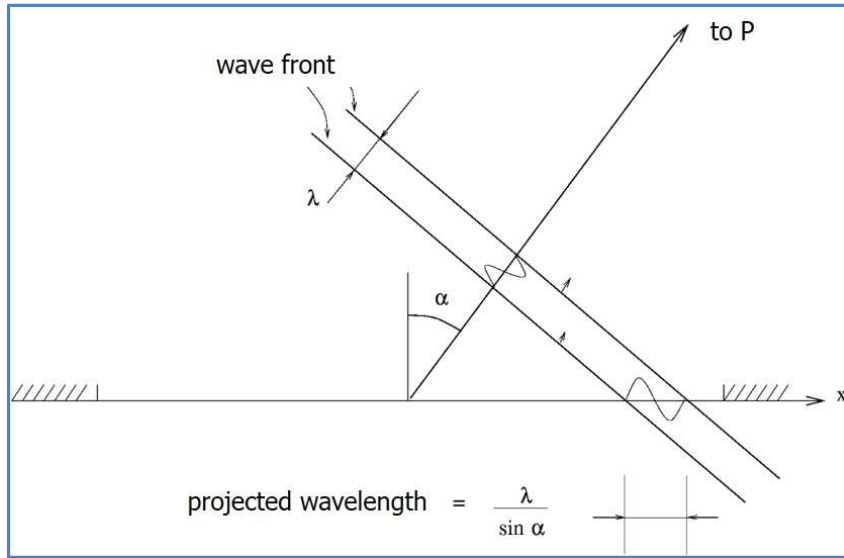


Figure 6.4: Plane wave with wavelength λ propagating in the direction α . Also indicated is the projected wavelength on the x -axis.

6.4 Phased array antennas

We have discussed the analogy between the diffraction pattern of an aperture and the transmission function of a continuous filter (the aperture illumination $a(x)$ is a continuous function of x). However, in acoustic imaging, radar and microwave technology etc. use is made of so-called ‘phased arrays’ consisting of discrete antenna elements. (The distance between the elements of the antenna is equal to Δ meter). Such ‘sampled’ antennas are the analogy of the discrete transversal filters of the previous chapter 5. This analogy holds for both the antenna in transmission and receiving mode, see figure 6.5.

The directionality of a phased array increases with $\frac{L}{\lambda}$, see figure 6.2 (and figure 6.6), hence long antennas have a significant directionality (given the wavelength λ). An advantage of phased arrays is that their beam direction can be electronically steered without the need to rotate the antenna mechanically.

Figure 6.5 shows a phased array antenna (both in transmission and receiving mode) consisting of $2M + 1$ elements along the x -axis. The element positions are $x_i = i\Delta$, $i = -M, \dots, M$ and the effective antenna length is $L = N\Delta = (2M + 1)\Delta$. Note that the effective length here is not equal to the actual array length $L = (N - 1)\Delta = 2M\Delta$, see also figure 5.1.

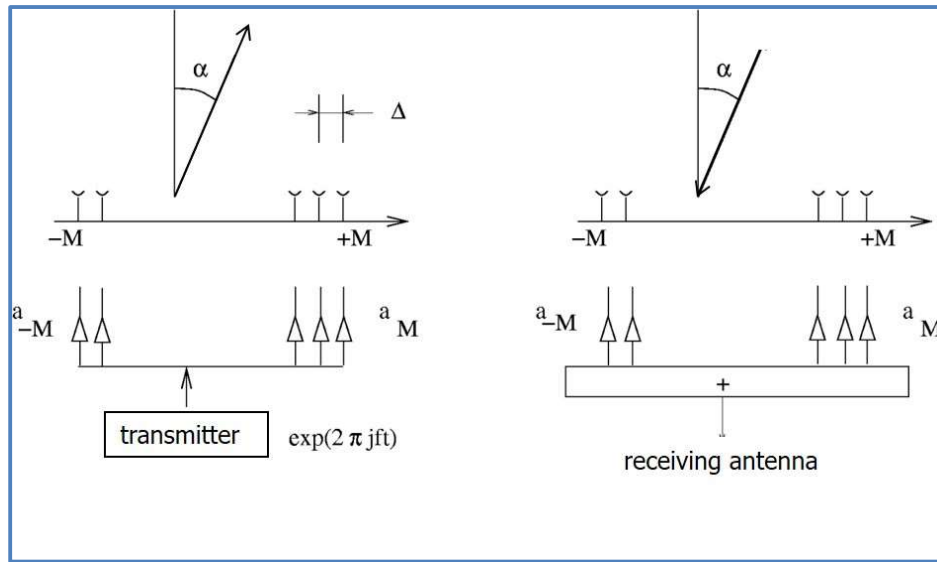


Figure 6.5: Phased array in transmission (left) and receiving (right) mode.

A directional beam centred around $\alpha = 0$ is obtained when all elements transmit the same signal $e^{2\pi j f t}$ (with $a_i = 1$, i.e. a uniform illumination). This results in a Fraunhofer pattern according to equation 6.4:

$$A(k) = \sum_{i=-M}^M e^{2\pi j k x_i} = \sum_{i=-M}^M e^{2\pi j k i \Delta} \quad (6.10)$$

which becomes the ‘digital sinc’ function of equation 5.2 (with f replaced by k):

$$A(k) = \frac{\sin(\pi k L)}{\sin(\pi k \Delta)}. \quad (6.11)$$

Now $A(k)$ is a periodic function in k (with period $1/\Delta$), in contrast to equation 6.6. Note that $A(0) = N$. Figure 6.6 shows $A(k)$ plotted as a function of k for $M = 5$ (and thus $N = 11$).

The Fraunhofer function $A(k)$ is, similar to the diffraction pattern of equation 6.6, the far field amplitude distribution of the antenna pattern, i.e. most radiation goes in directions around $\alpha = 0$ (the main lobe) and less radiation goes into other directions (the side lobes). Still, a significant amount of radiation (10-20 %) is emitted in these side lobe directions.

To create a narrow receiving beam at $\alpha = 0$ (see right part of figure 6.5) we have to add the signals from all array elements with $a_i = 1$ for all i . Then a plane wave from the direction $\alpha = 0$ gives the highest antenna output as all signals are in phase. Plane waves from other directions yield signals that are out of phase, at least to a certain extent, and hence result in a lower antenna output. In this

receiving mode, the beam pattern is also given by equation 6.11, but now $A(k)$ can be regarded as a sensitivity pattern of the antenna.

For both the transmitting and receiving mode of the phased array, we can electronically steer the beam in any desired direction by applying phase factors to the array elements according to

$$a_i = e^{-2\pi j k_0 x_i} = e^{-2\pi j k_0 i \Delta} \quad (6.12)$$

i.e. phase is linear in x . In transmission mode the individual array element signals are then $s_i(t) = e^{2\pi j f t} e^{-2\pi j i k_0 \Delta}$. Equations 6.10 and 6.11 now become

$$A(k) = \sum_{i=-M}^M e^{2\pi j (k-k_0)x_i} = \sum_{i=-M}^M e^{2\pi j i (k-k_0)\Delta} = \frac{\sin \pi(k-k_0)L}{\sin \pi(k-k_0)\Delta} \quad (6.13)$$

i.e. the periodic function of equation 5.4 (with f replaced by k). This $A(k)$ is the antenna pattern of equation 6.11 but shifted over the spatial frequency k_0 (and hence rotated over angle α_0 with $k_0 = \frac{\sin \alpha_0}{\lambda}$). Figure 6.7 shows $A(k)$ plotted as a function of k with $M = 5$ and $k_0 = 0.35 \frac{1}{2\Delta}$.

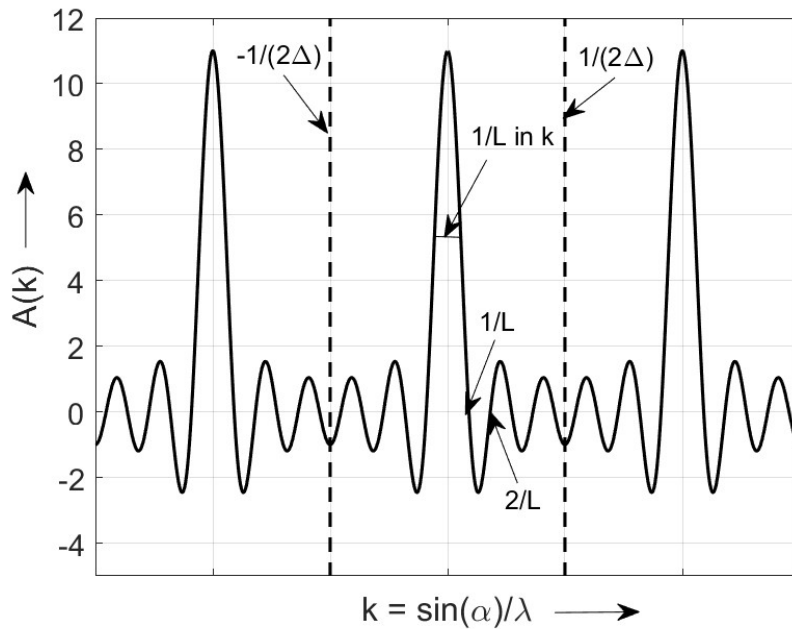


Figure 6.6: The function $A(k)$ cf. equation 6.11 and its properties (for $M = 5$).

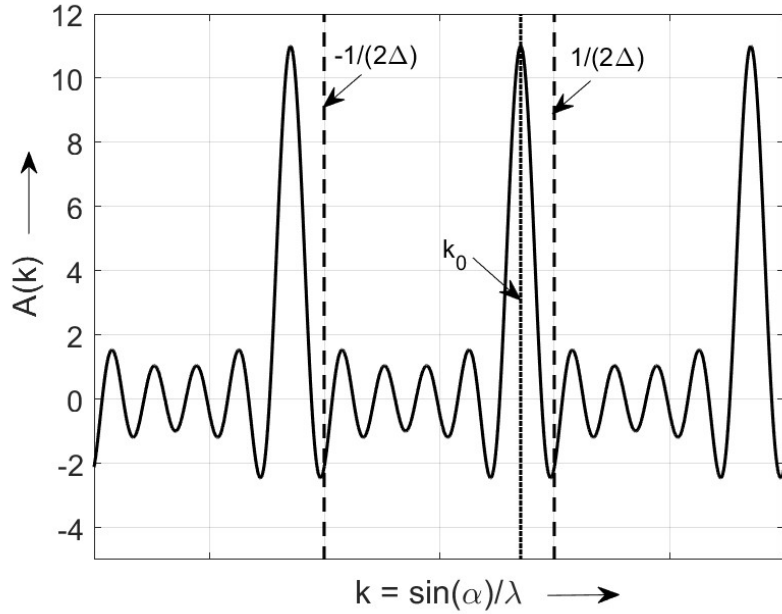


Figure 6.7: The function $A(k)$ cf. equation 6.13 and its properties (for $M = 5$ and $k_0 = 0.35$)

The phases according to equation 6.12 compensate the differences in travel time for a wave front in the direction k_0 in such a way that for this particular direction the $2M+1$ signals add up with the same phase and thus give a maximum output. In other words, by applying appropriate phase shifts to the array elements, one can steer the antenna beam in any desired direction from $k_0 = -\frac{1}{\lambda}$ to $k_0 = \frac{1}{\lambda}$ (or from $\alpha_0 = -\frac{\pi}{2}$ to $\alpha_0 = \frac{\pi}{2}$). Hence, the name 'phased array'. The beam steering is accomplished electronically, i.e. without any mechanical movement of the antenna.

As already mentioned, the 'digital sinc' function of equation 6.13 is a periodic function in k with period $1/\Delta$. Hence, this function is not only maximal when $k = k_0$ but also when

$$\pi(k - k_0)\Delta = \pm m\pi, \quad m = 1, 2, 3, \dots$$

or

$$\sin \alpha = \sin \alpha_0 \pm m \frac{\lambda}{\Delta}, \quad m = 1, 2, 3, \dots \quad (6.14)$$

When this equation in α has solutions, then at these values of α the function is maximal in addition to the maximum at the desired direction α_0 . Such undesired maxima are called ‘grating lobes’ and these have to be avoided. The grating lobe equation 6.14 has no solutions (for all values of α_0) when

$$\frac{\lambda}{\Delta} > 2 \quad \text{or} \quad \Delta < \frac{\lambda}{2} \quad (6.15)$$

i.e. grating lobes are avoided when the antenna element spacing is chosen to be less than half the wavelength of interest. Condition 6.15 is the spatial equivalent of the Nyquist sampling theorem (see section 2.3.2) and hence avoids ‘spatial alias’.

In section 5.3 we showed that the DFT can be considered as the output of a set of N transversal filters tuned at the frequencies $f_r = \frac{r}{N\Delta}$. Similarly, we can make the phased array antenna sensitive in N consecutive beams that simultaneously span the entire field of view. This is implemented by using N antenna ‘processors’ each with its own value of k_0 in formula 6.13, i.e.

$$k_0 = k_r = \frac{r}{N\Delta} \quad r = -M, \dots, +M. \quad (6.16)$$

Note: Section 5.5 introduced the concept of reducing the side lobe levels of the DFT by applying a weighting function to the time domain signal. Similarly, a reduction of the side lobe levels of the antenna pattern of equation 6.13 can be accomplished by applying a weighting function g_i to the phase factors of equation 6.12, i.e.

$$a_i = g_i e^{-2\pi j k_0 i \Delta}. \quad (6.17)$$

This results in strongly reduced side lobes at the expense of a slightly increased width of the beam.

6.5 Applications

Phased array antennas are applied in:

- radio communication ($L \approx 1 \text{ m}$)
- radar systems ($L \approx 1 - 10 \text{ m}$)
- imaging aircraft noise ($L \approx 1 \text{ m}$)
- seismic (for oil exploration and earth quake registration, $L \approx 100 \text{ m}$)
- sonar (for submarine detection and oil exploration, $L \approx 100 \text{ m}$)
- medical imaging ($L \approx 0.1 \text{ m}$)

The typical array length L is determined by the wavelength of interest used in these applications, since directionality scales with $\frac{L}{\lambda}$ (i.e. angular resolution in radians scales as $\frac{\lambda}{L}$). In most cases tens to hundreds of array elements are used.

6.6 Exercise

Consider a 1D phased array for imaging aircraft noise. The number of elements is $N = 11$ ($M = 5$) and the element spacing is $\Delta = 0.2$ m. Make a polar diagram of the sensitivity of the antenna pattern ($|A(k)|$ versus α) for a frequency of 850 Hz and $\alpha_0 = 0$ (array not steered) and $\alpha_0 = 45^\circ$ (array steered in the direction 45°). The sound speed in air is 340 m/s.

Chapter 7 Properties of noise signals – spectral analysis revisited

7.1 Introduction

In the previous chapters we already talked about noise signals, e.g. in section 4.5 where a useful narrow band signal buried in white noise was recovered by frequency domain filtering. In this chapter we discuss the properties of noise signals in more detail. We will discuss discrete noise signals r_k , i.e. rows of random variables sampled with sample distance Δ , see figure 7.1.

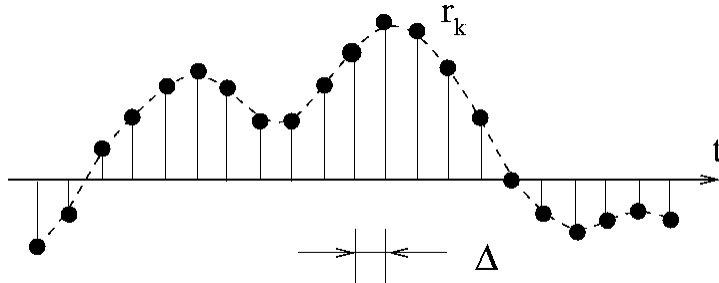


Figure 7.1: A noise signal r_k sampled with a sampling distance Δ .

We limit the discussion to so-called stationary noise signals, i.e. noise for which the statistical properties do not change with time. In general, stationary noise originates from sources for which the macroscopic physical conditions do not change. We subsequently treat four statistical characteristics of noise: mean, variance, covariance and spectrum.

7.2 Mean and variance

We only consider noise signals with mean or average value equal to zero, i.e.

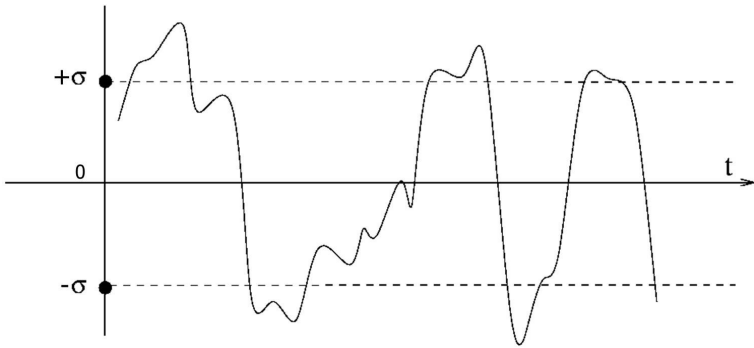
$$E(r) = \frac{1}{N} \sum_{k=0}^{N-1} r_k = \bar{r} = 0 \quad (7.1)$$

with E the expectation value operator.

The variance or averaged quadratic value of a noise signal (with $\bar{r} = 0$) is given by

$$E(r^2) = \frac{1}{N} \sum_{k=0}^{N-1} r_k^2 = \bar{r^2} = \sigma^2 \quad (7.2)$$

The standard deviation σ is a measure for the strength of the noise fluctuations, see figure 7.2.

Figure 7.2: A noise signal and its corresponding standard deviation σ .

7.3 Covariance

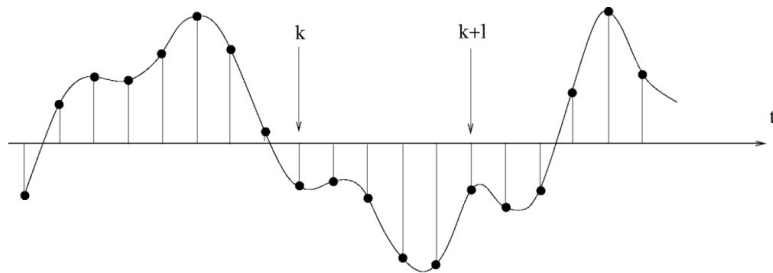
Consider the noise signal shown in figure 7.3. The covariance function of a noise signal is defined as

$$R_l = E(r_k r_{k+l}) = \frac{1}{N} \sum_{k=0}^{N-1} r_k r_{k+l} = \overline{r_k r_{k+l}} \quad (7.3)$$

which is equal to

$$R_{-l} = E(r_k r_{k-l}) = \frac{1}{N} \sum_{k=0}^{N-1} r_k r_{k-l} = \overline{r_k r_{k-l}}$$

i.e. the covariance function is a symmetric function: $R_l = R_{-l}$.

Figure 7.3: Noise samples k and $k+l$ in a discrete noise signal for defining the covariance function.

The covariance function R_l is a measure of the internal statistical coherence within the noise signal.

R_l has the following properties

$$\begin{aligned} l = 0 & \quad R_0 = \overline{r^2} = \sigma^2 \\ l \rightarrow \pm\infty & \quad R_l \rightarrow 0 \end{aligned} \quad (7.4)$$

i.e. for large l the statistical coherence is lost in all noise signals (no proof provided here for this).

In general, rapidly fluctuating noise signals have a short ‘correlation time’, i.e. a rapid decline of R_l to zero, while slowly fluctuating noise signals have a longer correlation time. This is illustrated in figures 7.4a and 7.4b for noise signals with bandwidths of 350 Hz and 50 Hz, respectively. (These signals were obtained by low-pass filtering a white noise signal). In fact, the correlation time is inversely proportional to bandwidth.

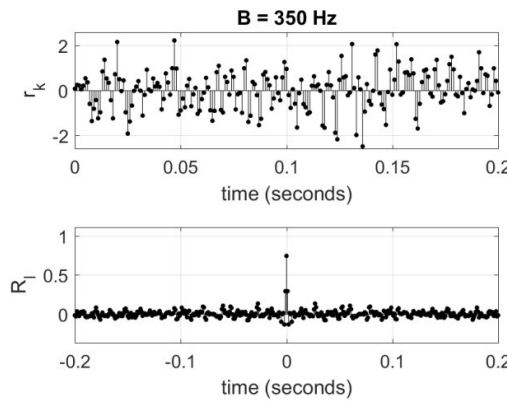


Figure 7.4a: Noise signal r_k (bandwidth 350 Hz) and corresponding covariance function R_l .

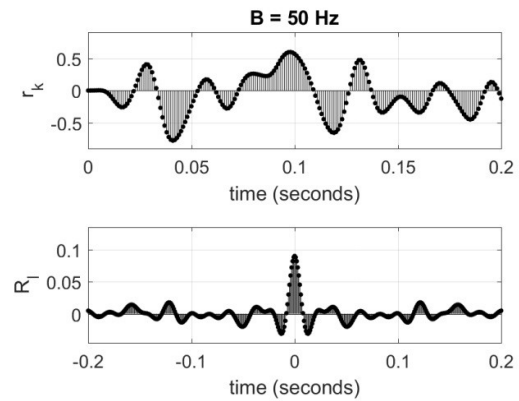


Figure 7.4b: Noise signal r_k (bandwidth 50 Hz) and corresponding covariance function R_l .

Note: The speed of fluctuation in a noise signal is not only reflected in the covariance function R_l , but also in the ‘spectrum’ $P(f)$ of the signal (spectrum is introduced in the next section). Hence, there is a relation between R_l and $P(f)$. This is the so-called Wiener-Khintchin relation, see section 7.5.

7.4 Spectrum

As with all discrete time signals with sample distance Δ , the frequency axis of a discrete noise signal ranges from $-\frac{1}{2\Delta}$ to $+\frac{1}{2\Delta}$ Hz. The ‘spectrum’ $P(f)$ of a (noise) signal indicates how the variance

σ^2 is distributed over these frequencies, see the example of figure 7.5 below. When the noise signal r_k has units of Volt, then variance σ^2 is in Volt² and spectrum $P(f)$ is in Volt²/Hz.

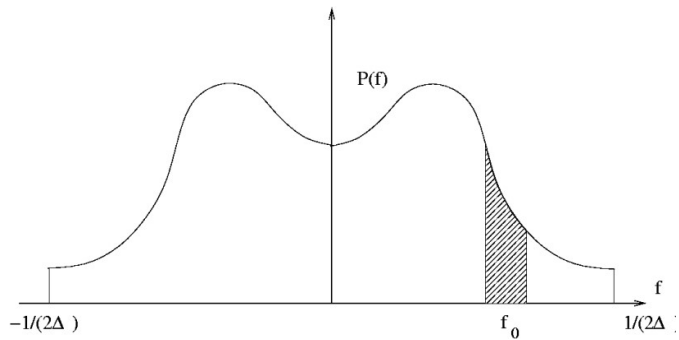


Figure 7.5: Example of a spectrum of a noise signal.

The variance of r_k in band df around frequency f is $P(f)df \text{ Volt}^2$. Hence,

$$\sigma^2 = \int_{-\frac{1}{2\Delta}}^{\frac{1}{2\Delta}} P(f)df. \quad (7.5)$$

From the definition of $P(f)$ (see below) and the Wiener-Khintchin relation (see section 7.5) it will follow that $P(f)$ is symmetrical, i.e.

$$P(-f) = P(f). \quad (7.6)$$

The spectrum is defined as follows. Filter the noise signal r_k with a filter with bandwidth B around frequency f_0 and with a transmission equal to 1 in the passband, see figure 7.6. The variance of the output signal y_k is $\overline{y^2}$. We then define $P(f_0)$ as

$$P(f_0) = \lim_{B \rightarrow 0} \frac{\overline{y^2}}{B} \quad (7.7)$$

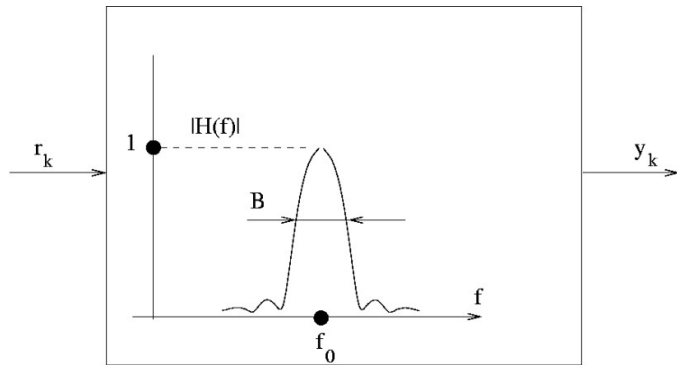


Figure 7.6: The bandpass filter used to define the spectrum of a (noise) signal.

For this filter we choose the transversal filter of section 5.2 (equation 5.3):

$$h_k = \begin{cases} \frac{1}{N} e^{2\pi j f_0 k \Delta} & k = -M, \dots, +M \\ 0 & \text{elsewhere} \end{cases} \quad (7.8)$$

with $N = 2M + 1$. The corresponding transmission function is (equation 5.4)

$$H(f) = \frac{\sin(\pi(f - f_0)L)}{N \sin(\pi(f - f_0)\Delta)}. \quad (7.9)$$

According to equation 5.5 the variance at the output of this filter then is

$$\overline{y^2} = \overline{\left| \frac{1}{N} \sum_{k=-M}^M r_k e^{-2\pi j f_0 k \Delta} \right|^2}. \quad (7.10)$$

This is the numerator in equation 7.7. The denominator of equation 7.7 is

$$B = \frac{1}{|H(f_0)|^2} \int_{-\frac{1}{2\Delta}}^{\frac{1}{2\Delta}} |H(f)|^2 df. \quad (7.11)$$

According to equation 7.9 we have $H(f_0) = 1$. The integral in equation 7.11 can be calculated with Parseval's equation.

Intermezzo: Parseval equation

For a (real) continuous signal $a(t)$ with Fourier transform $A(f) = \int_{-\infty}^{\infty} a(t) e^{-2\pi j ft} dt$ Parseval's equations reads $\int_{-\infty}^{\infty} |A(f)|^2 df = \int_{-\infty}^{\infty} a(t)^2 dt$ (provided the integrals exist).

For a (real) discrete time signal a_k with Fourier transform $A(f) = \Delta \sum_k a_k e^{-2\pi j fk\Delta}$ we have

$$|A(f)|^2 = A(f) A^*(f) = \left(\Delta \sum_k a_k e^{-2\pi j fk\Delta} \right) \left(\Delta \sum_{k'} a_{k'} e^{+2\pi j fk'\Delta} \right) = \Delta^2 \sum_k \sum_{k'} a_k a_{k'} e^{2\pi j f(k'-k)\Delta}.$$

$$\text{Hence, } \int_{-\frac{1}{2\Delta}}^{\frac{1}{2\Delta}} |A(f)|^2 df = \Delta^2 \sum_k \sum_{k'} a_k a_{k'} \int_{-\frac{1}{2\Delta}}^{\frac{1}{2\Delta}} e^{2\pi j f(k'-k)\Delta} df.$$

$$\text{The integral is already determined in chapter 1: } \int_{-\frac{1}{2\Delta}}^{\frac{1}{2\Delta}} e^{2\pi j f(k'-k)\Delta} df = \frac{1}{\Delta} \delta_{k'-k}.$$

Thus $\int_{-\frac{1}{2\Delta}}^{\frac{1}{2\Delta}} |A(f)|^2 df = \Delta \sum_k \sum_{k'} a_k a_{k'} \delta_{k'-k} = \Delta \sum_k a_k^2$, which is Parseval's equation for real discrete time signals.

Applying Parseval for the (complex) impulse response h_k of equation 7.8 (with Fourier transform $H(f) = \sum_k h_k e^{-2\pi j fk\Delta}$, i.e. without the Δ), we obtain

$$\int_{-\frac{1}{2\Delta}}^{\frac{1}{2\Delta}} |H(f)|^2 df = \frac{1}{\Delta} \sum_k |h_k|^2. \quad (7.12)$$

Hence, equation 7.11 becomes

$$B = \frac{1}{\Delta} \sum_k |h_k|^2 = \frac{1}{\Delta} \sum_k \frac{1}{N^2} = \frac{1}{N\Delta}. \quad (7.13)$$

(see also section 5.1, first note, which is proved here now).

The limit $B \rightarrow 0$ in equation 7.7 corresponds to $N \rightarrow \infty$. Hence, equation 7.7 (using equation 7.10 and 7.13) becomes

$$P(f_0) = \lim_{N \rightarrow \infty} N\Delta \overline{\left| \frac{1}{N} \sum_{k=-M}^M r_k e^{-2\pi j f_0 k \Delta} \right|^2} \quad (7.14)$$

which can be rewritten as

$$P(f_0) = \lim_{N \rightarrow \infty} \frac{1}{N\Delta} \overline{\left| \Delta \sum_{k=-M}^M r_k e^{-2\pi j f_0 k \Delta} \right|^2} \quad (7.15)$$

i.e. the averaged absolute value squared of the Fourier transform of an N -point part of the noise signal divided by the corresponding time $N\Delta$ of this Fourier transform. For obtaining the noise 'spectrum' or 'power spectral density' $P(f_0)$ we have to take the limit of this for $N \rightarrow \infty$.

Introducing

$$Q(f) = \frac{1}{N\Delta} \left| \sum_{k=-M}^M r_k e^{-2\pi j f_0 k \Delta} \right|^2 \quad (7.16)$$

then

$$P(f) = \lim_{N \rightarrow \infty} \overline{Q(f)} \quad (7.17)$$

with the smooth function $P(f)$ the true power spectral density (or spectrum), i.e. an intrinsic statistical property of the noise signal as a whole. $Q(f)$ is the absolute value squared of the Fourier transform of an arbitrary N -point part of the noise signal (divided by time $N\Delta$) and as such a realization (i.e. an estimate) of $P(f)$. Consequently, $Q(f)$ exhibits statistical fluctuations and is generally not a smooth function. The spectral details in $P(f)$ become more and more visible when increasing N (in equation 7.17), whereas the averaging of $Q(f)$ over many realizations reduces the statistical fluctuations. This is illustrated by the example at the end of section 7.6.

Note: When a noise signal $x(t)$ with spectrum $P_x(f)$ is put at the input of a filter with transmission function $G(f)$, then the spectrum of the output signal $y(t)$ is $P_y(f) = |G(f)|^2 P_x(f)$.

7.5 Wiener-Khintchin relation

According to the Wiener-Khintchin theorem, the power spectral density (or in short spectrum) $P(f)$ and covariance function R_l are each other's Fourier transform, i.e.

$$\begin{aligned} P(f) &= \Delta \sum_{l=-\infty}^{\infty} R_l e^{-2\pi j f l \Delta} \\ R_l &= \int_{-\frac{1}{2\Delta}}^{\frac{1}{2\Delta}} P(f) e^{2\pi j f l \Delta} df \end{aligned} \quad (7.18)$$

(without proof)

Notes:

- R_l follows from $P(f)$ and vice-versa, i.e. R_l and $P(f)$ provide the same statistical description of the noise signal r_k .
- For white noise we have $P(f) = P_0$, i.e. a constant. Then

$$R_l = \int_{-\frac{1}{2\Delta}}^{\frac{1}{2\Delta}} P(f) e^{2\pi j f l \Delta} df = P_0 \int_{-\frac{1}{2\Delta}}^{\frac{1}{2\Delta}} e^{2\pi j f l \Delta} df = \frac{P_0}{\Delta} \delta_l \text{ (see figure 7.7 below).}$$

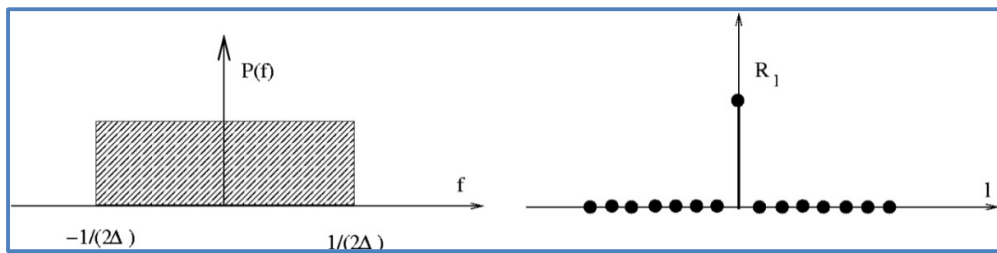
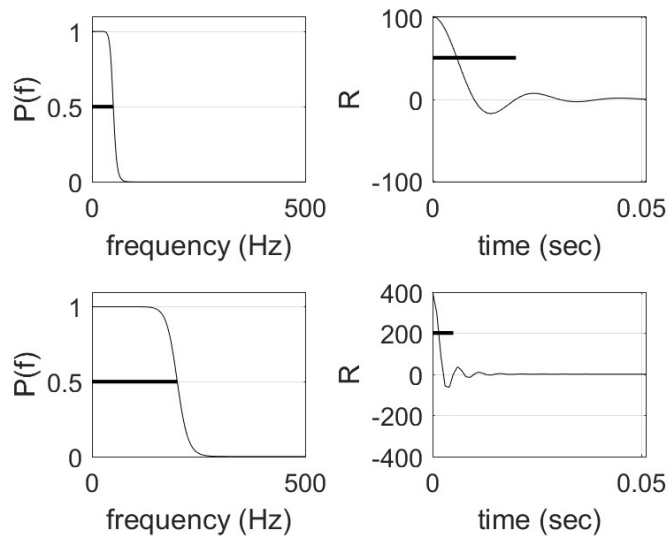


Figure 7.7: Spectrum (left) and covariance function (right) of white noise.

- Suppose $P(f)$ is a smooth function with bandwidth B , then R_l is a smooth function too with 'correlation time' $T_c \approx \frac{1}{B}$, see figure 7.8 below.

Figure 7.8: Spectrum $P(f)$ (left plots) and corresponding covariance function R_l (right plots) for noise signals with bandwidth $B = 50$ Hz (upper plots) and $B = 200$ Hz (lower plots). Bandwidth B and correlation length T_c are indicated by the horizontal thick black lines.

- Suppose $P(f)$ is a function with smallest detail of length W , then R_l is function with range, i.e. correlation time, $T_c \approx \frac{2}{W}$ and smallest detail of length $\sim 2\Delta$ (see figure 7.9).

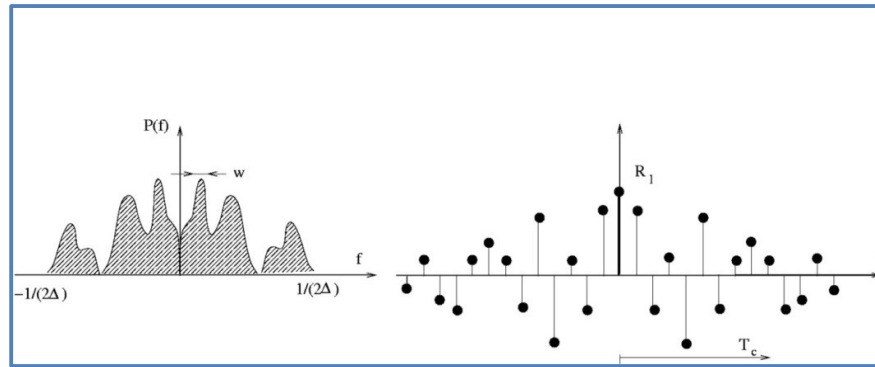


Figure 7.9: Spectrum (left figure) with smallest detail W and corresponding covariance function (right figure) with correlation time $T_c \approx 2/W$.

The above 4 notes not only refer to properties of $P(f)$ and R_l , but are properties of any Fourier transformation pair.

7.6 Spectral analysis

In practice the power spectral density $P(f)$ is determined according to its definition, equation 7.15, i.e. the following steps are taken:

- The noise signal is divided up in blocks of length N ;
- The DFT is computed for each data block $i = 1, \dots, I$ (i.e. there are I blocks in total). The DFT's have $\frac{N}{2}$ frequency channels, each with bandwidth $B = \frac{1}{N\Delta}$;
- The DFT's are squared and averaged over the I blocks.

These four steps, known in the literature as the ‘Bartlett method’, are illustrated in figure 7.10. We note that the total duration of the noise signal used is $NI\Delta$ seconds. In the ‘Welch method’ for determining the spectrum, the data blocks are half overlapping and a weighted DFT is used (see section 5.5).

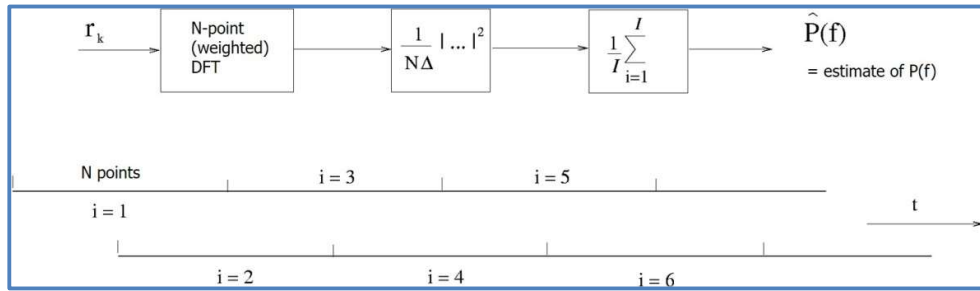


Figure 7.10: Block diagram illustrating the estimation of the spectrum of a (noise) signal.

When compared to the definition of $P(f)$, equation 7.15, this procedure leads to two types of errors. Hence, we obtain an estimate $\hat{P}(f)$ that differs from the true spectrum $P(f)$. First, N cannot be made infinite, the consequence of which is that the DFT channels have a finite bandwidth $B = \frac{1}{N\Delta}$, i.e. the spectral resolution is finite. Hence, $\hat{P}(f)$ is a smoothed version of $P(f)$:

$$\hat{P}(f) = \int |H(f' - f)|^2 P(f') df' = |H(f)|^2 \otimes P(f). \quad (7.19)$$

This illustrated by the example in figure 7.11a.

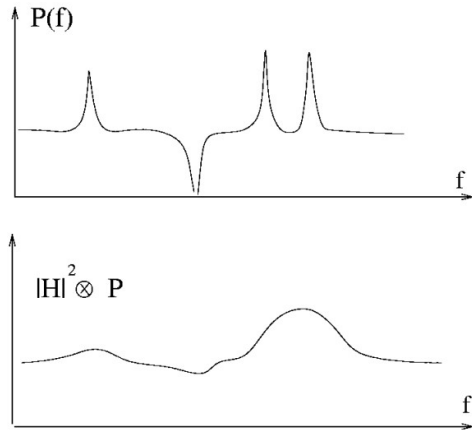


Figure 7.11a: True spectrum (top figure) and estimated spectrum (bottom figure) due to the finite resolution of the spectrum estimation method.

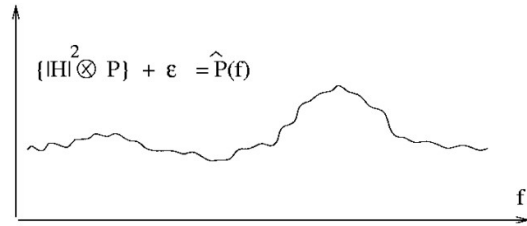


Figure 7.11b: Statistical uncertainty on the estimated spectrum (same example as that of figure 7.11a).

Second, the averaging is done over a finite number I of DFT's, which leads to a statistical uncertainty in $\hat{P}(f)$. Therefore,

$$\hat{P}(f) = |H(f)|^2 \otimes P(f) + \varepsilon(f). \quad (7.20)$$

The effect is shown in figure 7.11b for the same example as that of figure 7.11a. The frequency-dependent standard deviation of $\varepsilon(f)$ is approximately equal to $\frac{P(f)}{\sqrt{I}}$. The relative error is thus equal to $\frac{1}{\sqrt{I}}$, i.e. independent of $P(f)$. The relative error decreases with increasing I according to \sqrt{I} .

Another method for spectrum estimation, using the Wiener-Khintchin relation, is as follows. First, an estimate \hat{R}_l is made of the true covariance function R_l . If we average over NI data points (see figure 7.12), then we use a noise signal of equal length as that used in the previous method. Subsequently, we use the DFT (equation 7.18) to transform \hat{R}_l into an estimate $\hat{P}(f)$ of the true spectrum $P(f)$. This procedure leads to the same two errors. If \hat{R}_l is obtained for $l = -N, \dots, N$, then the estimate $\hat{P}(f)$ is obtained with the same spectral resolution equal to $B = \frac{1}{N\Delta}$. Further, \hat{R}_l values are averaged over NI points instead of an infinite number of points. The resulting statistical errors on \hat{R}_l will result in statistical errors on $\hat{P}(f)$ (obtained from the DFT of \hat{R}_l).

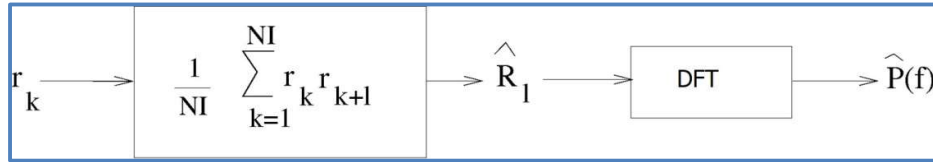


Figure 7.12: Block diagram illustrating the estimation of the spectrum of a (noise) signal using the covariance function and the Wiener-Khintchin relation.

Finally, spectral estimation using the Bartlett method is illustrated for a simulated noise signal sampled at $F = 1000$ Hz ($\Delta = 1$ ms). The signal is obtained by low-pass filtering white noise. The low-pass (elliptical) filter has a cut-off frequency of 250 Hz. The transmission function of the filter is chosen such that it generates a sharp peak in the resulting spectrum of the noise signal. The thick solid black lines in figures 7.13a and 7.13b indicate this true spectrum. For the spectral analysis we first set N to 512, resulting in a spectral resolution of $B = \frac{1}{N\Delta} = 2$ Hz, which is sufficient to resolve all details in $P(f)$, including the narrow peak. The averaging is performed over $I = 1, 10, 100$ and 1000 data blocks (each of $N = 512$ points). The results are presented in figure 7.13a. Indeed, the relative statistical errors behave as $\frac{1}{\sqrt{I}}$.

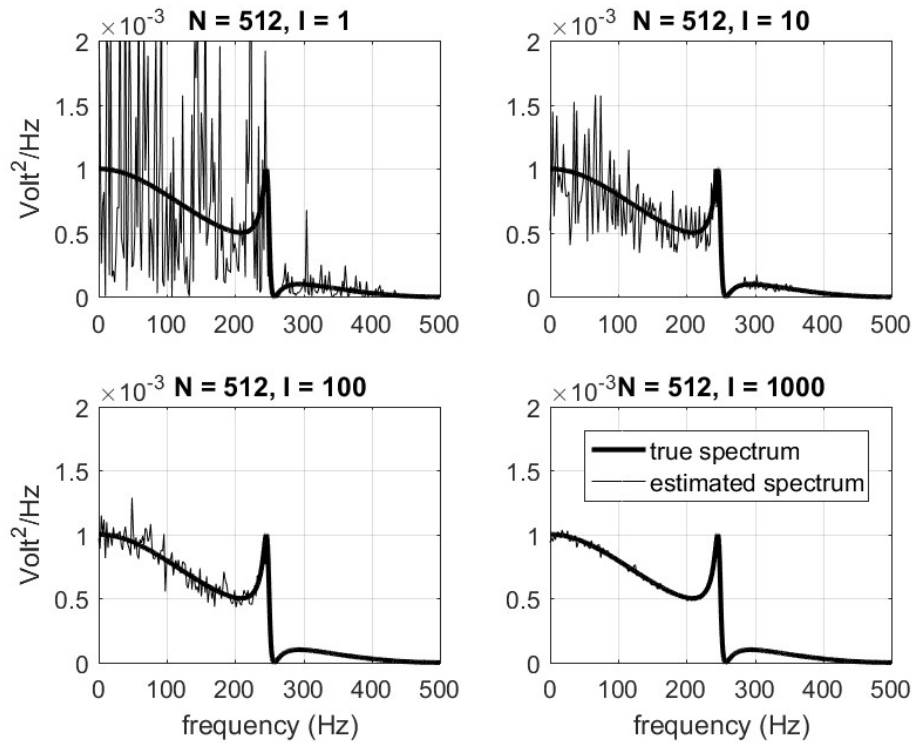


Figure 7.13a: Spectral estimation of a noise signal (sampled at 1000 Hz) for various values of I . The true spectrum and estimated spectrum are indicated by the thick and thin solid line, respectively. In this case the data blocks contain $N = 512$ points resulting in sufficient spectral resolution to resolve the narrow peak in the true spectrum.

Figure 7.13b shows similar results but now with N set to 64, i.e. the spectral resolution is now $B = \frac{1}{N\Delta} = 16$ Hz, which is insufficient to resolve the narrow peak in the true spectrum.

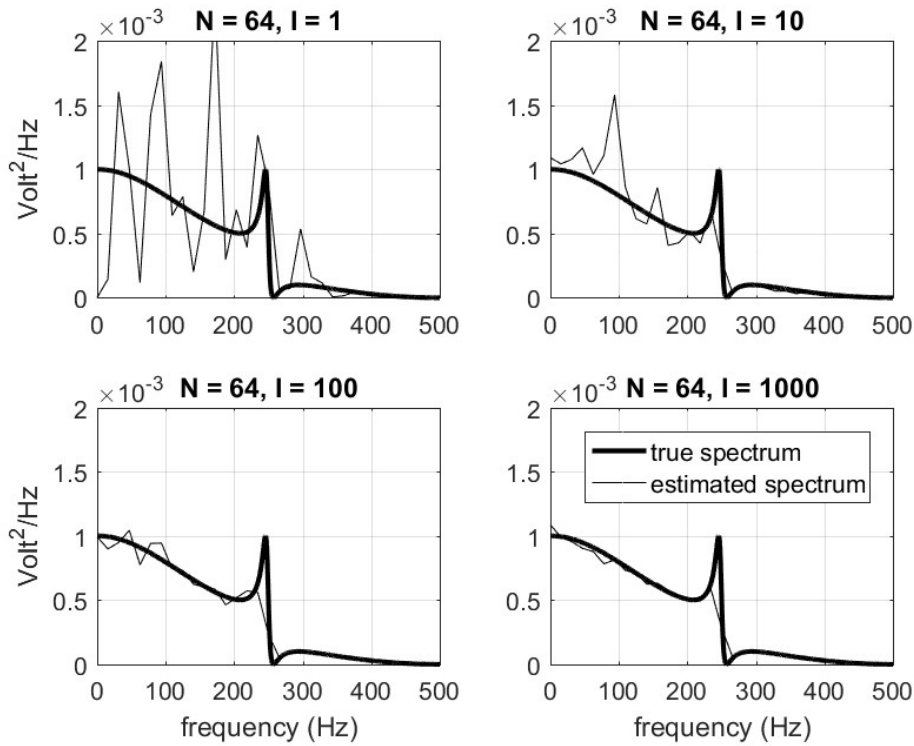


Figure 7.13b: Spectral estimation of a noise signal (sampled at 1000 Hz) for various values of I . The true spectrum and estimated spectrum are indicated by the thick and thin solid line, respectively. In this case the data blocks contain $N = 64$ points resulting in a spectral resolution that is insufficient to resolve the narrow peak in the true spectrum.

7.7 Exercise

Consider the continuous white noise signal $x(t)$ with spectrum $P_x(f) = P_0$ (in units V^2/Hz). The signal is put at the input of the simple low-pass filter (LPF) of question 2 of chapter 1. The time constant of the LPF is $\tau = RC$ and the output signal is denoted $y(t)$.

- (a) Calculate the spectrum $P_y(f)$ of $y(t)$.
- (b) Calculate the variance σ_y^2 of $y(t)$ by integration of the spectrum $P_y(f)$.
- (c) Calculate the covariance function $R_y(t)$ of $y(t)$ using the Wiener-Khintchin relation for continuous signals.
- (d) Make a sketch of $R_y(t)$ for a few values of the time constant $\tau = RC$ of the LPF.
- (e) What is $R_y(t=0)$? Compare your answer with that of question (b) and explain.

Note: Use the list of Fourier transform pairs of section 1.6.

Appendix Analog signal processing

Complex impedance and passive filters

Complex impedance of L, C and R

As a start we derive the formulas for the complex impedance for a capacitor, an inductor and a resistor. Subsequently, this is applied in simple passive analog filters using these devices.

We consider an (harmonic) electric current $I(t) = I_0 \cos(\omega t)$ with I_0 the current amplitude and $\omega = 2\pi f$ the radial frequency (and f the frequency in Hz). In complex notation the current reads

$$I(t) = I_0 e^{j\omega t} \quad (1)$$

For an inductor, see figure 1, the relation between the voltage V across the inductor and the current through it is given by

$$V(t) = L \frac{dI(t)}{dt} \quad (2)$$

with L the coefficient of self-induction of the inductor.



Figure 1: Inductor symbol.

Substitution of the equation for the current, equation (1), into equation (2) yields

$$V(t) = L j \omega I_0 e^{j\omega t}$$

Using $j = e^{\frac{1}{2}\pi j}$ this can be written as

$$V(t) = \omega L I_0 e^{j(\omega t + \frac{1}{2}\pi)} = V_0 e^{j(\omega t + \frac{1}{2}\pi)} \quad (3)$$

where we have introduced the voltage amplitude $V_0 = \omega L I_0$.

Going back to non-complex notation, this would read $V(t) = V_0 \cos\left(\omega t + \frac{1}{2}\pi\right)$, i.e. there is a phase shift of 90° between the current and the voltage across an inductor.

Now, the complex impedance of an inductor is defined as $Z_L = \frac{V}{I} = \frac{j\omega L I_0 e^{j\omega t}}{I_0 e^{j\omega t}}$, i.e.

$$Z_L = j\omega L \quad (4)$$

The inductive reactance is given as $X_L = |Z_L| = \omega L$ and has units Ohm.

Note: The same result can be obtained by going to the frequency domain using the Fourier transform, which is defined for signal $x(t)$ as

$$X(\omega) = \int_{-\infty}^{\infty} x(t) e^{-j\omega t} dt \quad (5a)$$

The inverse Fourier transform reads

$$x(t) = \frac{1}{2\pi} \int_{-\infty}^{\infty} X(\omega) e^{-j\omega t} d\omega \quad (5b)$$

We rewrite equation (2) as

$$v(t) = L \frac{di(t)}{dt} \quad (6)$$

now using lowercase symbols to indicate that we are in the time domain. We use the property that if X is the Fourier transform of x then $j\omega X$ is the Fourier transform of the derivative $x' = \frac{dx}{dt}$.

Hence, Fourier transforming equation (6) yields $V(\omega) = j\omega L I(\omega)$ with V and I the Fourier transform of v and i , respectively. Hence

$$Z_L = \frac{V(\omega)}{I(\omega)} = j\omega L \quad (7)$$

For a capacitor, see figure 2, the relation between the voltage V across the capacitor and the accumulated charge Q is given by

$$V = \frac{Q}{C} \quad (8)$$

with C the capacitance of the capacitor. We have $I(t) = \frac{dQ(t)}{dt} = I_0 \cos(\omega t)$ or in complex notation $I(t) = I_0 e^{j\omega t}$.



Figure 2: Capacitor symbols (left: fixed, right: variable).

Now

$$V = \frac{Q}{C} = \frac{1}{C} \int I(t) dt = \frac{1}{C} \int I_0 e^{j\omega t} dt = \frac{I_0}{j\omega C} e^{j\omega t} = \frac{I}{j\omega C}.$$

Hence, the complex impedance of a capacitor, being the ratio of V and I , becomes

$$Z_C = \frac{1}{j\omega C} \quad (9)$$

The capacitive reactance is given as $X_C = |Z_C| = \frac{1}{\omega C}$ and has units Ohm.

Using $\frac{1}{j} = e^{-\frac{1}{2}\pi j}$ we see that $V(t) = V_0 \cos(\omega t - \frac{1}{2}\pi)$ with voltage amplitude $V_0 = \frac{I_0}{\omega C}$.

Finally, as for a resistor $V = IR$ (Ohm's law), the complex impedance of a resistor is simply

$$Z_R = R \quad (10)$$

with R the resistance of the resistor (which is of course real-valued).

We will now consider the *LRC* series circuit depicted in figure 3. The current at all points in the circuit is the same and assumed to be given as $I(t) = I_0 \cos(\omega t)$ (or $I(t) = I_0 e^{j\omega t}$ in complex notation). With the expressions for the complex impedances derived above, the expression for the (AC) voltage V is easily found. The total impedance of the circuit is given by

$$Z = R + j\omega L + \frac{1}{j\omega C} = R + j \left(\omega L - \frac{1}{\omega C} \right) \quad (11)$$

Hence, the voltage reads

$$V = ZI = \left[R + j \left(\omega L - \frac{1}{\omega C} \right) \right] I_0 e^{j\omega t}$$

which can be written as

$$V = \sqrt{R^2 + \left(\omega L - \frac{1}{\omega C} \right)^2} e^{j\phi} I_0 e^{j\omega t} = V_0 e^{j(\omega t + \phi)}$$

with voltage amplitude $V_0 = I_0 \sqrt{R^2 + \left(\omega L - \frac{1}{\omega C}\right)^2}$ and phase angle $\phi = \tan^{-1} \left(\frac{\omega L - \frac{1}{\omega C}}{R} \right)$.

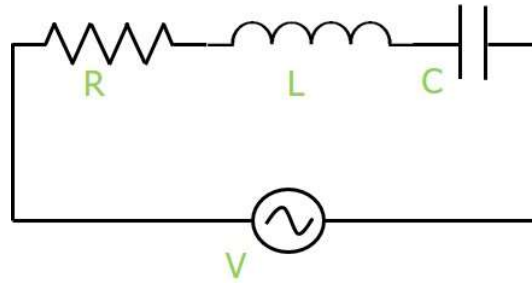


Figure 3: *RLC* series circuit.

The peak current in the *RLC* series circuit is given by

$$I_0 = \frac{V_0}{\sqrt{R^2 + \left(\omega L - \frac{1}{\omega C}\right)^2}} \quad (12)$$

which is maximum when $\omega L - \frac{1}{\omega C} = 0$ or $\omega_0 = \frac{1}{\sqrt{LC}}$ at which frequency the circuit is in resonance, see figure 4 where we plotted $\frac{I_0}{V_0}$ versus frequency for two values of R .

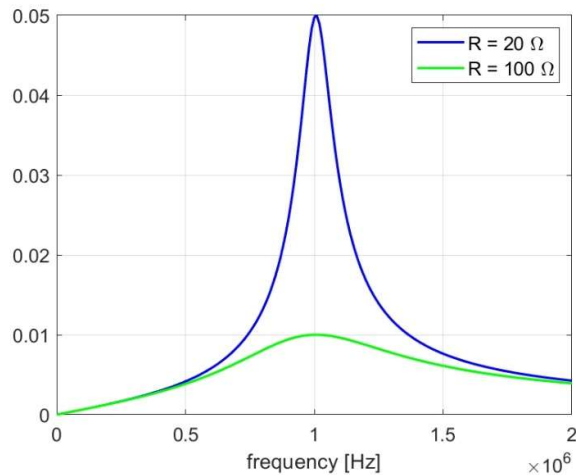


Figure 4: Resonance in an *RLC* series circuit for $L = 25 \mu\text{H}$ and $C = 1 \text{nF}$ ($f_0 = 1 \text{ MHz}$)

As a second example we consider the *LRC* parallel circuit of figure 5. Given the voltage $V(t) = V_0 \cos(\omega t)$ (or $V(t) = V_0 e^{j\omega t}$ in complex notation), what is the expression for total current leaving the source?

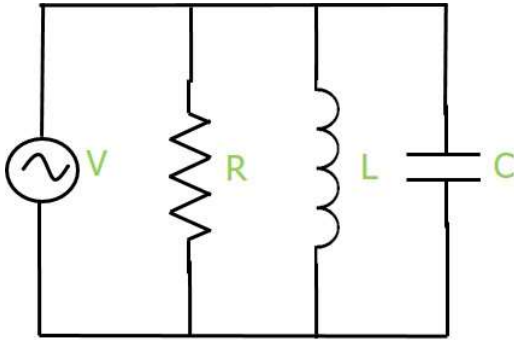


Figure 5: *RLC* parallel circuit.

Now, the total impedance Z of the circuit is determined by

$$\frac{1}{Z} = \frac{1}{Z_R} + \frac{1}{Z_L} + \frac{1}{Z_C} = \frac{1}{R} + \frac{1}{j\omega L} + j\omega C \quad (13)$$

Hence, the current is

$$I = \frac{V}{Z} = V \left(\frac{1}{R} + \frac{1}{j\omega L} + j\omega C \right) = V \left[\frac{1}{R} + j \left(\omega C - \frac{1}{\omega L} \right) \right]$$

which can be written as

$$I = V_0 e^{j\omega t} \sqrt{\frac{1}{R^2} + \left(\omega C - \frac{1}{\omega L} \right)^2} e^{j\phi} = I_0 e^{j(\omega t + \phi)}$$

with current amplitude $I_0 = V_0 \sqrt{\frac{1}{R^2} + \left(\omega C - \frac{1}{\omega L} \right)^2}$ and phase angle $\phi = \tan^{-1} \left[R \left(\omega C - \frac{1}{\omega L} \right) \right]$.

Passive analog filters

Passive low-pass, high-pass, band-pass and band-stop filters consisting of combinations of resistors, capacitors and inductors can be assessed by the complex impedance method developed in the previous section. In addition, the formula for a voltage divider using two resistors, see figure 6, is needed and given by

$$\frac{v_{out}}{v_{in}} = \frac{R_2}{R_1 + R_2}. \quad (14a)$$

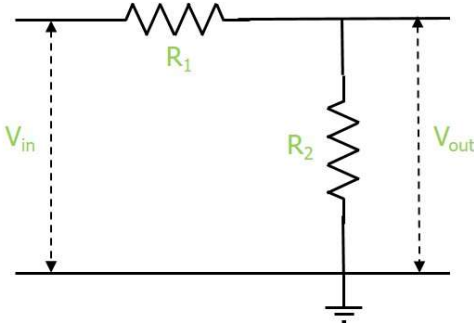


Figure 6: A simple voltage divider using two resistors R_1 and R_2 (which may be replaced by complex impedances Z_1 and Z_2 , respectively).

When the resistors R_1 and R_2 are replaced by the complex impedances Z_1 and Z_2 , respectively, then the relation between output voltage v_{out} and input voltage v_{in} is still given by

$$\frac{v_{out}}{v_{in}} = \frac{Z_2}{Z_1 + Z_2}. \quad (14b)$$

The ratio $\frac{v_{out}}{v_{in}}$ is called the transmission function $H(j\omega)$ of the filter.

As a first example we consider the filter depicted in figure 7. The transmission function or voltage amplification of this simple low-pass filter is given as

$$H(j\omega) = \frac{v_{out}}{v_{in}} = \frac{\frac{1}{j\omega C}}{R + \frac{1}{j\omega C}} = \frac{1}{1 + j\omega RC}. \quad (15)$$

A so-called Bode diagram of $H(j\omega)$ is given in figure 8 for $R = 850 \Omega$ and $C = 1 \mu\text{F}$. A Bode diagram shows plots of the absolute value (in dB) and phase (in degrees) of $H(j\omega)$ as a function of frequency (using a logarithmic frequency axis). The roll-off in the stop band of the filter is 6

dB/octave (1 octave being a factor 2 in frequency) or 20 dB/decade. In this case the cut-off frequency is $f_c = \frac{1}{2\pi RC} = 187$ Hz at which $|H(j\omega)| = \frac{1}{\sqrt{2}}$ (= -3 dB).

Note: A filter is fully characterized by its transmission function, which gives its behavior in the frequency domain. A filter is also fully determined by its impulse response $h(t)$ being the response of the filter to a Dirac delta function, i.e. $v_{in}(t) = \delta(t)$. $h(t)$ is the inverse Fourier transform of $H(j\omega)$.

In this case $h(t) = \frac{1}{RC} e^{-\frac{t}{RC}}$, $t \geq 0$.

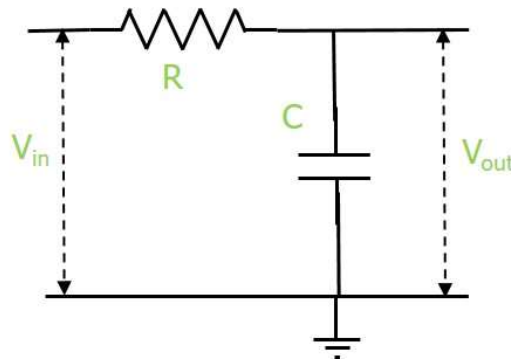


Figure 7: The simplest low-pass filter.

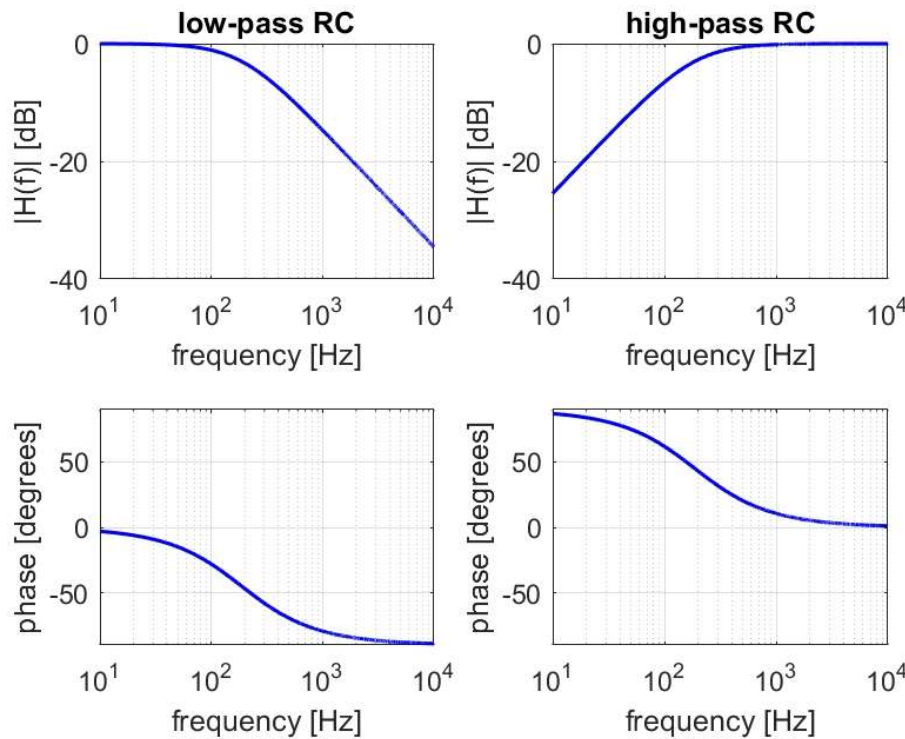


Figure 8: Bode plots of the low-pass RC filter (left) and high-pass RC filter (right).

Figure 9 shows the simplest high-pass filter, the transmission function of which is

$$H(j\omega) = \frac{V_{out}}{V_{in}} = \frac{R}{\frac{1}{j\omega C} + R} = \frac{j\omega RC}{1 + j\omega RC}. \quad (16)$$

The corresponding Bode plot is shown in figure 8, again for $R = 850 \Omega$ and $C = 1 \mu F$.

Note: The transmission function of this filter can be rewritten as $H(j\omega) = 1 - \frac{1}{1 + j\omega RC}$. The inverse Fourier transform of this, i.e. the impulse response, is $h(t) = \delta(t) - \frac{1}{RC} e^{-\frac{t}{RC}}$, $t \geq 0$.

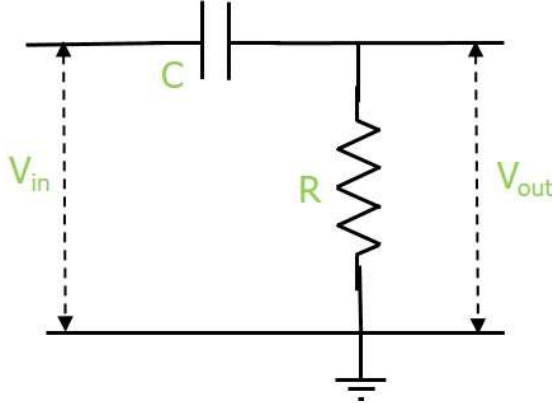


Figure 9: The simplest high-pass filter.

A simple band-pass filter can be made by adding an inductor parallel to the capacitor in the low-pass filter of figure 7, see figure 10. The transmission function of this filter is derived as follows. The impedances Z_1 and Z_2 (of equation 14b) are given by $Z_1 = R$ and $\frac{1}{Z_2} = \frac{1}{j\omega L} + j\omega C = j\left(\omega C - \frac{1}{\omega L}\right)$, i.e. the transmission function $H(j\omega)$ is thus

$$\frac{Z_2}{Z_1 + Z_2} = \frac{\frac{1}{j\left(\omega C - \frac{1}{\omega L}\right)}}{R + j\left(\omega C - \frac{1}{\omega L}\right)}. \text{ Hence,}$$

$$H(j\omega) = \frac{1}{1 + jR\left(\omega C - \frac{1}{\omega L}\right)}. \quad (17)$$

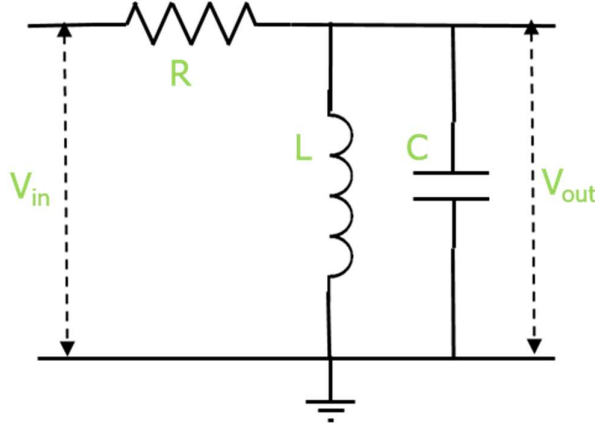


Figure 10: The simplest band-pass LRC filter.

The simplest band-stop filter using an inductor is shown in figure 11, the transmission function of which is

$$H(j\omega) = \frac{j\left(\omega L - \frac{1}{\omega C}\right)}{R + j\left(\omega L - \frac{1}{\omega C}\right)} \quad (18)$$

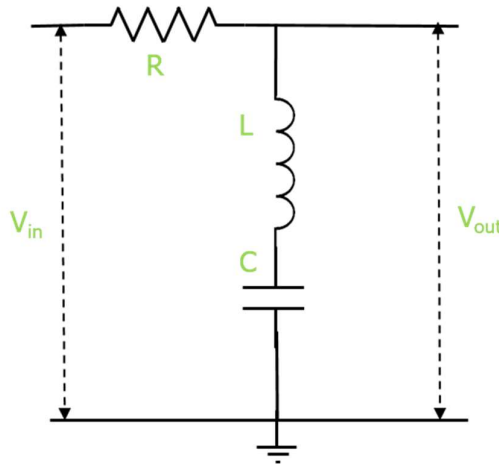


Figure 11: The simplest band-stop LRC filter.

Taking $C = 230 \text{ pF}$ and $L = 110 \mu\text{H}$, i.e. resonance frequency $f_0 = \frac{1}{2\pi\sqrt{LC}} = 1 \text{ MHz}$, we have

plotted $|H(j\omega)|$ and the phase of $H(j\omega)$ as function of frequency (on a linear frequency axis) in

figure 12. The resistance R for the band-pass filter and the band-stop filter is chosen as $10 \text{ k}\Omega$ and 100Ω , respectively.

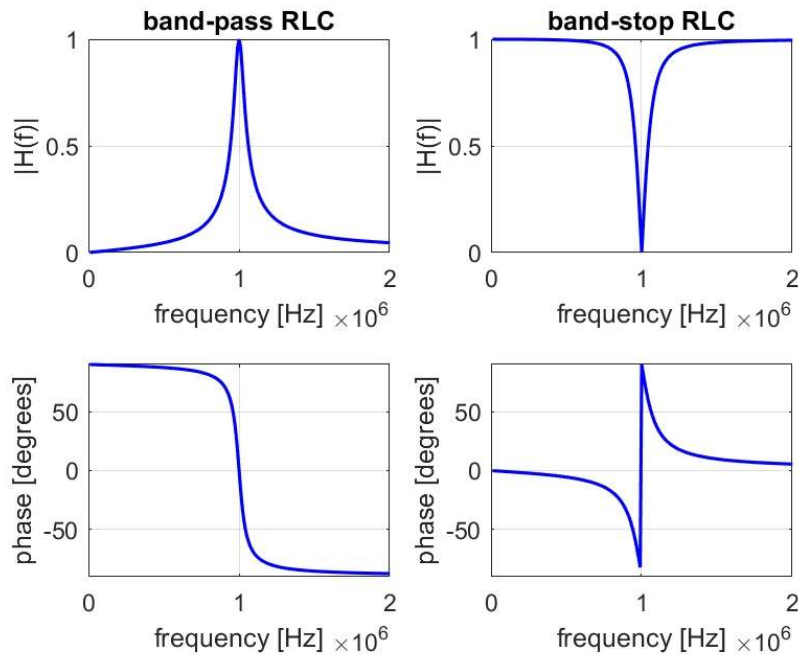
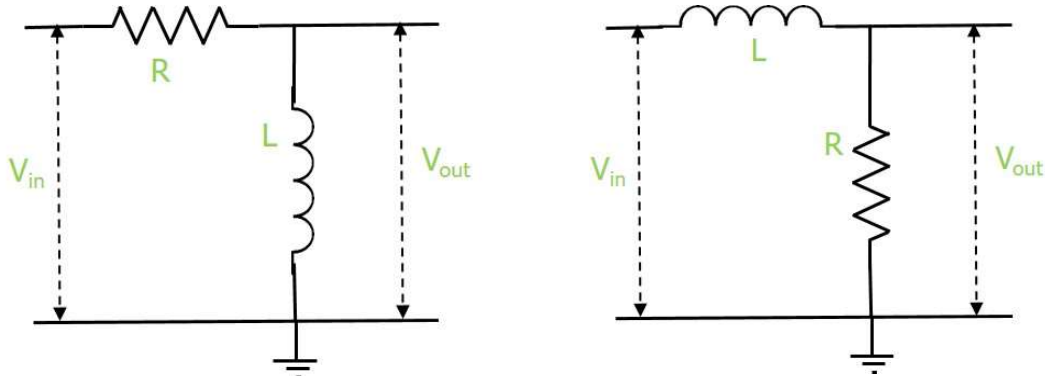


Figure 12: Plots of $H(j\omega)$ (absolute value and phase) for the RLC band-pass (left) and the RLC band-stop filter (right). The same values for L and C are taken (i.e. same resonance frequency being 1 MHz). For the band-pass filter $R = 10 \text{ k}\Omega$ and for the band-stop filter $R = 100 \Omega$.

Exercise

Consider the filters in the figure below. For both filters $R = 24 \Omega$ and $L = 20 \text{ mH}$.



Determine $H(j\omega)$ for the two filters and make plots of $|H(j\omega)|$ and the phase of $H(j\omega)$ as function of frequency. Which of the filters is a LPF and which is a HPF? What is the cut-off frequency of both filters? (Compare your results with those shown in figure 8).

Circuits with operational amplifiers and active filters

An operational amplifier, or OPAMP for short, is an amplifying device designed to be used with external feedback components (mainly resistors and capacitors). These components determine the resulting function or operation of the OPAMP. Depending on the feedback configuration, the amplifier can perform a variety of different functions, hence the name operational amplifier. In particular, active filters can be made with OPAMPS. It is a three-terminal device: two high-impedance inputs, the inverting input (denoted by a minus sign) and non-inverting input (denoted by a plus sign), and a low-impedance output. Figure 13 shows the electronic symbol of this ‘differential’ amplifier.

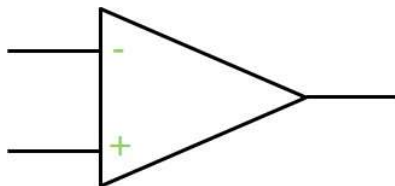


Figure 13: Electronic circuit symbol of the operational amplifier (OPAMP).

The properties of an (ideal) OPAMP are:

- very large amplification ($\sim 10^5$)
- very high input impedance ($\sim 10 \text{ M}\Omega$)
- very low output impedance ($\sim 100 \Omega$)
- sufficiently large bandwidth

Note: Although often omitted from circuit diagrams, OPAMPS require connections to a power supply (typically +15 V and -15 V) in order to function. For many OPAMPS the precise supply voltage is however not critical.

By amplification we mean the so-called ‘open-loop gain’ A , i.e. the gain obtained when no feedback is applied in the circuit. Then we have

$$v_{out} = A(v^+ - v^-) \quad (19)$$

A basic OPAMP circuit is shown in figure 14. The impedances Z_i and Z_f (denoted by the two rectangles in the figure) can be any combination of R , C (and L).

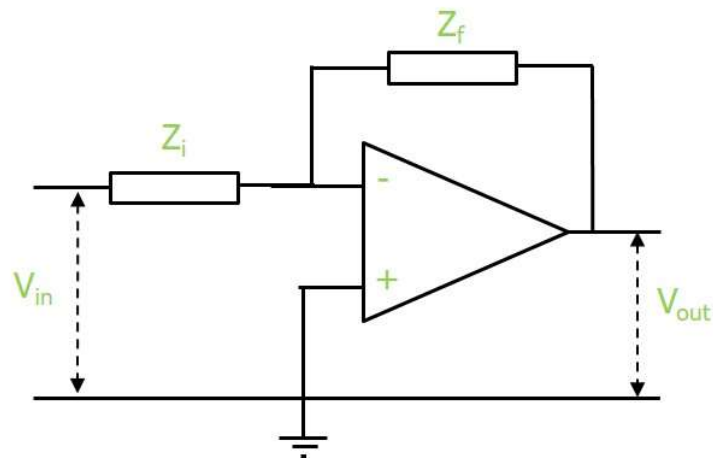


Figure 14: Basic OPAMP circuit.

The transfer function of this circuit is determined as follows. The current I_i and I_f through the impedance Z_i and Z_f , respectively, are given by $I_i = \frac{V^- - V_{in}}{Z_i}$ and $I_f = \frac{V_{out} - V^-}{Z_f}$. Assuming the input impedance of the OPAMP to be infinite, we have $I_i = I_f$. Further, according to equation (19) we have $v_{out} = A(V^+ - V^-) = -AV^-$.

After elimination of V^- the transmission function of this circuit is obtained as

$$H(j\omega) = \frac{v_{out}}{v_{in}} = -\frac{A}{(A+1)\frac{Z_i}{Z_f} + 1} \quad (20)$$

which simplifies to

$$\frac{v_{out}}{v_{in}} = -\frac{Z_f}{Z_i} \quad (21)$$

when we assume the open-loop gain A to be infinite (ideal OPAM: $V^- = V^+$, i.e. the inverting input is at ‘virtual earth’).

Note: Because of the complex impedances we are in the frequency domain and hence use capital letters for currents and voltages (but not for v_{in} and v_{out} to be consistent with equation 21).

Note: The impedances Z_i and Z_f (and feedback in general) will change the input and output impedance of the entire circuit (compared to those of the OPAMP only).

We study a special case of this circuit in more detail, i.e. the situation when $Z_f = R_f$ and $Z_i = R_i$.

Then, the amplification would be $\left| \frac{v_{out}}{v_{in}} \right| = \frac{R_f}{R_i}$, independent of the OPAMP parameters. However,

actually we have to use the exact equation 20 to see the full frequency behaviour of this amplifier. A good practical model for the OPAMP open-loop gain is

$$A = \frac{A_0}{1 + j\omega\tau}. \quad (22)$$

Typically, $A_0 \approx 10^5$ and the cut-off frequency f_c is around 100 Hz, i.e. $\tau = \frac{1}{2\pi f_c} \approx 1.6 \times 10^{-3}$.

Figure 15 shows the open-loop gain of the OPAMP together with the so-called ‘closed-loop gain’ of the circuit (i.e. equation 20) as a function of frequency. We have taken $\frac{R_f}{R_i} = 20$. For both gains we

plotted its absolute value in dB, i.e. $20^{10} \log |A|$ and $20^{10} \log \left| \frac{v_{out}}{v_{in}} \right|$ (with $\frac{v_{out}}{v_{in}}$ according to equation 20).

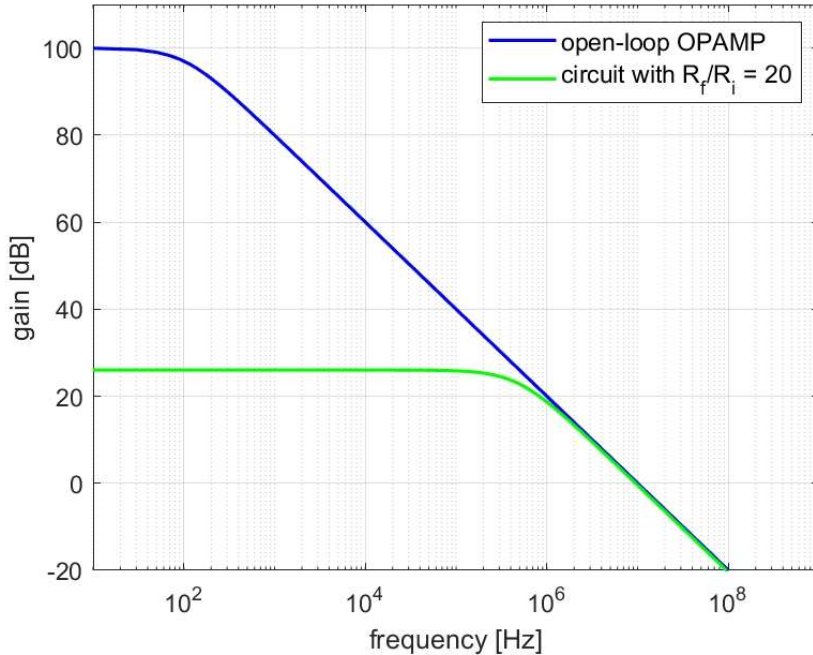


Figure 15: Open-loop gain of the OPAMP (blue line) and closed-loop gain of the circuit of figure 14 with $R_f/R_i = 20$ (green line) as a function of frequency. Note the logarithmic x-axis (frequency) and the dB scale on the y-axis (gain).

An interesting extension of this circuit is the sum circuit shown in figure 16.

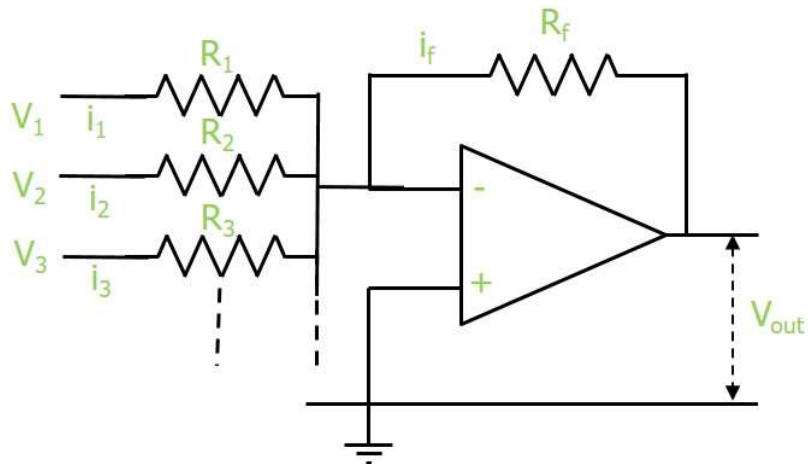


Figure 16: The summer circuit.

Assuming an ideal OPAMP (both open-loop gain and input impedance is infinite) we may write

$$i_1 + i_2 + i_3 + \dots = i_f.$$

Given the ideal OPAMP properties we have $V^- = V^+$ and since $V^+ = 0$ we may write

$$-\frac{V_1}{R_1} - \frac{V_2}{R_2} - \frac{V_3}{R_3} \dots = \frac{V_{out}}{R_f}.$$

Taking $R_1 = R_2 = R_3 = \dots = R_f = R$ we obtain

$$V_{out} = -(v_1 + v_2 + v_3 + \dots) \quad (23)$$

Note: When designing OPAMP circuits such as that shown in figure 16, we normally use resistors in the range 1 kΩ to 100 kΩ.

An important OPAMP circuit is the so-called buffer or voltage follower, which is shown in figure 17.

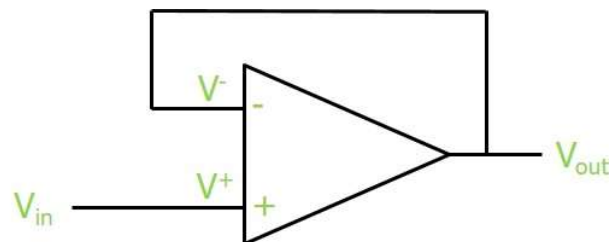


Figure 17: The buffer circuit.

We derive the transfer function of the buffer assuming the OPAMP open-loop gain is again

$A = \frac{A_0}{1 + j\omega\tau}$. Substituting $V^- = v_{out}$ and $V^+ = v_{in}$ in the basic OPAMP equation 19 yields

$$\frac{v_{out}}{v_{in}} = \frac{A}{A+1} = \frac{1}{1 + j\omega\frac{\tau}{A_0}} \quad (24)$$

i.e. the gain of the buffer is equal to 1 (0 dB) up to the new cut-off frequency $\frac{A_0}{2\pi\tau}$, which is A_0

higher than the cut-off frequency of the open-loop gain ($f_c = \frac{1}{2\pi\tau}$).

The result (as a Bode plot) is shown in figure 18 (for $A_0 = 10^5$ and cut-off frequency $f_c = 100$ Hz, i.e.

$$\tau = \frac{1}{2\pi f_c} \approx 1.6 \times 10^{-3}$$

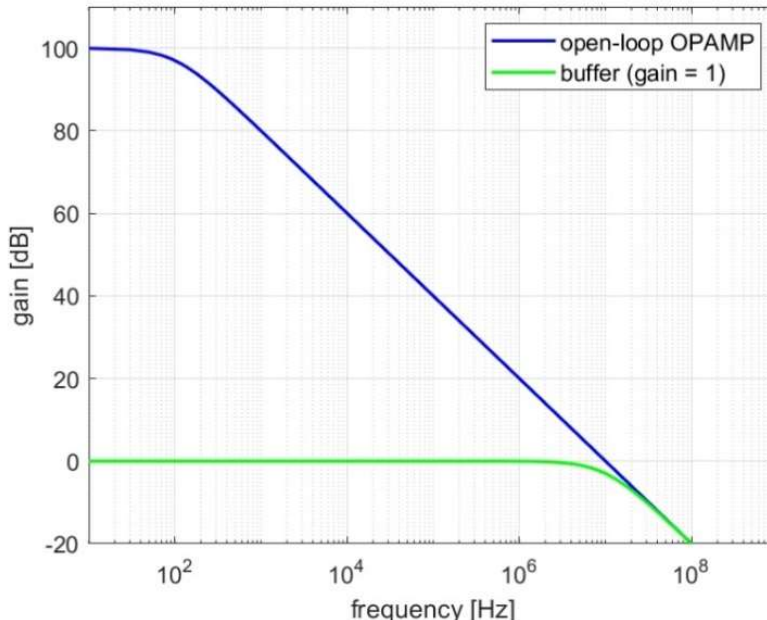


Figure 18: Open-loop gain of the OPAMP (blue line) and closed-loop gain of the buffer (green line) as a function of frequency. Note the logarithmic x-axis (frequency) and the dB scale on the y-axis (gain).

An illustrative application of the buffer is a band-pass filter consisting of a series connection of a high-pass RC filter and a low-pass RC filter with the buffer in between, see figure 19. Due to the high input impedance of the buffer (i.e. the high-pass RC filter is not loaded) and the low output impedance of the buffer, the transmission function of this circuit is given by the product of the transmission functions of the subsequent filters (equations 16 and 15), i.e.

$$H(j\omega) = \frac{j\omega\tau_1}{1+j\omega\tau_1} \cdot \frac{1}{1+j\omega\tau_2} \quad (25)$$

with $\tau_1 = R_1 C_1$ and $\tau_2 = R_2 C_2$.

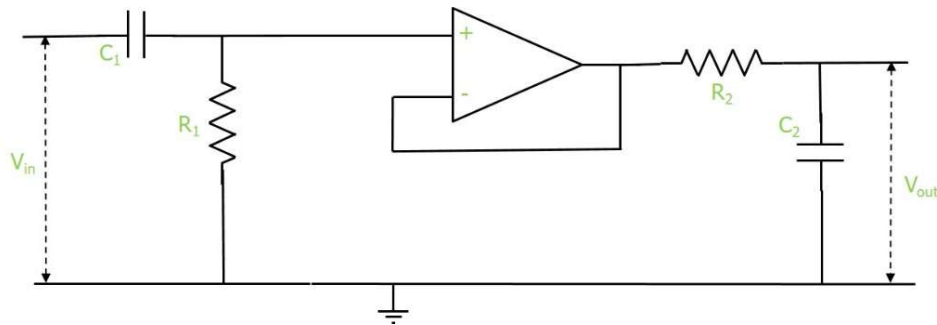


Figure 19: Band-pass filter consisting of a series connection of a high-pass RC filter, a buffer and a low-pass RC filter.

Figure 20 shows a Bode plot of the transmission function of the band-pass filter with cut-off frequencies equal to $\frac{1}{2\pi\tau_1} = 300$ Hz and $\frac{1}{2\pi\tau_2} = 15$ kHz.

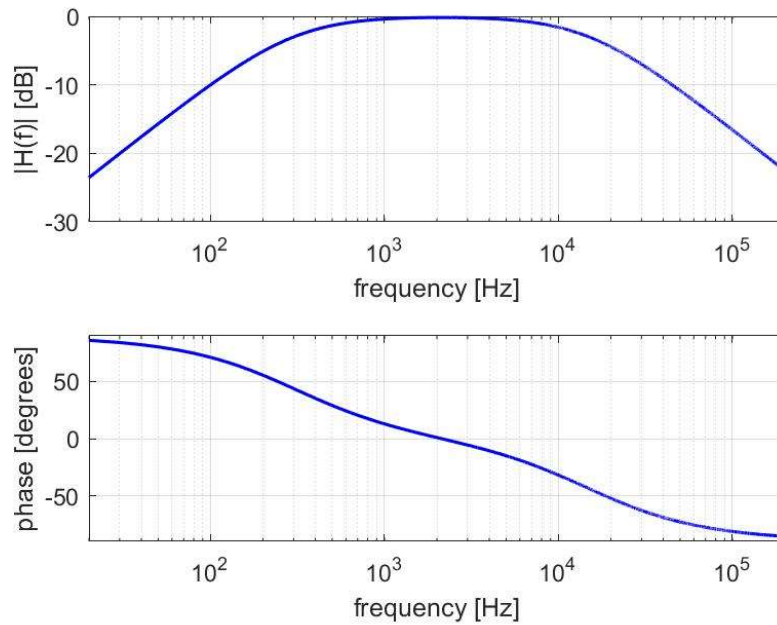


Figure 20: Bode plot of the BPF of figure 19 with cut-off frequencies 300 Hz and 15 kHz.

Figure 21 shows two more examples of important OPAMP circuits, i.e. the integrator and the differentiator. For the integrator we have (see equation 21)

$$\frac{v_{out}}{v_{in}} = -\frac{Z_f}{Z_i} = -\frac{1}{j\omega RC}.$$

Going to the time domain, using the inverse Fourier transform, we obtain

$$v_{out}(t) = -\frac{1}{RC} \int v_{in}(t) dt. \quad (26)$$

For the differentiator we have

$$\frac{v_{out}}{v_{in}} = -\frac{Z_f}{Z_i} = -\frac{R}{\frac{1}{j\omega C}} = -j\omega RC.$$

In the time domain this becomes

$$v_{out}(t) = -RC \frac{dv_{in}(t)}{dt}. \quad (27)$$

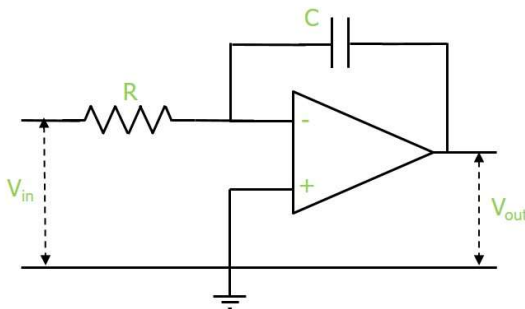


Figure 21a: Integrator circuit.

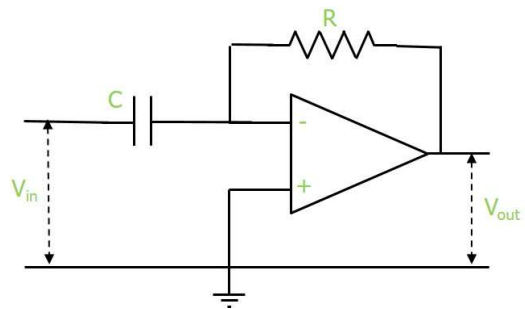


Figure 21b: Differentiator circuit.

We now treat an important 2nd order active low-pass filter, i.e. the so-called 'Sallen-Key' configuration shown in figure 22.

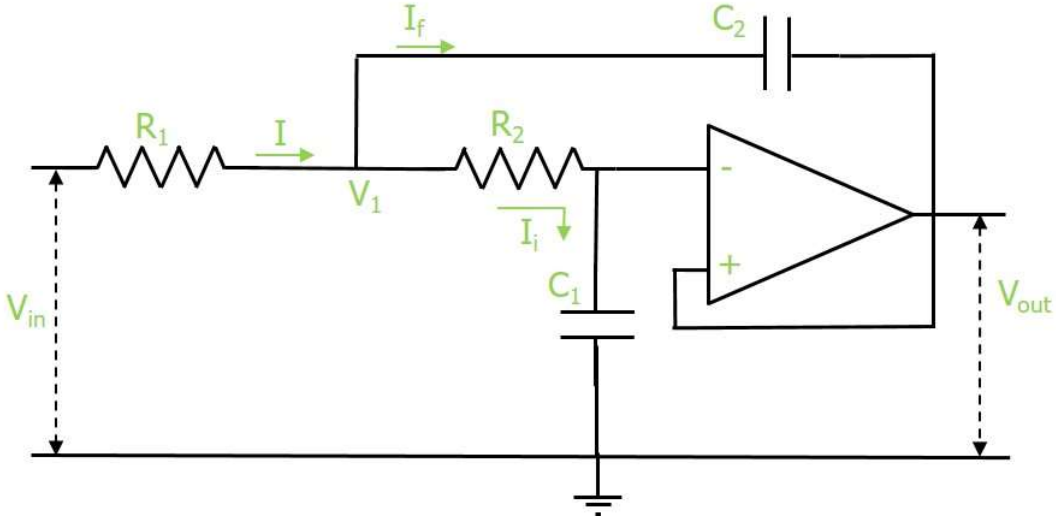


Figure 22: The second-order low-pass Sallen-Key configuration.

Given the (ideal) OPAMP properties we have $v_{out} = V^- = V^+$. Also, $V^+ - V_1 = I_i R_2$. Eliminating V^+ from these two equations yields

$$v_{out} - V_1 = I_i R_2.$$

Further the following equations hold for this circuit:

$$\begin{aligned} v_{out} &= -\frac{I_i}{j\omega C_1} \\ V_1 - v_{in} &= IR_1 \\ v_{out} - V_1 &= \frac{I_f}{j\omega C_2} \\ I &= I_i + I_f \end{aligned}$$

Eliminating the currents I , I_i and I_f and V_1 from these five equations yields the transmission function

$$\frac{v_{out}}{v_{in}} = \frac{1}{1 + j\omega C_1(R_1 + R_2) - \omega^2 R_1 C_1 R_2 C_2}. \quad (28)$$

The cut-off frequency of the filter is given by $\frac{1}{2\pi\sqrt{R_1 C_1 R_2 C_2}}$.

Figure 23 gives a Bode plot of a low-pass filter consisting of two Sallen-Key stages in series (i.e. a so-called 4th order Butterworth filter). The parameters of the first filter are: $R_1 = 2.21 \text{ k}\Omega$, $R_2 = 2.49 \text{ k}\Omega$,

$C_1 = 6.2 \text{ nF}$ and $C_2 = 7.5 \text{ nF}$ (cut-off frequency 9.95 kHz). The parameters of the second filter are: $R_1 = 1.58 \text{ k}\Omega$, $R_2 = 2.21 \text{ k}\Omega$, $C_1 = 2.4 \text{ nF}$ and $C_2 = 18 \text{ nF}$ (cut-off frequency 12.96 kHz). The effective cut-off frequency of this 4th order filter is 11.2 kHz.

Also shown in the figure is the Bode plot of a low-pass filter consisting of four simple first-order low-pass RC filters in series (see figure 7 and equation 15). The series connection of this filter is done with buffers, figure 17. The R and C (same for all four stages) are chosen such that the cut-off frequency is also 11.2 kHz. Obviously, the 4th order Butterworth filter outperforms this more simple configuration.

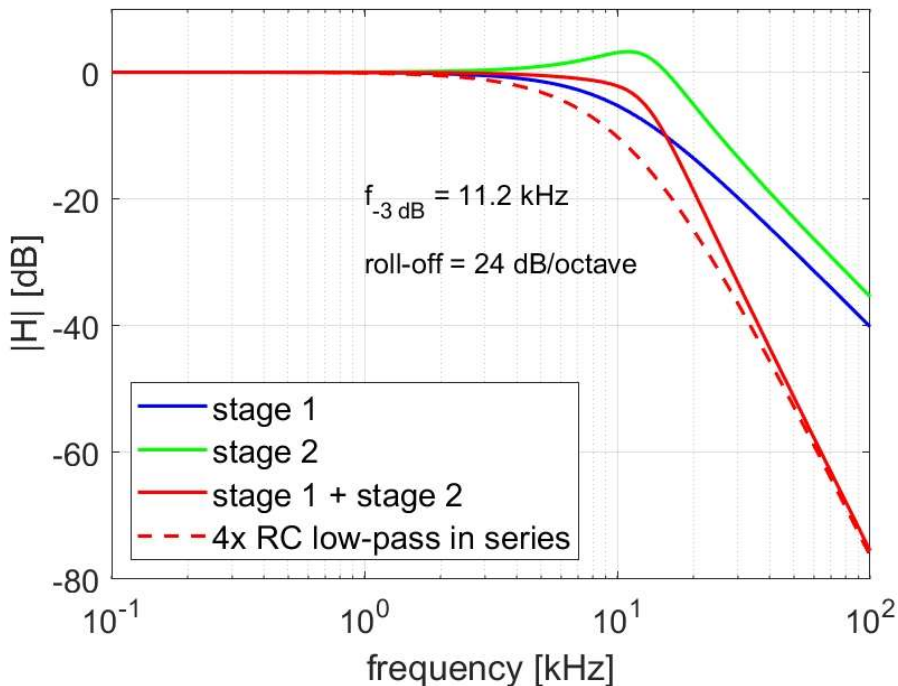


Figure 23: Bode plots of a two-stage Sallen-Key low pass filter (red curve) and a low-pass filter consisting of four first-order low-pass RC filters (dashed red curve). The two filters have the same cut-off frequency (11.2 kHz).

Note: Exchanging the resistors and the capacitors in the circuit of figure 22 results in a 2nd order active *high-pass* filter (in the Sallen-Key configuration).

Finally, we discuss the so-called ‘comparator’, a simple but frequently used OPAMP circuit that, in a way, forms a bridge between analog and digital circuits. The circuit is shown in the left part of figure 24. In the figure also the supply voltages $-V_S$ and $+V_S$ are indicated. Basically, it is an OPAMP circuit without feedback.

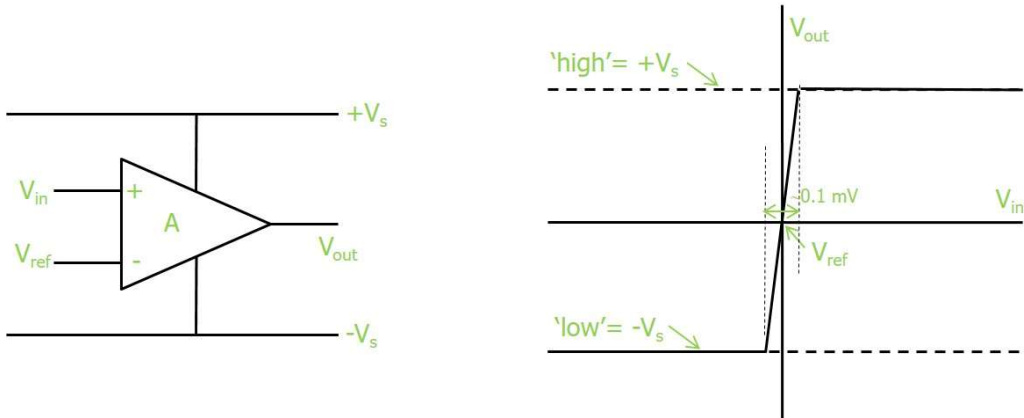


Figure 24: Comparator circuit (left) and output behaviour as a function of input voltage (right).

A comparator compares the magnitude of two voltage inputs and determines the largest. The OPAMP equation $v_{out} = A(V_{in} - V_{ref})$ here becomes

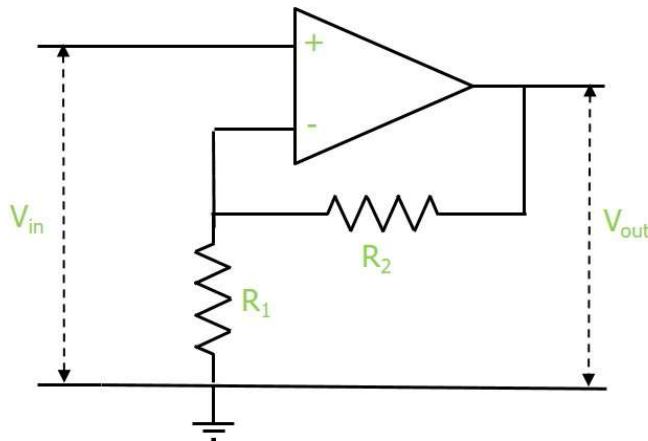
$$v_{out} = A(V_{in} - V_{ref}). \quad (29)$$

Due to the very high open-loop gain A , the output either swings fully to the positive supply voltage $+V_s$ ($V_{in} > V_{ref}$, output state 'high') or fully to the negative supply voltage $-V_s$ ($V_{in} < V_{ref}$, output state 'low'). This is illustrated in the right part of figure 24. Hence, in this circuit the OPAMP is used in saturation, i.e. non-linear mode. There is however a small range of values of V_{in} around V_{ref} (about 0.1 mV, see figure) where the OPAMP behaves linearly.

Exercises

Question 1

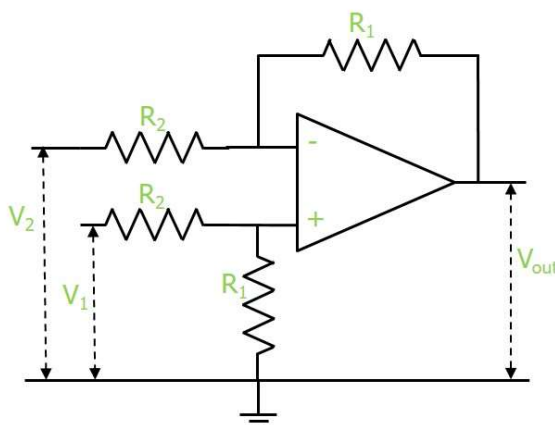
When taking $Z_f = R_f$ and $Z_i = R_i$ in the OPAMP circuit of figure 14, an *inverting* amplifier is obtained with a gain equal to $-\frac{R_f}{R_i}$ (assuming the OPAMP to be ideal). Show that the OPAMP circuit shown below, again assuming an ideal OPAMP, is a *non-inverting* amplifier with gain $1 + \frac{R_2}{R_1}$.



Question 2

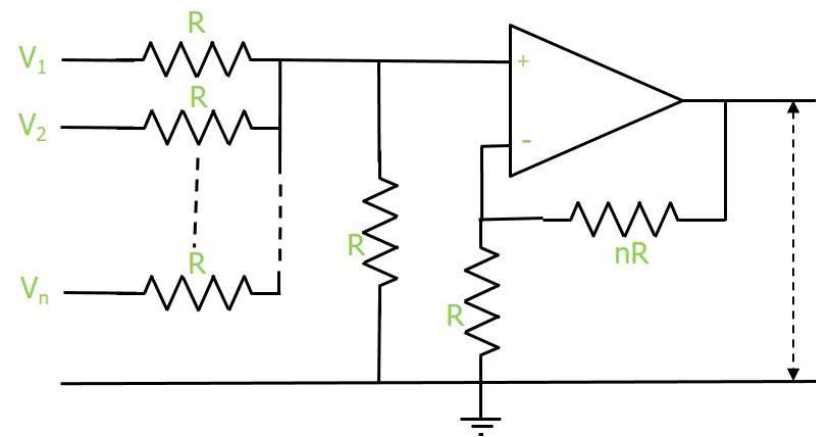
Show that for the OPAMP circuit shown below, the output voltage is given by $V_{out} = \frac{R_1}{R_2}(V_1 - V_2)$.

Assume the OPAMP to be ideal. The circuit is a *subtractor* capable of subtracting one signal from another signal.



Question 3

Show that for the OPAMP circuit shown below, the output voltage is given by $v_{out} = v_1 + v_2 + \dots + v_n$. Assume the OPAMP to be ideal. This circuit is a *non-inverting adder* (of an arbitrary number of signals).



Data acquisition systems

Analog signals are often converted into a digital form, e.g. binary words, since digital data can be more easily processed, transmitted and stored. Digital data are also less susceptible to noise. This section describes the major stages of a typical data acquisition system, starting from the process of sampling to the hardware required to convert these samples into digital form. It will be shown that the OPAMP again turns out to be an essential building block of the hardware.

Sampling is already discussed in chapter 2. We saw that the Shannon-Nyquist theorem answers the question of how fast a time-varying analog signal needs to be sampled such that the original analog signal can be fully recovered from the samples without loss of information. The theorem states that the sampling rate or sampling frequency F must be greater than at least twice the highest frequency present in the signal. This minimum sampling frequency is called the Nyquist rate. A lower sample frequency leads to so-called aliasing, see section 2.4. It should be noted that the Nyquist rate is determined by the highest frequency present in the analog signal and not by the highest frequency of interest. Hence, unwanted high-frequency components in the signal must be removed before sampling. This is accomplished by an anti-alias filter (which is a low-pass filter LPF, see section 2.4.2 and the previous sections of this appendix). As LPFs are not perfect, sampling is performed at about 20 % above the Nyquist rate to accommodate the finite roll-off of the filter's stop band. Often, a 4th or 6th order Butterworth filter as described in the previous section (figure 22) is used as an anti-alias filter.

Note: Binary numbers are similar to decimal numbers, except that they have a base of 2 instead of 10. Each digit takes only two values, i.e. 0 ('low') and 1 ('high'). A binary word of length n is denoted $s_{n-1}s_{n-2}s_{n-3}\dots s_1s_0$ (with $s_i = 0,1$) and can be converted to decimal form according to $s_{n-1}2^{n-1} + s_{n-2}2^{n-2} \dots s_12^1 + s_02^0$. s_{n-1} is the most significant bit (MSB) and s_0 is the least significant bit (LSB). Example: the 5-bit digital word $11010 = 1 \times 2^4 + 1 \times 2^3 + 0 \times 2^2 + 1 \times 2^1 + 0 \times 2^0 = 26$.

Sampling an analog signal comprises the instantaneous reading of the signal's magnitude and converting it into a digital form, e.g. an n -bit digital word. The opposite, i.e. reconstruction, is to convert the digital word back to the corresponding analog value. These two operations are performed by analog-to-digital converters (ADCs) and digital-to-analog converters (DACs). An n -bit converter corresponds to 2^n quantisation levels and the related resolution is $\frac{100\%}{2^n}$. In many applications 8 bits are sufficient (0.4 % resolution). Converters up to 20 bits are available (resolution 10^{-4} % or 1 ppm). The time required for the conversion is referred to as the settling time.

The simplest form of DAC is the so-called 'binary-weighted resistor method', see figure 25.

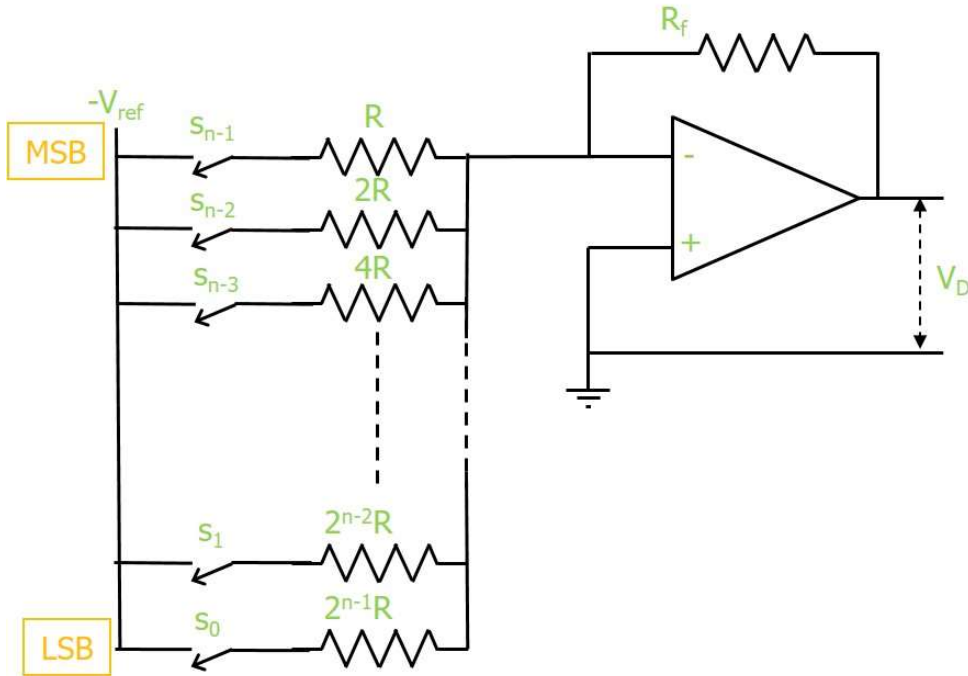


Figure 25: Circuit of a DAC utilizing the binary-weighted resistor method.

In this circuit each input controls a switch that connects a resistor to a constant reference voltage $-V_{ref}$. A switch is closed when the corresponding bit is set to 1 (an open switch means 0). If the switch connected to the MSB is closed, while all others being open, the output voltage of the DAC is

$$V_D = -IR_f = -R_f \left(-\frac{V_{ref}}{R} \right) = \frac{V_{ref}R_f}{R}$$

If the switch connected to the next MSB is closed (all others being open), the DAC output voltage is

$$V_D = \frac{V_{ref}R_f}{2R}$$

If the switch connected to the LSB is closed (all others being open), the DAC output voltage is

$$V_D = \frac{V_{ref}R_f}{2^{n-1}R}$$

The input to the OPAMP is at virtual earth. Hence, the fact that one switch is closed will not affect the current injected by another switch. The currents may therefore be summed, i.e. the DAC output voltage is

$$V_D = \frac{V_{ref} R_f}{R} \left(\frac{s_{n-1}}{1} + \frac{s_{n-2}}{2} + \frac{s_{n-3}}{4} + \dots + \frac{s_1}{2^{n-2}} + \frac{s_0}{2^{n-1}} \right)$$

given the digital input $s_{n-1}s_{n-2}s_{n-3}\dots s_1s_0$.

Note: In practice the DAC is implemented using transistors as electronic switches.

Note: The resistors in this type of DAC have a large spread of values (from R to $2^{n-1}R$). For a 10-bit DAC this range is 1 to 500, which can become unpractical and not precise enough (due to e.g. unequal temperature coefficients of resistors with considerable different resistance). More clever resistor chain methods however exist, such as the $R - 2R$ method (a description of which is beyond the scope of this reader).

A number of techniques are available today for analog-to-digital conversion. Perhaps the most frequently used form of ADC is that utilizing the so-called ‘successive approximation method’, the (simplified) circuit of which is shown in figure 26.

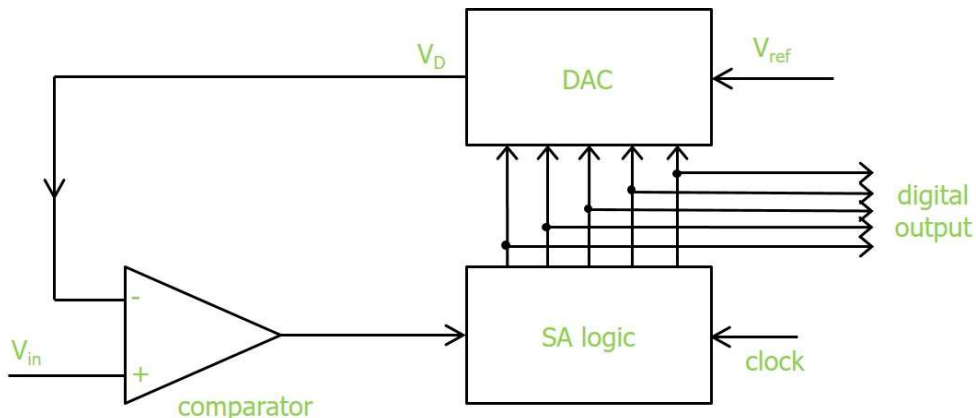


Figure 26: Circuit of an ADC utilizing the successive approximation method.

Basically, this type of ADC comprises of a DAC, a comparator (described at the end of the previous section) and digital circuitry containing the logic for the successive approximation (SA). The latter is denoted in the figure as ‘SA logic’. The input to the DAC is an n -bit digital word generated by the SA logic (in the figure $n = 5$). Initially, all n bits are set to 0 and then the MSB is set to 1. The digital word is converted by the DAC to an analog value corresponding to half the full range of the DAC. (The DAC’s full range is equal to V_{ref} , see figure 26). This value is compared with the analog input signal value V_{in} using the comparator, the output of which is fed into the SA logic. If this comparison shows that the DAC output V_D is less than V_{in} , the MSB is left at 1, otherwise it will be reset to 0. In both situations the SA logic then sets the next MSB to 1 and again V_D is compared to V_{in} . In this way each bit of the input to the DAC is set one by one and its correct state determined, i.e. 0 or 1. The conversion is completed when all n bits of the DAC input have been set correctly. The process is

illustrated in figure 27 for a 5-bit SA ADC for 4 values of V_{in} , i.e. $V_{in} = 0.2V_{ref}$, $V_{in} = 0.4V_{ref}$, $V_{in} = 0.6V_{ref}$ and $V_{in} = 0.8V_{ref}$. In the simulation shown in this figure the settling time per bit is assumed to be 1 μ s. (The typical total settling time of an 8-bit ADC is in the range 1-10 μ s and 10-100 μ s for a 12-bit ADC. Anyhow, the ADC's settling time is linearly proportional to the number of bits n).

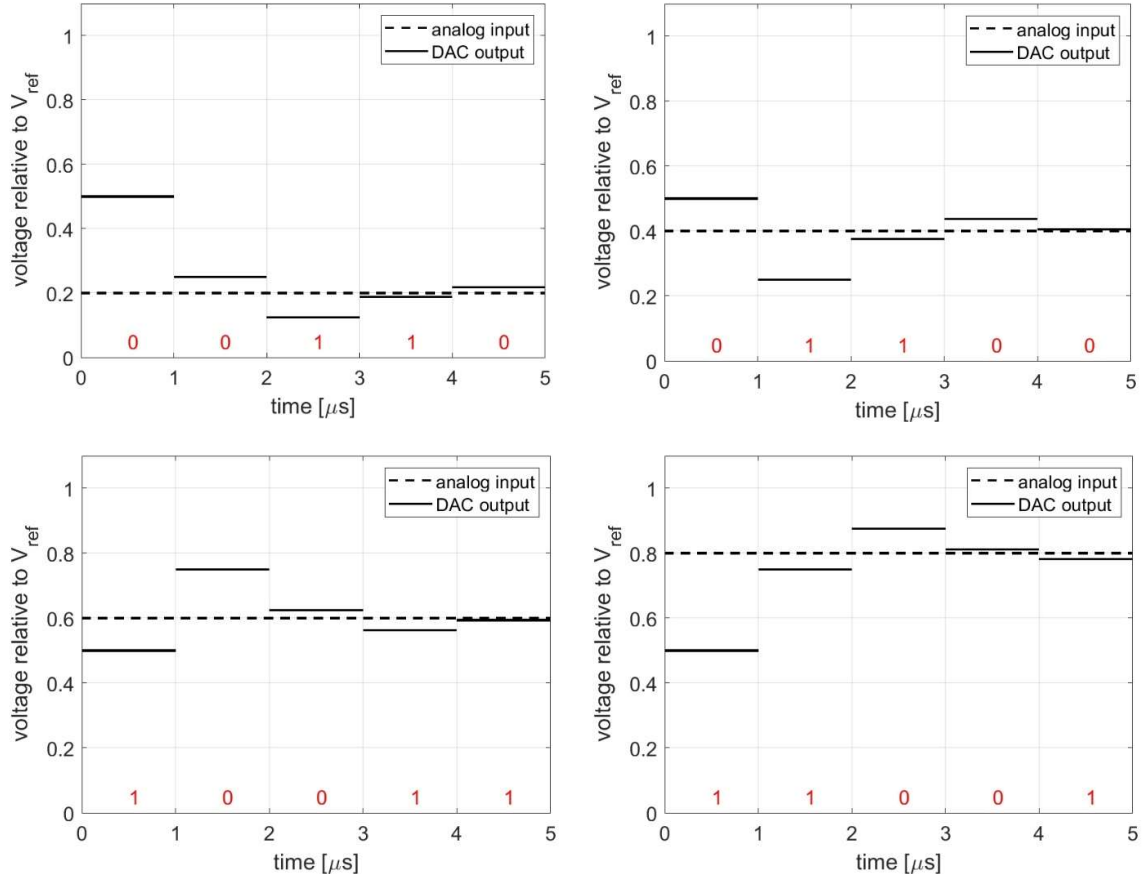


Figure 27: The successive approximation at work for a 5-bit ADC for several values of the input voltage (relative to the ADC's full range). The obtained digital output is shown in red at the bottom of each figure.

Note:

When performing analog-to-digital conversion for a (rapidly) time-varying analog signal it is often required to sample the signal and then hold its value constant for a certain (short) time. In this way the ADC's input signal does not change during the conversion process. A circuit able to perform this function is the 'sample-and-hold gate' shown in figure 28. Basically, the circuit consists of a capacitor and a switch. When the switch is closed, the capacitor quickly charges so that its voltage, which is equal to the output voltage V_{out} of the circuit, equals the input voltage V_{in} . If the switch is subsequently opened, the capacitor holds its charge and hence V_{out} remains constant. So, the circuit

samples a varying voltage by *closing* the switch and then *holds* that value by *opening* the switch, hence the name ‘sample-and-hold gate’.

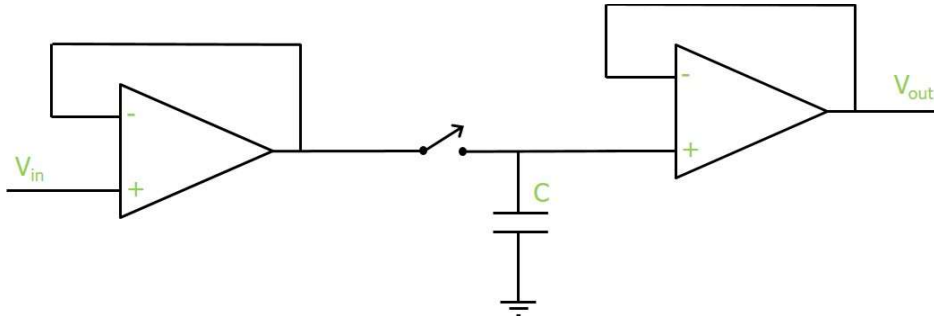


Figure 28: Circuit of a sample-and-hold gate.

As in practice the source of V_{in} has a finite output resistance and the capacitor will be connected to a load (e.g. the ADC), unity gain buffers (as described in the previous section) are used at the input and the output. The switch is implemented using a (field-effect) transistor as electronic switch.

A typical circuit of a data acquisition system for multiple analog inputs (in this case m analog signals) is shown in figure 29. A separate ADC for each input signal can be chosen, but a more economic solution is to use a so-called ‘analog multiplexer’. Basically, this device is an electrically controlled switch that accomplishes each analog signal to be connected subsequently to a single ADC. The necessary sequence and timing is determined by control signals from the electronic system (e.g. a microcomputer). To preserve the relationship between the input signals, e.g. their phase difference, all input signals are sampled simultaneously using a sample-and-hold gate for each input channel. (Acoustic imaging is an example of an application where this is important). As shown in the figure an anti-alias filter is used for each channel input.

Note: Today, integrated circuits (IC) exist that contain all elements depicted in figure 29. Such IC’s are denoted ‘single-chip data-acquisition systems’.

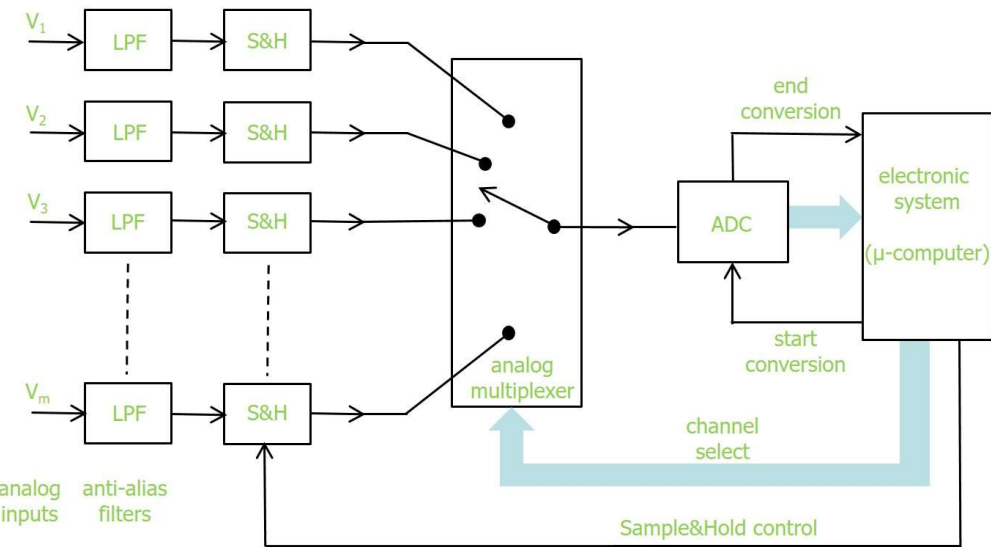


Figure 29: A typical circuit of a data acquisition system for m analog input signals.

Exercise

Consider a microcomputer-based data acquisition system cf. figure 29 that senses simultaneously eight analog input signals. These signals originate from sensors that produce useful signals with a bandwidth of 1 kHz. It is however known that the sensors pick up higher-frequency noise. It is required that the signals are measured with a resolution of at least 1 %.

- What is the required cut-off frequency of the LPF anti-alias filters?
- What is the Nyquist rate and the related practical (and safe) value of the sampling frequency?
- What is the corresponding minimally required sampling rate of the ADC?
- To what settling (conversion) time of the ADC does your answer to question (c) correspond?
- How many bits are required for the ADC? Is your answer possible with today's ADC devices given your answer to question (d)?